Investigations of the Temporary Adhesive of Acorn Barnacle Cypris Larvae

Joshua Raine

Submitted to Newcastle University in Partial fulfilment of the requirements for the degree of Doctor of Philosophy

School of Natural and Environmental Sciences

December 2020

Abstract

During its life cycle, an acorn barnacle spans multiple niches, from a free-swimming larva to a sessile adult. Settlement is permanent and therefore the individual must locate an optimal site for access to food and reproductive partners. To this end, the final larval stage, the cyprid, is well adapted for the purpose of surface exploration and selection. In order to adhere while exploring in dynamic environments, the cyprid secretes a proteinaceous temporary adhesive from the third antennular segment. This adhesive material is uncharacterised, and the descriptions of its secretory system almost half a century old. However, there is evidence that this temporary adhesive has some homology with the pheromone responsible for gregariousness in barnacles, the settlement-inducing protein complex, as both induce gregarious settlement, and they share an immunoreactive epitope(s).

This work aimed to re-examine the location of the temporary adhesive glands, and associated secretion pathways, in acorn barnacles. Additionally, it aimed to characterise the temporary adhesive protein(s) using a multi-omics approach validated by expression studies, and assess the involvement of the settlement-inducing protein complex in the temporary adhesive system. Evidence is presented that the temporary adhesive gland is located in the proximal first antennular segment, and that the system is structured differently to that of stalked barnacles. The identity of the temporary adhesive protein(s) remained elusive, but a pathway to identification was developed and candidates presented. Finally, the settlement-inducing protein complex, as it exists in adult barnacles, may not be involved in temporary adhesion. Instead, a substantially different analogue is present.

Acknowledgements

I would like to express my deepest thanks to the many people who have assisted with the creation of this thesis over the four years.

Firstly, to Tony Clare and Nick Aldred, for their tireless supervision and help with experiments and editing, without whom this endeavour would not have been possible.

Secondly to Ali Miserez, Lok Jun Jie, and Shawn Hoon, for their wonderful welcome at NTU, Singapore, and help in creating the *B. amphitrite* larval transcriptome.

Thirdly to Serena Teo and Serina Lee at NUS and TMSI, for providing cyprids during the time spent working in Singapore.

Fourth, to Tracey Davey and Ross Laws at the EMRS Newcastle, for assisting in collection and analysis of the SBF-SEM datasets for 3D-modelling.

Fifth, to Achim Treumann and Andrew Porter at NUPPA, for performing the peptide fingerprinting analysis.

Sixth, to Aisling Smith and Sean McTierney at the MBA, Plymouth, for allowing me to tag along on their sampling cruises in search of barnacles.

Seventh, to all the family and friends who offered support and encouragement when it was needed most.

And finally, my thanks to Sharon, for her immeasurable patience, understanding and love throughout the years.

Table of contents

List of Figures

List of Tables

Chapter 1. Literature Review

1.1. Introduction

The oceans of the world contain over 200,000 known species, with an estimated 1.5 million still to be discovered (Bouchet, 2006, Horton *et al.*, 2020). As oceans are dynamic environments, with currents and waves consistently transporting essential nutrients, gametes and waste, many species have adopted life strategies that forego movement altogether. These species are completely sessile, attaching themselves to the benthos or other organisms. However, the dynamic environment, which supports these sessile organisms, also threatens their existence, as being transported away from their preferred habitat would likely result in death. Thus, sessile marine organisms, such as mussels and barnacles, employ adhesives to ensure that they remain attached in the ideal location.

The subject of marine biological adhesives is of practical interest primarily for two reasons. First, synthetic adhesives able to bind and persist in the marine environment have proven difficult to manufacture. Gaining a better understanding of biological adhesives may lead to new avenues to develop these products. Secondly, many sessile marine organisms use their adhesives to attach to artificial structures or vessels, fouling them and often impairing their function. It follows that studies on the adhesive mechanisms of these organisms could help inform the development of fouling-resistant surfaces.

This work will focus on the bioadhesion of acorn barnacle (order Sessilia; suborder Balanomorpha) cypris larvae as the cyprid represents the key stage in a barnacle's life cycle that determines its permanent settlement location. Bioadhesion performs a vital function, allowing the larvae to explore and select surfaces. Interfering with this process can prevent or redirect settlement. Understanding the cypris larvae adhesive system is therefore of importance to the areas of both antifouling and ecological research. While adult barnacle bioadhesion has been comparatively well characterised (Kamino, 2016), there is little information on the adhesive systems of cyprids. Modern developments in 'omics and electron microscopy technology are able to overcome previous barriers to study through more sensitive techniques, making now the opportune time to elucidate this pivotal process of the barnacle life cycle.

1.2. Barnacles

Barnacles are arthropods belonging to the subphylum Crustacea, and class Cirripedia. Famously studied and classified by Charles Darwin (1853; 1854), Cirripedia are the only crustaceans that are sessile in their adult stage but possess a life cycle that spans both free swimming planktonic and sessile benthic forms (figure 1.1). The superorder Thoracica contains both stalked and acorn barnacles. While the body of stalked barnacles is contained within a shell atop a muscular stalk distal to the substratum, the body and shell of acorn barnacles are instead attached directly to the substratum (Perez-Losada *et al.*, 2008). Of the acorn barnacles, the family Balanidae are the focus for the present work.

1.2.1. Life Cycle

The life cycle of an acorn barnacle comprises nauplii, the cyprid, and the adult (figure 1.1). In some cases, these can be further subdivided (Chan *et al.*, 2017). For this review, the main focus will be on the larval stages, and the cyprid in particular.

Nauplii are the stages of barnacle development occurring immediately following hatching and release (Anderson, 1993). There are typically six naupliar stages, all of which are planktonic, and all but the first stage are planktotrophic among Sessila (Anderson, 1993). The first-stage nauplius moults soon after hatching and release from the adults, then develops through the planktotrophic stages over the course of days to weeks, depending upon the species and environment (figure 1.1) (Anderson, 1993; Pechenik, 1999). The accumulation of nutritional resources is a primary function of the naupliar stages as any deficiency due to sub-optimal conditions, be it temperature or food availability, can carry into the lecithotrophic cyprid stage and negatively impact fitness (Pechenik *et al.*, 1993; Anil *et al.*, 2001).

The cyprid stage is typically the seventh larval stage, following the nauplius stage (figure 1.1). The primary function of all barnacle cypris larvae is to find a suitable settlement site for metamorphosis into the juvenile stage. The major structures involved in settlement are the antennules, which are adapted as both sensory and adhesive organs (Nott and Foster, 1969; Aldred and Clare 2009). Unlike the nauplii,

cypris larvae are lecithotrophic and therefore have finite energy reserves for pre-settlement behaviour and metamorphosis.

Once settled, the cyprid metamorphoses into a juvenile barnacle, which begins feeding again and grows over time into the adult, reproductively mature, barnacle. Most barnacles are simultaneous hermaphrodites (Hoch *et al.*, 2016), and act as ‘females’ and ‘males’ as the situation requires. Typically, an individual will become ‘female’ first, releasing pheromones to trigger nearby conspecifics to become ‘male’ and increasing the size of their oviducal glands (Hoch *et al.*, 2016). The conspecific ‘male’ extends its penis in search of the mantle cavity of the ‘female’. Once inseminated, the eggs are subsequently laid, fertilized and then brooded within the mantle cavity until external stimuli trigger their hatching and subsequent release as stage 1 nauplii, beginning the life cycle anew (Crisp and Spencer, 1958; Walker, 1977.

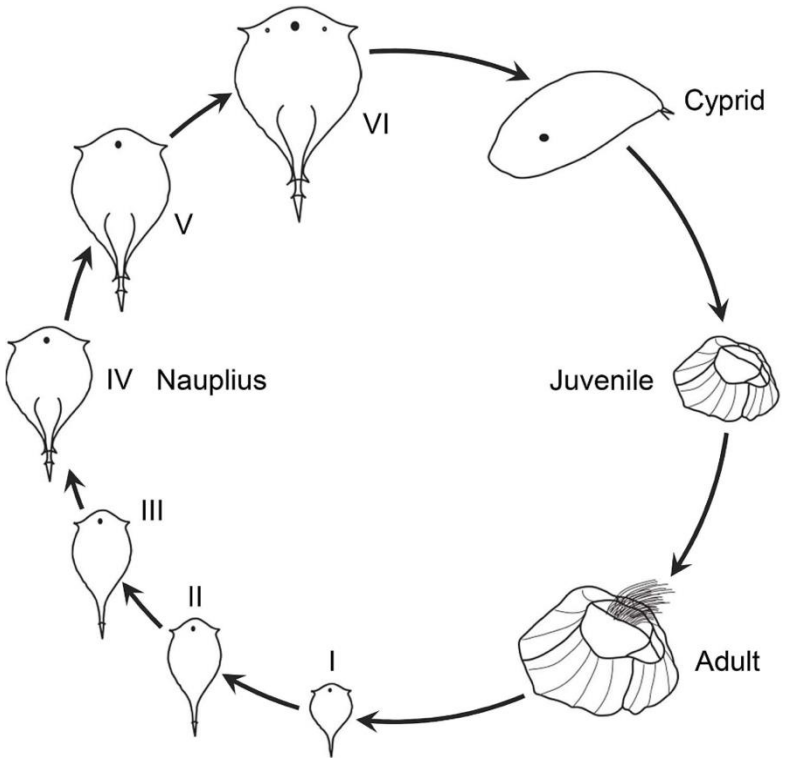

Figure 1.1. Life cycle of a typical acorn barnacle. Nauplius = the first larval stages following hatching from eggs brooded by adults. The planktonic nauplius feeds and develops through six stages over the course of days or weeks. Cyprid = final stage nauplii metamorphose into cyprids, losing the ability to feed and leaving the plankton to search for a suitable settlement location. Juvenile = a cyprid that finds an attractive substrate attaches permanently, metamorphosing into a juvenile barnacle which regains the ability to feed by filtering the water column. Adult = surviving juveniles will develop into adult barnacles. The adults are hermaphrodites and will reproduce with nearby conspecifics. Eggs are brooded in the mantle cavity until they hatch as stage one nauplii, and the cycle repeats. Figure adapted from Liang *et al.* (2019).

1.2.2. Larval Morphology

The body of a nauplius has a characteristic 'shield' shape, with numerous protruding appendages, including fronto-lateral horns and a posterior spine, which increase surface area and buoyancy. Cyprids swim using their thoracic appendages (Anderson, 1993). A nauplius begins life with a single eye, which it keeps through stages 1-4, whereupon it develops paired compound eyes in the 5th and 6th stages (Anderson, 1993). Towards the end of the 6th naupliar stage, production of the cyprid major protein, a vitellin-like protein, is activated, providing sustenance for the lecithotrophic cypris larval stage alongside lipid reserves (Lucas *et al.*, 1979; Satuito *et al.*, 1996; Shimizu *et al.*, 1996; *Chen et al.*, 2011).

The larval barnacle undergoes some dramatic morphological changes as it transitions into a cyprid (figure 1.1). The protruding appendages for assisting buoyancy mostly are lost, as is the 'shield' shape of the body, as the larva takes on a laterally compressed oval shape. Proteins relating to signal transduction, moulting and energy production increase in abundance significantly from the nauplius to cypris stage, but the overall proteome remains largely similar, up until the cyprid permanently attaches to the surface (Thiyagarajan and Qian, 2008). The appendages typically retained following metamorphosis are located on the ventral side: six pairs of thoracopods for swimming, and a pair of specialised antennules, comprising four segments (Nott and Foster, 1969; Anderson, 1993; Høeg and Møller, 2006).

The first antennular segment is connected directly to the anterior mantle, functioning primarily to rotate and orient the appendage to obtain maximum articulation during exploration (Nott and Foster, 1969; Lagersson and Høeg, 2002). As such, it does not possess any sensory setae.

The second segment is inflexible, with a single seta on the distal end from the first segment (Nott and Foster, 1969; Høeg, 1987). In *Balanus amphitrite* (=*Amphibalanus amphitrite*), and perhaps other intertidal species, the lateral cuticle of the second segment is altered to be 'rippled' allowing stretching and thus increased flexibility during close searching and providing resistance to sudden changes in flow (Lagersson and Høeg, 2002). This alteration is not present in parasitic rhizocephalan barnacles, indicating a specific adaptation for the dynamic and heterogeneous intertidal habitat (Lagersson and Høeg, 2002).

The third segment is the antennular disc, which is bell-shaped and responsible for adhering to the substratum that is being explored. Species-specific variation is present, but it appears the shape is often conserved among barnacles of similar habitats. For instance, species that occupy areas of hard substrata share a circular antennular disc, while the disc of epiphytic species is more elliptical (figure 1.2) (Chan *et al.*, 2017). The disc is coated with cuticular villi and surrounded by either a velum in rocky shore species, or a skirt of short but wide cuticle flaps in species which occupy other niches, such as epiphytic or sublittoral barnacles (figure 1.2) (Al-Yahya *et al.*, 2016; Chan *et al.*, 2017). The reasons for these morphological divergences have not been studied in detail, however, they likely correspond to niche specific requirements. The greater hydrodynamic forces and surface rugosity in rocky shore environments would make the flexible velum a more appropriate adaptation than potentially rigid cuticle flaps. The morphology of the villi also varies between species, but no clear correlation has been made with the preferred habitat (Al-Yahya *et al.*, 2016).

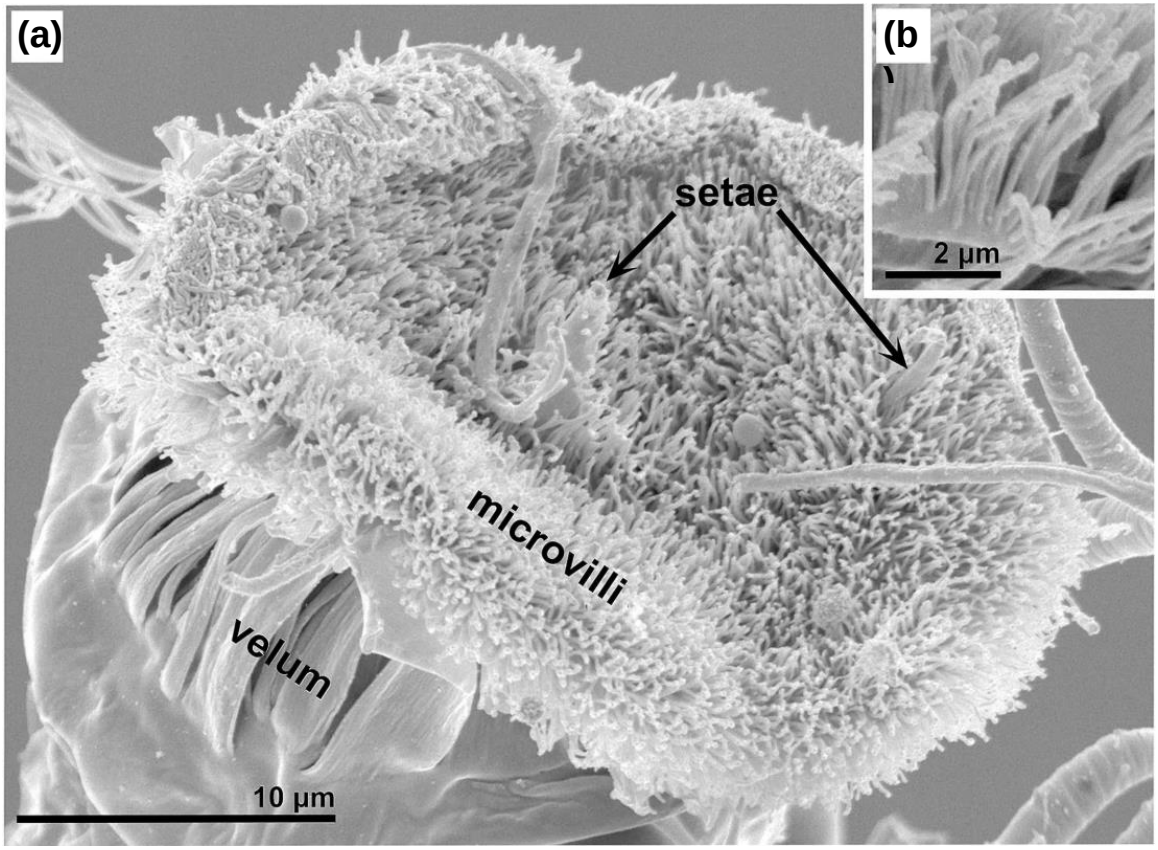

Figure 1.2. SEM images of a *Balanus improvisus* cyprid antennular disc. **(a)** = the bottom of the third antennular segment, or disc, is roughly circular and coated with numerous microvilli. Sensory setae are present to allow detection of a suitable substratum during exploration; **(b)** = A closer view of the villi covering the disc surface. Adapted from Aldred *et al.* (2013) and Liang *et al.* (2019).

The third segment also possesses a number of sensory organs: the axial sensory organ lies at the centre of the disc, adjacent to the central cement duct opening; the post-axial sensory organ is located amongst the villi; and two radial sensory organs are found on the edge of the disc (Nott, 1969). Each has an open-ended hair revealing them as chemosensory organs, which are believed to assist in surface selection, as well as identifying conspecific settlement signals (Nott and Foster, 1969; Clare and Nott, 1994; Bielecki *et al.*, 2009; Maruzzo *et al.*, 2011).

Finally, the fourth segment protrudes horizontally from the third segment at an angle of 45 to 90 degrees. It is cylindrical and possesses the greatest abundance of sensory setae, both chemosensory and mechanosensory, of any of the antennular segments (Nott and Foster 1969; Abramova *et al.*, 2019a). The expression of chemo- and mechanosensory receptor proteins changes over the course of settlement, from free swimming to surface exploration (Abramova *et al.*, 2019a). The cyprid flicks this segment regularly to improve the access of odour molecules to receptors, increasing the rate of flicking when cues are detected (Lagersson and Høeg, 2002; Elbourne and Clare, 2010; Maruzzo *et al.*, 2011). Utilising the antennule, the cyprid larvae explores and selects a surface on which to settle permanently and metamorphose into a juvenile. Once settled, the protein expression patterns become more concurrent with the proteome that can be observed in newly metamorphosed juveniles (Thiyagarajan and Qian, 2008).

1.2.3. Settlement

Cyprids are not passive in their dispersal and settlement patterns. Their ability to actively swim and explore the benthos in response to cues has been widely documented (Knight-Jones and Crisp, 1953; Knight-Jones, 1955; Eckman, 1990; Mullineaux and Butman, 1991; Hills et al. 1998; Dreanno *et al.*, 2007; Elbourne *et al.*, 2008; Prendergast *et al.*, 2008; Gatley-Montross, 2017; Larsson *et al.*, 2016; Aldred *et al.*, 2018). Cyprid settlement is permanent and thus critical to survival and reproductive success. When selecting a surface, a cyprid will typically follow a well-documented pattern of behaviours (Crisp, 1976). These early behavioural observations remain robust (Aldred et al., 2018). It begins with swimming, then

proceeds into substratum exploration, (Lagersson and Høeg, 2002; Maleschlijski *et al.*, 2015; Larsson *et al.*, 2016).

Swimming behaviours can be divided into spiralling, swimming, and sinking depending on the orientation and velocity as the cyprid moves through the water column (Maleschlijski *et al.*, 2015). Swimming and spiralling are both relatively high velocity movements with the cyprid actively propelling itself with its thoracapods. However, swimming generally occurs in a single direction, while spiralling is characterised by tight helical turns (Maleschlijski *et al.*, 2015). Conversely, sinking is a passive behaviour, characterised by low velocity vertical movement towards the substratum via gravity. The swimming activities comprise approximately two thirds of the cyprid's time for *B. amphitrite*, with substratum exploration taking up the other third. When attempting to settle under turbulent flow, the cyprids swim more, exhibiting positive rheotaxis, and settle during lulls in flow velocity (Larsson *et al.*, 2016). The critical velocity above which cyprids struggle to settle is based on swimming speed, not adhesion strength, as the values determined for *B. improvisus* were between 0.1 and 0.2 ms^{-1} (Larsson *et al.*, 2016). These velocities do not provide enough shear stress to overcome the temporary adhesion strength. Therefore, settlement in flow appears to be a voluntary behaviour (Mullineaux and Butman, 1991; Larsson *et al.*, 2016). *B. amphitrite*, on the other hand, rejects surfaces for settlement more often in high flow compared to low flow environments (Mullineaux and Butman, 1991).

Substratum exploration begins when the cyprid contacts a surface with its antennules and can be divided into distinct phases: wide searching, close searching, inspection, and settlement (Crisp 1976; Hills *et al.*, 2000; Lagersson and Høeg, 2002; Aldred *et al.*, 2010; Maleschlijski *et al.*, 2015; Alsaab *et al.*, 2017; Aldred *et al.*, 2018). Bipedal walking during searching involves the paired antennules contacting the surface, one at a time (Crisp 1976; Aldred *et al.*, 2013b; Maleschlijski *et al.*, 2015; Aldred *et al.*, 2018). While the antennules are in contact with the substratum, the cyprid senses the surface to determine its suitability for settlement. Wide searching is characterised by linear movement at relatively high velocities. If the cyprid finds the surface potentially suitable, it will proceed to close searching (Crisp 1976; Aldred *et al.*, 2018). If a surface is rejected, the cyprid may return to one of the swimming behaviours outlined above. During close searching, the velocity of the cyprid decreases; it travels shorter distances and changes direction with increased frequency, thus allowing more detailed

sensing of the surface (Crisp 1976; Alsaab *et al.*, 2017; Aldred *et al.*, 2018). Inspection was defined by Crisp (1976) as the final stage prior to settlement. The cyprid remains stationary, attached by one antennule while it probes the immediate vicinity with the other. However, Aldred *et al.* (2018) observed this behaviour during all surface exploration phases. The strict order described by Crisp (1976) can thus be short-circuited at any phase, with the cyprid returning to an earlier stage. Nevertheless, inspection behaviour is a good indicator of the propensity to settle. The terminal step is always fixation, as the process is irreversible once the permanent cement is secreted, followed by metamorphosis into the juvenile barnacle. Catecholamines, dopamine and noradrenaline, stimulate secretion of the permanent adhesive (Okano et al., 1996). Dopamine has been identified in other crustacean systems, is present in cyprids, and stimulates exploration and attachment, along with serotonin (Yamamoto et al., 1996 Yamamoto et al., 1999).

These settlement behaviours are influenced by the properties of the substratum, with surface microtopography being a particularly important factor, although the responses are not uniform between species (Yule and Walker, 1984; Berntsson *et al.*, 2000; 2004; Prendergast *et al.*, 2008; Aldred *et al.*, 2010; Chaw *et al.*, 2011). *Semibalanus balanoides* cyprids spent more time engaging in close searching behaviour on rough surfaces (Yule and Walker, 1984; Prendergast *et al.*, 2008), while *B. improvisus* cyprids exhibit a preference for smooth surfaces (Berntsson *et al.*, 2000; 2004). *B. amphitrite* appears to exhibit selection based on the size of micro-topographical features (Aldred *et al.*, 2010; Chaw *et al.*, 2011). In general, *B. amphitrite* cyprids tended to exhibit preferences for features in which their attachment disc, or the whole cyprid could fit, providing resistance to drag forces while exploring. The exception to this behaviour was observed when exploring surfaces with features below 30 µm in size. It was hypothesised that the surface roughness splits the point of contact, improving adhesion strength, but additionally these micro-topographical features would in turn provide an improved substrate to which adult cement could bond post-metamorphosis (Aldred *et al.*, 2010; Chaw *et al.*, 2011). The preference exhibited by *S. balanoides* for rough surfaces bearing larger features can likely be attributed to the increased size of the cyprid compared to *B. amphitrite* (Yule and Walker, 1984; Prendergast *et al.*, 2008). Assaying settlement preferences of *S. balanoides* against larger micro topographical features may result in a similar pattern being observed as

in *B. amphitrite*, since ~350 µm have been the largest features tested so far (Yule and Walker, 1984; Prendergast *et al.*, 2008). The preference of *B. improvisus* for smooth surfaces is less clear, as the cyprids are similar in size to *B. amphitrite,* with both species settling in dynamic intertidal environments, and thus benefiting from reduced drag forces (Berntsson *et al.*, 2000; 2004). Evidently, further research in this area is required to fully elucidate these phenomena, and how they vary between species.

In addition to microtopography, surface colour has been indicated to influence settlement. *S. balanoides* and *Elminius modestus* cyprids, when exploring identical surfaces, which differ only in colour, displayed significantly stronger adhesion on the darker surfaces, reds, blues and blacks (Yule and Walker, 1984; Robson *et al.*, 2009; Matsumura and Qian, 2014). Therefore, the cyprid is playing an active role in surface

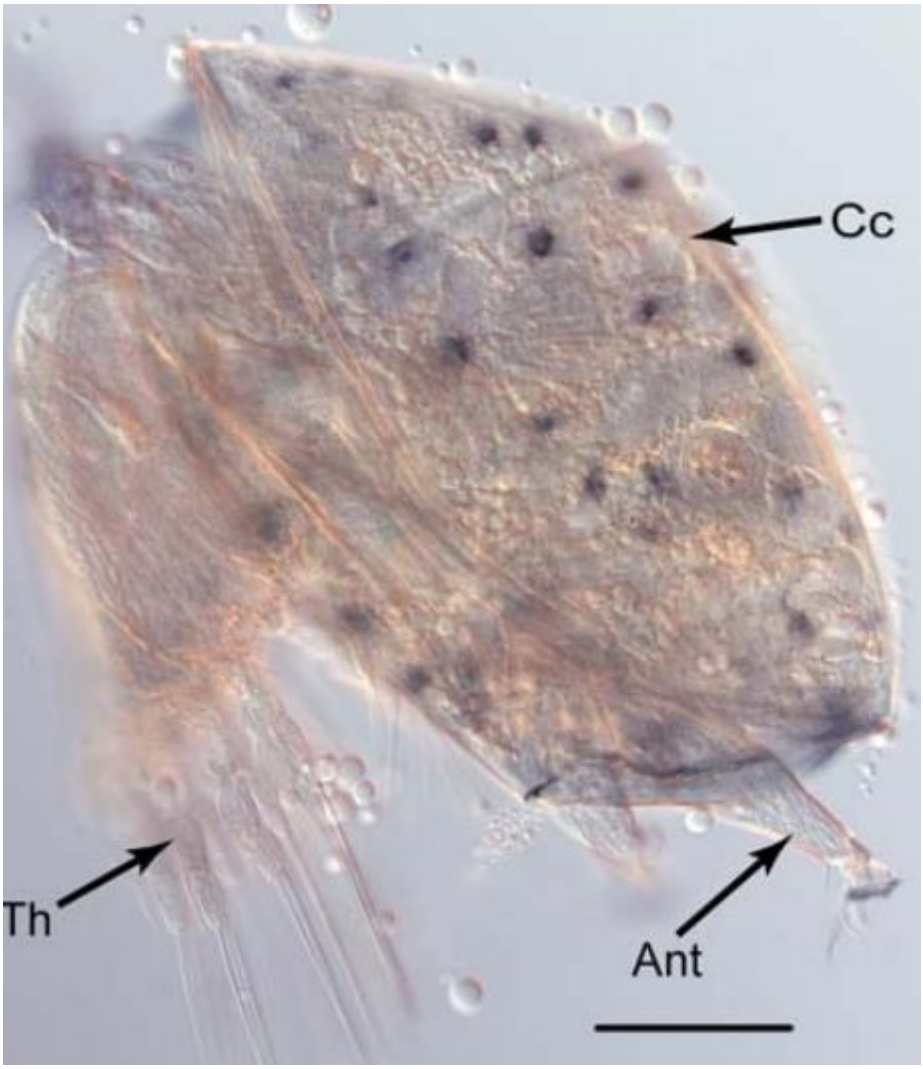

Figure 1.3. Whole mount in-situ hybridisation of a Balanus amphitrite cyprid. Lateral view, purple spots indicate the expression of mannose receptor genes in carapace pores. Ant = antennule; Cc = cyprid bivalve carapace; Th = thoracopod. Scale bar = 100 µm. Figure adapted from Chen *et al.* (2011).

selection, not simply settling where adhesion is the strongest. Adult *B. amphitrite* shells have been demonstrated to auto-fluoresce red, perhaps indicating that cyprid vision and colour preferences play a role in gregarious settlement (Matsumura and Qian, 2014).

Beyond their basic physical properties, marine surfaces, unless newly immersed, are biofilmed, which can influence the settlement behaviour of cyprids. Data on the influence of bacterial biofilms on cyprid settlement is inconsistent, with reports of both inhibition (Maki *et al.*, 1988; Olivier *et al.*, 2000), and stimulation of settlement (Qian *et al.*, 2003; Patil and Anil, 2005; DeGregoris *et al.*, 2012; Baragi and Anil, 2017). However, the majority of studies have been performed with axenic biofilms under laboratory conditions, thus the relevance to real world settlement behaviours is limited. The current best hypotheses are that the cyprids are capable of detecting bacterial and diatom exudates from communities associated with their preferred habitats, or even those which grow upon conspecifics, and are stimulated to settle by them (Patil and Anil, 2005; DeGregoris *et al.*, 2012). Cyprids do appear to collect their own bacterial community during the settlement process, however. *S. balanoides* cyprid microbiomes during settlement were distinct from the communities present during the planktonic larval phase, and the surrounding environment (Aldred and Nelson, 2019). This microbiome was consistent over multiple reproductive seasons, suggesting that this microbial community may play an important role in the metamorphosis or early development of settled cyprids (Aldred and Nelson, 2019).

During the settlement process, cyprids also alter their behaviours based on chemical cues and signals. The abundance, or scarcity, of certain inorganic ions can inhibit settlement. Magnesium and potassium ions in high abundances inhibited settlement, while low abundances of calcium ions did the same (Rittschof *et al.*, 1986; Clare 1996). It is hypothesised that the reduced settlement under calcium-limiting conditions is related to the requirement for calcium during metamorphosis and test production (Rittschof *et al.*, 1986).

More complex molecules also influence settlement behaviours in cyprids. Mannose sugars stimulate exploration, settlement, and metamorphosis (Khandeparker *et al.*, 2002). During the cyprid stage, mannose and tyrosine kinase receptor expression increased, located on pores and setae of the carapace, but not the antennules (figure

1.3) (Chen *et al.*, 2011). Other sugars, such as glucose, inhibited settlement, so there is likely a specificity to the mannose sugar moieties (Khandeparker *et al.*, 2002). The response to mannose sugars is currently hypothesised to be related to the settlement-inducing protein complex (SIPC), a key conspecific chemical signal in the gregarious settlement process of cyprids. This will be discussed further in 1.2.4. The SIPC is not the only gregarious chemical signal to settlement, however, as adult barnacles release a waterborne pheromone that stimulates increased swimming and settlement (Rittschof et al.,1985; Endo *et al.*, 2009; Elbourne and Clare 2010). The waterborne pheromone, first demonstrated in *S. balanoides* by Rittschof et al., (1985), has since been observed in *B. amphitrite* (Tegtmeyer and Rittschof 1989; Clare and Matsumura 2000; Clare and Yamazaki 2000; Browne and Zimmer, 2001; Endo *et al.*, 2009; Elbourne and Clare, 2010). These studies concurred that the waterborne pheromone is a small peptide(s) under 5kDa (Tegtmeyer and Rittschof, 1989), although some estimate a mass of 500Da or lower (Clare and Matsumura *et al.*, 2000; Elbourne, 2008). However, there is not yet a consensus as to the composition of the peptide(s) in question, if the signal is a peptide at all, as synthetic peptides bearing basic amino acids on the C-terminal positively induced settlement in some cases (Tegtmeyer and Rittschof 1989; Browne and Zimmer, 2001), but not others (Clare and Yamazaki, 2000). More recently, a 32kDa protein which acts as a waterborne settlement pheromone was isolated from *B. amphitrite* (Endo *et al.*, 2009), and several homologues of this protein described in the transcriptome of *S. balanoides* (Abramova *et al.*, 2019b). The occurrence of six homologues in *S. balanoides* suggests that the waterborne settlement pheromone may in fact be a mixture of proteins, as opposed to a singular molecule (Abramova *et al.*, 2019b). Also, because the C-terminus regions of these homologues were similar in mass to the peptides described previously, it has been posited that the peptides which act as the waterborne cue are cleavage products from a larger protein (Rittschof, 1993; Abramova *et al.*, 2019b). There is, however, no direct evidence that these proteins are released into the water column by the adult barnacle.

The settlement signals and cues discussed here must all be considered in the context of the finite lifespan of a cyprid. As previously mentioned, cypris larvae are lecithotrophic and therefore have finite energy to consume when searching for a suitable settlement location. This energy comes from stored lipids and the ‘cyprid

major protein' (CMP), which decrease significantly in amount within the cyprid as they age over the course of two to four weeks (Lucas *et al.*, 1979; Satuito *et al.*, 1996). This gives the larvae a limited amount of time to settle before their fitness is reduced and they may be less able to metamorphose, and less likely to survive post-metamorphosis (Pechenik *et al.*, 1993). As such, barnacle cyprids become less selective as to their settlement site the longer they are forced to search. For example, *B. amphitrite* cyprids up to five days old explore unfavourable surfaces less frequently than older cyprids (Miron *et al.*, 2000). Close searching and inspection behaviours became less frequent in *B. amphitrite* and *S. balanoides* cyprids that were over five days old, indicating reduced selectivity (Elbourne and Clare, 2010; Aldred *et al.*, 2018). The competency of *B. amphitrite* appears to be maximal in 3-day-old cyprids, and declines thereafter (Rittschof *et al.*, 1984; Satuito *et al.*, 1996; Miron *et al.*, 2000; Maréchal *et al.*, 2012). Fortunately for the study of larval behaviours, cyprids of the most commonly studied species are capable of being stored at <5°C for 14 days without exhibiting any notable decrease in CMP abundance or settlement ability (Satuito *et al.*, 1996). It is estimated that it takes ~40-60% of the energy reserves of the cyprid to undergo metamorphosis into a juvenile barnacle, and as such the importance of energy conservation to a cyprid seeking to settle cannot be understated (Thiyagarajan *et al.*, 2003).

The metamorphosis of cyprids post-settlement is governed by hormones (Freeman and Costlow, 1983; Clare *et al.*, 1992; Yamamoto *et al.*, 1997a; 1997b; Smith *et al.*, 2000). Hormones analogous to those described in insects stimulated metamorphosis of *B. amphitrite* cyprids, with concentration-dependant variations depending on the compound (Freeman and Costlow, 1983; Clare *et al.*, 1992; Yamamoto *et al.*, 1997a; 1997b; Smith *et al.*, 2000). Low ambient concentrations (0.1 µM) of methyl farnesoate inhibited metamorphosis, while ten- and hundred-fold increases of the same compound stimulated it (Yamamoto *et al.*, 1997a; Smith *et al.*, 2000). However, the cyprids metamorphosed without settling, and in many cases exhibited abnormalities (Yamamoto *et al.*, 1997a; Smith *et al.*, 2000), indicating that a mix of hormones are required for successful metamorphosis. One such hormone that has been studied is 20-hydroxyecdysone, the prohormone of the insect moulting hormone, ecdysone (Freeman and Costlow, 1983; Clare *et al.*, 1992; Yamamoto *et al.*, 1997b). In settlement assays, this hormone acted inversely to methyl farnesoate, with ambient concentrations above 10 µM inhibiting metamorphosis, while ten- to one thousand-

fold lower concentrations simulated settlement and metamorphosis (Freeman and Costlow, 1983; Clare *et al.*, 1992; Yamamoto *et al.*, 1997b). The responses of cyprids to these hormones changed when exposed to both compounds, however (Yamamoto *et al.*, 1997b). Prior exposure to 20-hydroxyecdysone prevented metamorphosis stimulation by methyl farnesoate, and 20-hydroxyecdysone became an inhibitor to metamorphosis when cyprids were first exposed to methyl farnesoate (Yamamoto *et al.*, 1997b). More recently, transcriptomic analysis of stage six nauplii and cyprids highlighted an upregulation of B-type allatostatin expression during these phases (Yan *et al.*, 2012). These neuropeptide hormones have been described as inhibitors of juvenile hormones in insects, thus it is hypothesised they perform a similar role in cyprid metamorphosis by inhibiting methyl farnesoate production (Lorenz *et al.*, 1995; Yan *et al.,* 2012). It is unlikely that these hormones and their interactions alone comprise the suite of those involved in the cyprid metamorphic process, and there is yet more research to be done to glean a comprehensive picture.

1.2.4. The Settlement-Inducing Protein Complex

Due to their sessile nature, sexual reproduction most commonly occurs between barnacles in close proximity, thus a preference for gregarious settlement is shared by a majority of acorn barnacles, first documented by Knight-Jones (1955) and Crisp (1953), and widely studied since (Matsumura *et al.*, 1998; Clare and Matsumura*,* 2000; Khandeparker *et al.*, 2002; Head *et al.*, 2003; 2004; Dreanno *et al*., 2006a; 2006b; 2006c; 2007; Elbourne *et al.*, 2008; Kotsiri *et al.*, 2018). Gregarious settlement requires that exploring cypris larvae can sense conspecific adults, and the settlement-inducing protein complex (SIPC) is a pheromone that fills this requirement.

The SIPC is a glycoprotein of high molecular mass, 262kDa in total and ~170kDa, not glycosylated (Dreanno *et al.*, 2006c). There is also some evidence that SIPC occurs as a dimer, as Matsumura *et al.* (1998) found the mass to be between 200 and 400kDa.The full sequence is 5,202bp and the open reading frame codes for 1,547 amino acids. Some homology (25%) is shared with thioester-containing proteins (TEP) in the α_2-macroglobulin (A2M) sub-family; 31% with *Ornothodoros moubata* (tick) A2M and 29% with *Limulus* sp. (horseshoe crab) A2M. The SIPC of *B. amphitrite* may not

be a TEP, however, as it does not possess the sequence ‘GCGEQ’, which is characteristic of the majority TEPs.

Three subunits of 76kDa, 88kDa, 98kDa make up the protein, with the 88kDa and 98kDa subunits originating from the N-terminus, while the 76kDa subunit originates from the C-terminus (Dreanno *et al.*, 2006c). Each of these subunits is individually capable of stimulating settlement of cyprids with equal efficacy to the whole protein (Matsumura *et al.*, 1998). Each subunit contains sugar chains which bind to lentil lectin (*Lens culinaris* agglutinin LCA) and jack bean lectin (ConA), both of which have a high affinity for mannose (Matsumura *et al.*, 1998). Adding LCA reduces SIPC-induced settlement, while exposure to mannose increases metamorphosis rates, with no response to other sugars (Matsumura *et al.*, 1998; Khandeparker *et al.*, 2002). More recently, the glycans present on the SIPC were isolated, showing them to be a high mannose type (Pagett et al., 2012). This evidence suggests that the sugar complexes of the SIPC play a role in its detection and conspecific settlement induction. Indeed, sugars have been observed bound selectively to the sensory organ of the third antennular segment (Khandeparker *et al.*, 2002). Mannose sugars in isolation stimulated minor increases in settlement and metamorphosis in *B. amphitrite* cyprids, below the magnitude of responses observed to adult extracts (Khandeparker *et al.*, 2002; Pagett et al., 2012). This indicates that while the sugars play a part in the settlement process, other factors are involved (Khandeparker *et al.*, 2002; Pagett et al., 2012).

The SIPC induces permanent settlement in cyprids, with an EC_{50} of just 100 ng per 0.8 cm^2 (Dreanno *et al.*, 2007). The SIPC is present in the cuticular slips covering the calcified parietes of adults, and all other organs that have cuticle tissue (Dreanno *et al.*, 2006b). It has also been recently posited that the SIPC takes on a secondary role, regulating calcite crystal formation in the parietes and thus improving resistance to water erosion (Zhang *et al.*, 2016). Estimates suggest that up to 11 µg of the SIPC is expressed per cm^2 of adult cuticle, provided that 100% of the SIPC is expressed at the surface; more than enough to stimulate larval settlement (Dreanno *et al.*, 2006c). However, more recent evidence indicates the SIPC and the settlement response is more complex. *B. amphitrite* cyprids were induced to settle only by low concentrations of recombinant waterborne SIPC, while higher concentrations had the opposite effect, causing a reduction in settlement (Kotsiri *et al.*, 2018). This differential, concentration-

dependent response would allow cyprids to settle gregariously, facilitating reproduction with neighbouring individuals, while also exhibiting the territoriality described by Crisp (1961), reducing intraspecific competition. The method of action for this putative dual response is found on the SIPC molecule itself as, when separated, the N-terminus of the protein stimulated settlement, while the C-terminus inhibited it (Kotsiri *et al.*, 2018). The receptors responsible for this behaviour have not yet been isolated, however, some potential candidates have been identified amongst antennular chemoreceptors by Abramova *et al.* (2019a). It is worth noting, however, that this purported dual action is directly contrasted by the observations of settlement stimulation by all subunits of SIPC, which originate from both the N- and C-terminals (Dreanno *et al.*, 2006c). Further study is evidently required to fully elucidate this phenomenon, given that the SIPC is typically a surface-bound protein, and indeed verify that the recombinant SIPC is equivalent to that produced *in vivo*.

The SIPC is not only limited to adult barnacles, as it has also been identified in all larval cuticles (Dreanno *et al.*, 2006b). In nauplii, the SIPC occurs predominantly within the gut, antennae, and mouthparts, while in cyprids it is found in the eyes, antennules, thoracopods, epidermis, and cuticle (Dreanno *et al.*, 2006b). While present in all larvae, expression of the SIPC increases dramatically in the cyprid stage (Kotsiri *et al.*, 2018). This is supported by the observations of Hills *et al.*, (1998), in which *S. balanoides* was stimulated to begin close searching and inspection by crushed conspecific cyprids. The SIPC, or a homologue, was also found to be present in cyprid footprint deposits by antibody staining performed by Dreanno *et al.* (2006a). It is likely that this is what allows cyprids to display gregarious settlement tendencies even without adults present (Clare *et al.*, 1994; Head *et al.*, 2003; 2004; Elbourne *et al.*, 2008). In *B. improvisus* and *B. amphitrite*, between three and five cyprids are required to stimulate gregarious settlement after two days (Head *et al.*, 2003; 2004; Elbourne *et al.*, 2008). After one day, however, while *B. improvisus*, still exhibited gregarious settlement with only three cyprids present, *B*. *amphitrite* required ten (Head *et al.*, 2004). This variation among species indicates a species-specific difference in either cue production or detection threshold (Head *et al.*, 2004). Regardless of the specifics, the occurrence of this phenomenon means that the number of cyprids assayed simultaneously for settlement behaviours should be given careful consideration (Clare *et al.*, 1994; Head *et al.*, 2003; 2004; Elbourne *et al.* 2008). Nevertheless, the cyprid

age seemingly has no influence over the sensitivity to gregarious settlement cues in *S. balanoides* and *B. amphitrite* (Elbourne and Clare, 2010); however previous evidence suggests that as cyprids age, they lose some ability to respond to chemical cues to settlement (Rittschof *et al.*, 1984; Holm *et al.*, 2000; Head *et al.*, 2004).

The SIPC is not identical among all acorn barnacles and it is thought that these differences facilitate conspecific settlement. While some inter-specific commonalities are present, differences in both the amino acid sequence, and potential glycosylation sites have been highlighted (Kato-Yoshinaga *et al.*, 2000; Dreanno *et al.*, 2007; Yorisue *et al.*, 2012). Antibodies raised against the 76kDa subunit of *B. amphitrite* SIPC also bound to SIPC-like proteins purified from *B. improvisus, E. modestus,* and *M. rosa*, while those raised against the 88kDa and 98kDa subunits did not (Dreanno *et al.*, 2007). Furthermore, *B. amphitrite* SIPC induced settlement of these species, albeit less than the conspecific signal (Kato-Yoshinaga *et al.*, 2000; Dreanno *et al.*, 2007). It is thought that the phylogenetic relationship between species influences the receptivity to inter-specific SIPC, with more distantly related species showing more divergence in SIPC structure, and thus stimulating a reduced settlement response due to the lack of specificity (Kato-Yoshinaga *et al.*, 2000; Dreanno *et al.*, 2007). An orthologue to the SIPC has also been identified in *Balanus glandula*, termed MULTIFUNCin (Ferrier *et al.*, 2016; Zimmer *et al.*, 2016). This cuticular glycoprotein shares a 78% homology with the SIPC, a similar molecular mass of ~200kDa, occurs natively as a 400kDa dimer, and fragments with a 98kDa subunit (Ferrier *et al.*, 2016; Zimmer *et al.*, 2016). Given the similarities, MULTIFUNCin is likely to be the SIPC of *Balanus glandula*. Like the SIPC, MULTIFUNCin stimulates settlement in conspecific cypris larvae, but also attraction of *Acanthinucella spirata*, a predatory whelk species (Ferrier *et al.*, 2016; Zimmer *et al.*, 2016). The role of the SIPC as a cue to attract predators in other barnacle species has yet to be explored. Given the importance of gregarious settlement cues to the barnacle life strategy, and the uniformity of this strategy amongst acorn barnacles, it is unsurprising that the SIPC and its homologues share such similarities.

1.3. Bioadhesion

Unsurprisingly for an infraclass which spends a considerable portion of its life cycle sessile, bioadhesion is vitally important to the Cirripedia. This bioadhesion is facilitated by a suite of adhesive proteins and associated secretory systems (Walker, 1971; Walker and Yule, 1984; Yule and Walker, 1987; Dreanno *et al*., 2006a; Phang *et al.*, 2008; Aldred *et al.*, 2013a; 2013b; Kamino, 2013; Gohad *et al.*, 2014; Yap *et al.*, 2017; Fears *et al.*, 2018; Schultzhaus *et al.*, 2019; Aldred *et al.*, 2020). As each stage of the barnacle life cycle requires its own specialised adhesives, the expression of these proteins changes throughout the life cycle (Thiyagarajan and Qian, 2008). This area of the review will focus on these specialised adhesives and their biological systems.

1.3.1. Adults

The adult cement is expressed in basal soft tissue from glands and secreted into the adhesive joint between the surface and the barnacle approximately 35-40 days after metamorphosis (Yule and Walker, 1987). This cement layer is typically a few µm thick and is transparent, providing an estimated attachment strength of ~9 x 10^5 N m^{-2} by *S. balanoides* adults to slate (Yule and Walker, 1984; 1987). The adult barnacle also secretes more cement as it grows to remain firmly adhered to the substratum. The secretion of cement is believed to be linked to the moult cycle (Fyhn and Costlow, 1976), however cement production seems to be constitutive, as there is no observable change in cement gene expression before, during or after the moult cycle (Burden *et al.*, 2014; De Gregorio *et al.*, 2015; Wang *et al.*, 2015). Furthermore, prior to cement secretion, *B. amphitrite* has been observed to release a fluid with a high abundance of phenol chemistries, lipids, and reactive oxygen species. This is hypothesised to function as a ‘cleaning’ fluid, removing biofilms and allowing uninterrupted access of the bulk cement to the substratum (Fears *et al.*, 2018). Phenol chemistries have long been thought to be associated with cross linking in barnacle cement (Walker, 1970; 1971), and *B. amphitrite* was also found to secrete a novel peroxinectin enzyme, which oxidises phenolic chemistries. Thus, it is possible this ‘cleaning fluid’ then cross links and forms part of the cement (So *et al.*, 2017). It is also possible that the source of the phenol content in BCS1 was this ‘cleaning fluid’ (So *et al.*, 2017).

Evidence of a juvenile cement also exists, which is secreted within 1 day of settlement and metamorphosis (Yule and Walker, 1984; 1987). It was originally believed that the cyprid cement served as the sole adhesion mechanism during this time, however *S. balanoides* attachment strength was found to be far stronger in practice than if this was the case and increased over 14 days. Furthermore, this adhesive strength was ~5.5x weaker than that provided by the adult cement (Yule and Walker, 1984; 1987). Recent observations by Essock-Burns *et al.* (2017) support this hypothesis. During metamorphosis, a material comprised of phosphoproteins was released into the barnacle-substrate interface, which may be the juvenile cement (Essock-Burns *et al.*, 2017). This substance, and the developing cuticle, was rich in reactive oxygen species, potentially contributing to oxidative cross linking (Essock-Burns *et al.*, 2017). Much like the 'cleaning fluid' of adults, this substance may also act as an antimicrobial mechanism, as during *B. amphitrite* settlement, bacteria associated with the adhesive plaque died off over time (Essock-Burns *et al.*, 2017).

Given the estimated attachment strength of adult cement at ~9 x 10^5 N m^{-2}, barnacle cement is not particularly strong in comparison to current, man-made adhesives. It is, however, on par with, or superior to, the adhesives of other marine organisms, such as mussels and limpets (Yule and Walker, 1987). Despite this, the barnacle adult cement is distinct from all other marine biological adhesives, and seemingly more complex. No homology has been found with tubeworm or mussel adhesives, and there is a notable absence of DOPA in the barnacle cement, which is present in the adhesives of these organisms (Kamino, 2013). Some homology to silk proteins has been observed, however (So *et al.*, 2016).

The components of the barnacle adult cement were originally characterised in *Megabalanus rosa*. Six component cement proteins, with molecular masses of 100, 52, 68, 19, 20k & 16kDa were partially characterised (Kamino *et al.*, 1996; 2000; Mori *et al.*, 2007; Urushida *et al.*, 2007; Kamino, 2013; 2016). Homologues of these proteins have been found in other acorn barnacles, such as *B. amphitrite* (He *et al.*, 2013; Jonker *et al.*, 2014; He *et al.*, 2018).

The 52 & 100kDa proteins are hydrophobic, highly insoluble bulk proteins with a low abundance of cysteine (Cys) residues (<1.5%). Intramolecular disulphide bonds are protected from denaturing by the external hydrophobicity, which contributes to the

insolubility (Kamino *et al.*, 2000; 2012; 2016). The corresponding proteins in *B. amphitrite* share a similar amino acid composition, with slight variation in Cys and hydrophobic amino acid abundances (Kamino, 2016). It is also worth noting that the 100kDa protein has been identified in both adult and cyprid cement glands indicating that it is a core component of barnacle adhesives used at multiple life stages (He *et al.*, 2018). Reports indicate that between 5-50% of bulk cement is comprised of amyloid proteins, which form a beta sheet secondary structure, and serve together as an insoluble framework for other proteins to embed into (Sullan et al., 2009; Barlow *et al.*, 2010; Kamino *et al.*, 2016). Kamino *et al.* (2000) estimated that almost 90% of the 100kDa cement protein of *M. rosa* takes on this conformation.

The 68kDa component of the cement is hydrophilic, with >60% composed of serine (Ser), threonine (Thr), glycine (Gly), and alanine (Ala). The primary structure has two regions. Firstly, the N-terminus region is long and rich in the aforementioned Ser, Thr, Ala, and Gly amino acids, which includes hydroxyl groups with the potential to displace surface-bound water, thereby facilitating contact between the adhesive and the surface. The C terminus is short, and is comprised of more hydrophobic amino acids, and proline (Pro) and tryptophan (Trp) instead. The protein is, therefore, more likely to pack tightly into a hydrophobic core (Kamino *et al.*, 2016).

The 20kDa cement protein is also hydrophilic, with many charged amino acids such as histidine (His), Cys, and aspartic/glutamic acid (Asp/Glu) and is comprised of six repeated sections. While present in low abundance, when folded, the charged amino acids present on the surface of the protein, facilitating good adsorption to calcite, and are thus hypothesized to bond with the calcareous base of the barnacle (Mori *et al.*, 2007; Kamino *et al.*, 2016). Two homologues of the 20kDa protein have been characterised in *B. amphitrite*, both in the adult cement, and the cyprid permanent cement glands, with each homologue being unique to either the α or β granules of the latter (He *et al.*, 2013). The cyprid permanent cement is discussed further in section 1.3.2.

The 19kDa protein is very similar in nature to the 68kDa protein and was originally hypothesised to have a similar role (Urushida *et al.*, 2007; Kamino *et al.*, 2016). When isolated from *M. rosa*, the 19kDa protein displayed strong adsorption to a range of surface chemistries and shared a high level of homology with those of *B. improvisus*

and *B. albicostatus* (Urushida *et al.*, 2007). Furthermore, all three were rich in Ser, Thr, Ala, Gly, valine (Val) and lysine (Lys) residues, much like the 68kDa protein (Urushida *et al.*, 2007). In the case of *B. amphitrite*, these residues formed a repeating pattern of simple amino acids with little to no modification or charge, interspersed with charged regions (So *et al.*, 2016; 2019). A recent study found that the 19kDa protein naturally aggregates into amyloid fibrils in seawater, more akin to the 52 and 100kDa proteins, in addition to less saline and more acidic conditions hypothesised to be present in the cement glands (Liu *et al.*, 2017; Liang *et al.*, 2018). Furthermore, the assembly time of these amyloid fibrils is comparable to the curing time of the adhesive, suggesting an involvement in the polymerisation process, as opposed to the 68kDa protein acting to displace water on hydrated surfaces (Liu *et al.*, 2017; Liang *et al.*, 2018). Amyloid fibrils pre-assembled in acidic conditions also retained their structure when exposed to alkaline environment, potentially highlighting the role of pre-curing prior to cement secretion (Liang *et al.*, 2018). A recombinantly expressed version of the 19kDa *B. amphitrite* protein successfully bound to naturally deposited barnacle plaques, further supporting its role in polymerisation (So *et al.*, 2019).

There is evidence to suggest that the precise roles of barnacle cement protein components could vary between species as, in contrast to *M. rosa* discussed above, the 19kDa cement protein of the stalked barnacle *Pollicipes pollicipes*, displays low adsorption to most surfaces (Tilbury *et al.*, 2019). In addition, the charge of the protein differs between species. For example, the *B. amphitrite* 19kDa cement protein is positively charged in seawater, while that of *M. rosa* is negatively charged (Wang *et al.*, 2018). This difference may facilitate improved adhesion in varied ecological niches. Desipite functional differences, some cement proteins appear to be partially conserved between taxa (Jonker *et al.*, 2014). Antibodies raised against *B. amphitrite* 52 and 68kDa cement proteins, reacted with cement proteins in the stalked barnacle *Lepas anatifera*. Moreover, the 100kDa, 20kDa, and 19kDa proteins of the acorn barnacles *B. amphitrite, B. improvisus, M. rosa* possess some homology (~20-65%) with these proteins in *P. pollicipes* (Jonker *et al.*, 2014).

Finally, the 16kDa protein is the only non-novel one, as it shares 47% homology with lysozyme P from *Drosophila melanogaster* (Kamino, 2016). This protein is active against gram positive bacterial membranes, and so is likely a lysozyme itself, and thus

could act to disrupt biofilms from surfaces and protect from microbial degradation of the cement.

In *B. amphitrite,* and potentially other acorn barnacle species that possess analogous cement proteins, the cement is released in two distinct stages, likely linked to the moult cycle (Burden *et al.*, 2012; 2014; Golden *et al.*, 2016). The first phase is released at the edge of the expanding base of the barnacle, displacing water bound to the surface, and as such may contain the 68, 16 and 19kDa proteins. This then forms amyloid fibrils upon the release of the second phase, potentially containing the 100 & 52kDa proteins, which doubles the adhesion strength with no alteration to the thickness of the adhesive layer (Burden et al., 2012; 2014). The 20kDa component meanwhile may remain in contact with the base of the barnacle based on its affinity for calcite (Mori *et al*., 2007). Lysyl oxidase has been hypothesised to have a role in the curing of the cement (So *et al.*, 2017).

When attempting to adhere to more challenging surfaces, however, the cement formation can change quite dramatically. When secreted onto hydrophilic green mussel shells, a natural antifouling surface, the cement becomes thicker and more viscous, which reduces its adhesion strength (Raman *et al.*, 2013). Likewise, on polydimethylsiloxane (PDMS) based fouling-release coatings, the cement layer becomes white and rubbery, as opposed to its usual translucent form, and increases in thickness up to 1mm. (Berglin, and Gatenholm, 2003; Ahmed *et al.*, 2014). This change in composition appears to result from reduced crosslinking and polymerisation, and a higher water content (Wiegemann and Watermann, 2003). Despite changes to the cement the barnacles remain adhered, though are more vulnerable to removal by shear stress (Kavanagh *et al.*, 2005).

Overall, the cement of adult acorn barnacles is a complex mixture of adhesive proteins that displays great adaptability to a range of surfaces, even those designed to prevent adhesion. This proves to be a challenge when designing anti-fouling and fouling-release surfaces to combat barnacle biofouling.

1.3.2. Cyprid Permanent Adhesion

The cyprid permanent adhesive (syn. cyprid cement) is secreted once the cyprid has found a location to settle and metamorphose into a juvenile. The permanent adhesive is predominantly proteinaceous, since it stained positive for protein in histochemical studies and was removed from surfaces by serine proteases (Walker, 1971; Aldred *et al.*, 2008). However, it appears that the nature of the adhesive is not constant, as it only remained vulnerable to degradation by serine proteases for up to 15 hours post settlement (Aldred *et al.*, 2008). Following this period, the adhesive developed a more crystalline structure as it cured. It is thought that the adhesive cures via quinone tanning, due to the cement glands containing phenols (Walker, 1971), a reduction observed in pull-off length of deposited proteins via AFM over time (Phang *et al.*, 2006), and the presence of copper in adhesive deposits, which may be associated with polyphenol oxidase curing mechanisms (Senkbeil *et al.*, 2015). However, the reported curing time varies. The changes observed by Phang *et al.* (2006) began to occur within just 45 minutes, as opposed to the 15 hours previously observed by Walker (1971). In addition, Schmidt *et al.* (2009) documented a high abundance of polar hydroxyl groups, and incorporation of water into the cured adhesive. The water was hypothesised as facilitating curing and adhesion, while the hydroxyl groups were thought to aid in wetting of surfaces with high energy (Schmidt *et al.*, 2009). Recent transcriptomic and proteomic analyses have revealed lysyl oxidase present in the cyprid cement glands (Yan *et al.*, 2020). This enzyme is putatively involved in adult cement curing, and thus may also act to cure the cyprid cement (So *et al.*, 2017; Yan *et al.*, 2020) Carotenoids, common crustacean proteins linked to membrane support and antioxidant activity, were also observed on the edge of the area coated by the permanent adhesive, possibly due to contact made between peripheral cuticular villi or the velum, and the substratum (Schmidt *et al.*, 2009).

The cyprid permanent adhesive is produced and stored within a pair of glands in the main body of the cyprid (Walker, 1971; Gohad *et al.*, 2014). This gland is comprised of two major cell types, termed α and β, which are filled with distinct granule types. The α cells produce and contain a proteinaceous adhesive in small, spherical vesicles, while the β cells produce larger vesicles, of irregular shape, rich in lipids (Walker, 1971; Aldred *et al.*, 2013a; Gohad *et al.*, 2014). In addition, the periphery of the β cell vesicles of *Balanus amphitrite* have recently been shown to contain chitin, a component typically found in crustacean carapaces (Aldred *et al.*, 2020). The adhesive is then

kept temporarily in a collecting duct until required, whereupon it is secreted rapidly via coordinated muscle contraction and valve control (Nott, 1969; Okano *et al.*, 1996). Secretion of the permanent adhesive is comprised of two phases, but forms three distinct layers on the surface, observable by TEM (Walker, 1971). The first phase is released from the β cells, as the lipidaceous components displace water and create a favourable environment for the introduction of the second phase of bulk phosphoproteins, released from the α cells (Aldred *et al.*, 2013a; Gohad *et al.*, 2014). When the permanent adhesive is secreted, the chitin present at the periphery of the β vesicle is deposited between the lipid and protein components and is integral to the continued adhesion of the cyprid (figure 1.4) (Aldred *et al.*, 2020). It may be this chitin that constitutes the third cement layer observed by Walker (1971).

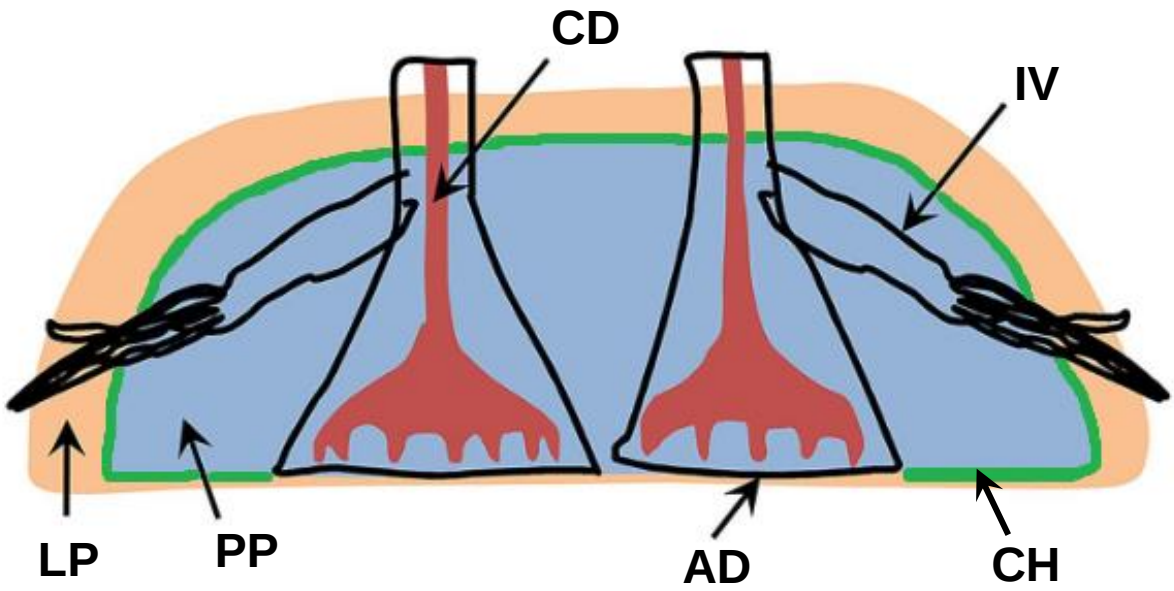

Figure 1.4. Schematic of the cyprid permanent cement plaque during settlement. CD = Cement duct; IV = fourth antennular segment; LP = lipid phase; PP = protein phase; AD = attachment disc; CH = chitin layer. Figure adapted from Liang et al. (2019).

Exposing adhered cyprids to chitinase results in close to 100 percent removal over eight hours, but has no effect on juveniles or adults, indicating either the importance of chitin to the adhesive mechanism decreases over time, or access of the enzyme to the substrate is reduced by subsequent secretions (Aldred *et al.*, 2020). This ‘two-phase’ descriptor of the cyprid permanent adhesive system may not comprise the complete picture, however, as four distinct granule types were described within the

cement gland of *B. improvisus*, suggesting that the system may be more complex, although the lack of corroborating evidence leaves the potential that these granules were an anomaly or misidentified, being at different stages of maturation (Ödling *et al.*, 2006).

Interestingly, there is evidence that the cyprid permanent adhesive is related to the adult cement secreted following metamorphosis, at least in part. Homologues of the 20kDa and 100kDa adult cement proteins (see 1.3.1.) are present in the cyprid cement glands (figure 1.5) (Chen *et al.*, 2011; Gohad *et al.*, 2014; He *et al.*, 2018), despite, prior genetic investigations having determined that genes relating to adult cement production were not expressed in the cyprid stage (Kamino and Shizuri, 1998).

The proteinaceous component of the permanent adhesive is purported to be comprised of small proteins, 20-43kDa, and 66kDa (Al-Aidaroos *et al.*, 2016).

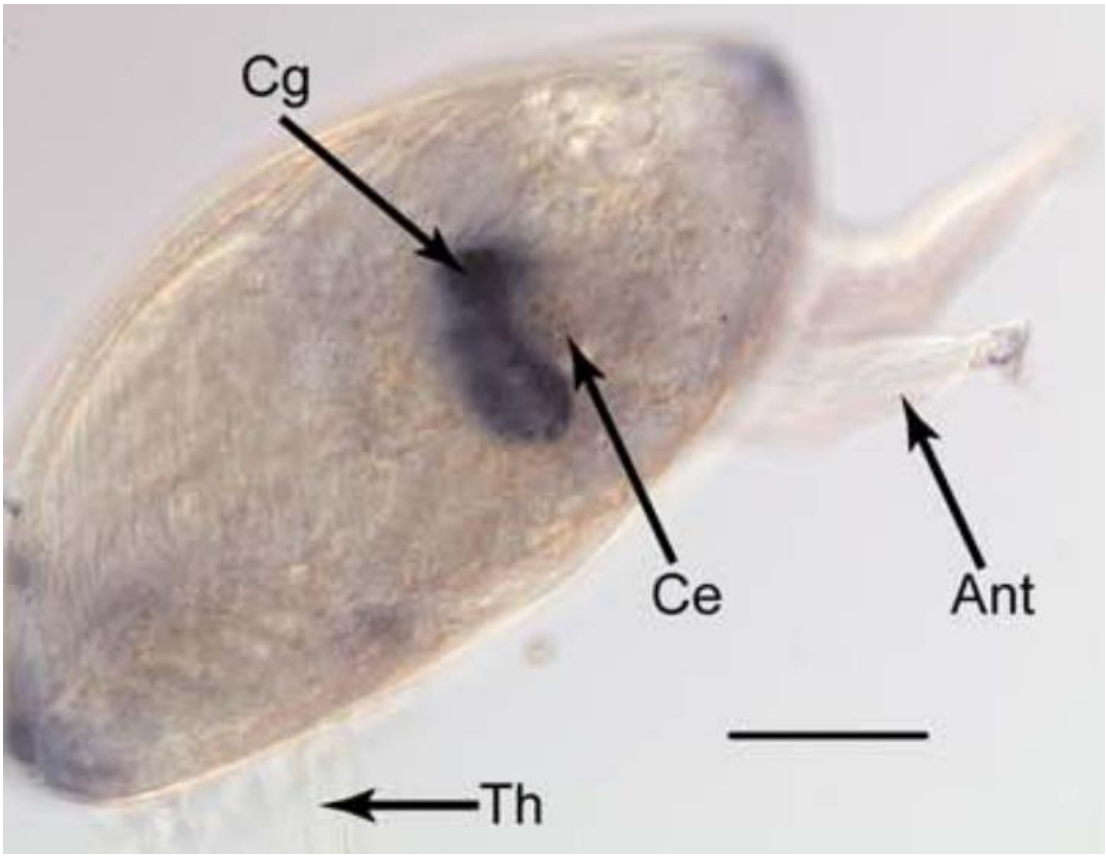

Figure 1.5. Whole mount in-situ hybridisation of a *Balanus amphitrite* cyprid. Lateral view, the purple area in the permanent cement gland indicates the expression of genes homologous to the *Megabalanus rosa* 20kDa adult cement protein. Ant = antennule; Cg = permanent cement gland; Th = thoracopod; Ce = Compound eye Scale bar = 100 µm. Figure adapted from Chen *et al.* (2011).

However, recent analysis of *Megabalanus volcano* cement glands identified four putative cement proteins of much higher molecular weight, 52-130 kDa (Yan *et al.*,

2020). Beyond this, the structure of the adhesive proteins remains unknown. Increased spreading of the adhesive has been observed on hydrophobic, low energy surfaces, although due to the multiple component nature of the adhesive, measuring factors such as contact angle proves difficult (Aldred *et al.*, 2013a). Due to the lack of information, the extent to which inter-specific variation occurs in the cyprid permanent adhesive, and how this relates to surface selection, is unknown.

1.3.3. Cyprid Temporary Adhesion

As previously discussed, during surface exploration a cyprid contacts the substratum with the third antennular segment of its antennules, which provide an adhesive force (Walker and Yule, 1984; Dreanno *et al*., 2006a; Phang *et al.*, 2008; 2010 Aldred e*t al.*, 2013). Cyprids are relatively large larvae, *S. balanoides* can reach over 1mm in length, and thus are subject to drag forces when exploring turbulent and dynamic areas (Eckman *et al.*, 1990). As a result, their adhesion must be highly resistant and resilient.

It was previously thought that the third antennular segment (attachment disc) acted as a suction cup (Saroyan, 1968), however, under closer examination by scanning electron microscopy it appears that this is unlikely to provide the adhesive force (Nott, 1969). The villi close to the circumference of the disc would interfere with the formation of a seal, and the overlapping nature of the cuticle segments make the velum unsuitable to form a continuous seal with the substratum (Nott, 1969).

Now, the prevailing consensus is that cyprids secrete an adhesive material from the base of the third antennular segment, allowing them to temporarily adhere to the benthos as they explore (Walker and Yule, 1984; Dreanno *et al*., 2006a; Phang *et al.*, 2008; Aldred *at al.*, 2013, Di Fino, 2015). This consensus stemmed from the discovery that material ‘footprints’ were deposited on explored surfaces. Investigation of these footprint deposits has indicated that they indeed possess adhesive properties.

1.3.3.1. The Temporary Adhesive

The footprint material left behind by exploring cyprids was originally determined to be proteinaceous by histochemical staining (Walker and Yule, 1984), supported by the later discovery that it is vulnerable to degradation and removal by proteases (Aldred *et al.*, 2008). The size of the deposit depends upon the surface and the species, but usually covers an area equal in size to the attachment disc of the cyprid, and is estimated at between 1-20nm thick (figure 1.6) (Phang *et al.*, 2008; Phang *et al.*, 2010; Di Fino, 2015). The deposit is distributed evenly beneath the disc, except in the centre, where less material is present. It is likely that little or no adhesive is secreted from around the axial sensory organ located in the concave central disc region. Atomic force microscopy (AFM) indicates that the footprint material deposited by exploring cyprids is porous and composed of proteinaceous nanofibrils, either bundled or singular. Singular fibres are approximately 20nm wide. These fibrils typically adopt an orientation parallel to the circumference of the footprint, potentially stemming from the detachment of the disc from the surface (figure 1.6d) (Phang *et al.*, 2010). A similar style of fibril construction can be observed in diatom adhesive mucilage (Higgins *et al.*, 2002).

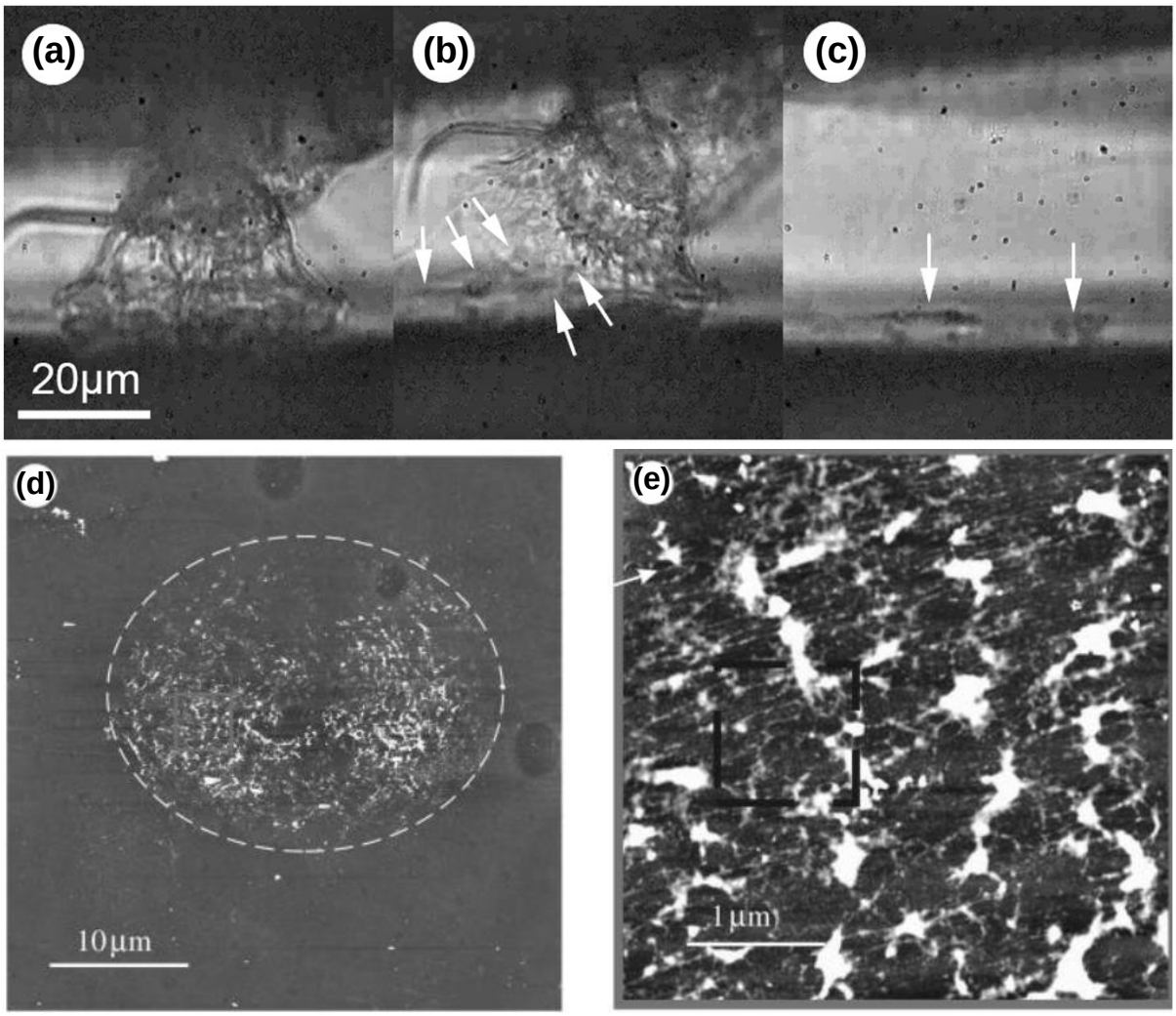

Figure 1.6. (a-c) = The deposition process of temporary adhesive footprints by *Semibalanus balanoides* cyprids. **(a)** = The attachment disc is in contact with the surface to which the cyprid is adhering, attached by the temporary adhesive protein; **(b)** = The cyprid detaches its disc from the substratum through mechanical force. The white arrows highlight the stretching and breaking of the elastic temporary adhesive proteins. **(c)** = The cyprid has detached from the surface and moved on, leaving behind a footprint deposit of its temporary adhesive material. **(d-e)** = Atomic force microscopy micrograph of a Balanus amphitrite temporary adhesive footprint deposit. **(d)** = The footprint deposit is indicated by the white fibres. It is circular and ~30 µm in diameter, correlating with the shape and size of the attachment disc. The central area has little to no deposited material, as this is where the axial sense organ would contact the substratum. **(e)** = A closer view of the fibrous structure of the deposited proteins. Individual nanofibrils can be observed in the dashed box. Figures adapted from Phang *et al.* (2010) and Aldred *et al. (*2013b).

When subjected to a pulling force in AFM force mode, the adhesive of *Balanus amphitrite* displays a 'saw-tooth' pattern on its force-extension curve, indicating the presence of sacrificial bonds as the bundles of nanofibrils are stretched (Phang *et al.*, 2010). When these sacrificial bonds break, requiring between 220 and 580pN of force (20nm tip diameter), it results in a sudden loss of tension as the energy is dissipated and the protein unfolds. The adhesive is, however, capable of reforming some of these

sacrificial bonds within 500ms when not under tension, although longer relaxation times of 5-10 seconds are required to regain its full strength (Phang *et al.*, 2010). This resilience to change would prove highly beneficial for a cyprid exploring in highly dynamic environment, such as the intertidal zone where *B. amphitrite* often occurs, as it would not be easily removed. However, if the fibrils are extended too far, >700nm, the force-extension behaviour changes, and the fibrils begin to exhibit more elastic properties, until complete breakage at 10 µm extension (Phang *et al.*, 2010). Cyprids on surfaces can rapidly increase their adhesion strength, with the force required to detach them increasing by up to three orders of magnitude over the course of 15 minutes, although whether the cyprid is beginning settlement and this strength stems from its permanent adhesive, or if the cyprid is at rest and using its temporary adhesive, is unknown (Eckman *et al.*, 1990). The age of a cyprid also alters the tenacity of its temporary adhesion. Shiomoto *et al.* (2019) documented that cyprid temporary adhesion is over 20 times stronger in 21-day-old *Megabalanus rosa* cyprids than 3-day-old cyprids, correlating with the observations of Yule and Crisp (1983) that the later *S. balanoides* cyprids were collected in the fouling season, and thus more likely to be older cyprids, the stronger temporary adhesion they exhibited. It is worth noting, however, that the experiments of Shiomoto *et al.* (2019) were performed on hydrophilic surfaces, therefore it is unclear if the change is due to a natural phenomenon, or a specific change in the adhesive chemistry increasing affinity for those surface chemistries over time. In addition to age and attachment time, cyprids have also displayed the ability to increase their temporary adhesion strength in response to surfaces coated with conspecific protein extracts (Yule and Crisp, 1983). Whether this is a response to conspecific cues stimulating increased temporary adhesive secretion, or if the temporary adhesive has greater affinity for compounds within these extracts in unknown.

The relationships between temporary adhesion strength, settlement rate and surface chemistry are complex, variable between species and not yet fully understood. The temporary adhesive has displayed variation in the amount deposited and adhesion strength to different surface chemistries depending on species.

Amine-terminated glass, a hydrophilic surface, collected a three-fold greater abundance of *S. balanoides* footprint materials in comparison to methyl-terminated glass, a hydrophobic surface (Phang *et al.*, 2008). Whether this is due to an increased

affinity of the temporary adhesive proteins to the hydrophilic surface, resulting in less removal and therefore greater deposits, and/or if the detection of a more favourable surface by receptors on the cyprid stimulates increased secretion of the temporary adhesive, is unknown. There is some uncertainty on the issue, however, as Phang *et al.* (2009) later observed a greater affinity of the adhesive proteins for hydrophobic CH_3- AFM tips than hydrophilic Si3N4- tips, although the adhesive remained strongly attached to the hydrophilic amine-terminated surfaces. Furthermore, the observation of adhesive peeling on hydrophobic methyl-terminated glass indicates that the bond between the adhesive and the surface was weaker than that between the adhesive and the attachment disc, contrary to observations on the hydrophilic surface. This suggests that while greater deposition is related to surface wettability, other factors may play a role in adhesive strength (Phang *et al.*, 2008).

The temporary adhesive of *B. amphitrite* however, has been reported to behave differently. The adhesive of this species exhibited a three-fold greater adhesive strength to hydrophobic surfaces versus hydrophilic, in addition to increased spreading of the adhesive over the surface (Guo *et al.*, 2014; Di Fino, 2015). The high affinity for hydrophobic surfaces displayed in these studies may indicate that the adhesive is hydrophobic itself, which would support its putative function to displace water from the adhesive disc (Guo *et al.*, 2014; Di Fino, 2015). However, reports vary in terms of the volume of adhesive deposited. Di Fino (2015) recorded increased volumes of adhesive material deposited on hydrophobic, negatively charged surfaces, over hydrophilic surfaces with a positive charge, while Guo *et al.* (2014) reported no differences. The apparent variation observed between these studies may be due to the surfaces used, for while their wettability was the factor being tested and the tested surfaces exhibited comparable contact angles, Guo *et al.* (2014) did not report the surface energies of the substrates being tested (Di Fino, 2015). Surface energy has been indicated to play an important role in settlement of cyprids, to the point where it has been hypothesised that surface energy and charge are more important to the surface selection process than wettability (Maki *et al.*, 1994; Aldred *et al.*, 2010; Petrone *et al.*, 2011; Di Fino *et al.*, 2014; Gatley-Montross *et al.*, 2017; Aldred *et al.*, 2019). The affinity of the *B. amphitrite* temporary adhesive to hydrophobic surfaces is strange given that *B. amphitrite* has been reported to either settle preferentially on hydrophilic surfaces (O'Connor & Richardson 1994; Finlay *et al.*, 2010) or display no preference for

settlement based on surface wettability (Maki *et al.*, 1994; Guo *et al.*, 2014; Gatley-Montross *et al.*, 2017). However, Petrone *et al.* (2011) and Di Fino *et al.* (2014) both observed an increase in settlement of *B. amphitrite* cyprids on hydrophobic, low energy surfaces in comparison to those with high energy. A correlation between settlement and surface charge was observed, with negatively charged self-assembled monolayers (SAMs) stimulating greater settlement than those with no charge, and positively charged SAMs inducing the least settlement (Petrone *et al.*, 2011; Di Fino *et al.*, 2014). This indicates that cyprids may detect and utilise information on surface charge when selecting settlement sites, a phenomenon that may have evolved due to the abundance of negatively charged surfaces that occur in the marine environment.

Finally, the temporary adhesion strength of *B. improvisus* displays a similar trend to *B. amphitrite* but tends to deposit a lower volume of material (Di Fino 2015). Again, hydrophobic interactions were the strongest, while positively charged surfaces were weakest, and the high affinity for hydrophobic surfaces resulted in a thin footprint deposit, but with a large area, as the substance spread over the surface (Di Fino 2015). Unlike *B. amphitrite*, however, this affinity for low energy, hydrophobic surfaces correlates with the reported settlement behaviours exhibited by *B. improvisus*. Preferential settlement on hydrophobic surfaces has repeatedly and significantly been reported for this species, in addition to reduced settlement and exploration on hydrophilic surfaces with higher surface energies (O'Connor and Richardson 1994; Dahlström *et al.*, 2004; Di Fino *et al.*, 2014: Gatley-Montross *et al.*, 2017: Abramova, 2019). The question of whether the increased settlement in response to surface chemistry is a 'passive' decision based on affinity of the temporary adhesive, or a more 'active' decision whereby the cyprid can sense the surface properties, remains. Recent evidence from Abramova (2019) suggests the latter, as *B. improvisus* larvae exhibited differential gene expression depending on the surface chemistry of the substratum being explored. Between five and ten times more genes are upregulated during the close search and early settlement behaviours on hydrophobic surfaces, as opposed to hydrophilic (Abramova, 2019). Despite this, wettability is again, unlikely to be the sole factor in the determination of a suitable substrate by a cyprid, as Aldred *et al.* (2019) documented variability in settlement rates of *B. improvisus* cyprids on surfaces with similar total surface energies, but which varied in their ratios of dispersive to polar interactions. Despite all the works highlighted here, the inter-specific variations in

temporary adhesive strength and settlement preferences in response to surface chemistries have yet to be comprehensively understood, as have the impacts of even minor differences in surface properties.

The work published on interactions between the temporary adhesive material and various surface chemistries has facilitated the beginnings of characterisation of this substance. As previously discussed (1.2.4.), the cyprid temporary adhesive is either partially or completely comprised of the SIPC, or an analogue (Dreanno *et al.*, 2006a). The potential involvement of the SIPC in the temporary adhesion process has recently been highlighted through demonstration of its strong adsorption to a range of surface chemistries (Petrone *et al.*, 2015). A structurally similar protein, an α_2-macroglobulin (A2M), adsorbed only to positively charged surfaces via electrostatic interactions, while the SIPC behaved more akin to fibrinogen, a 'sticky' protein, adsorbing to a variety of surfaces, be they hydrophobic or hydrophilic. Adsorption of the SIPC increased on surfaces which possessed a charge, either positive or negative, while the adsorption rates on all surfaces indicated irreversible attachment (Petrone *et al.*, 2015). This could be why the cyprid must mechanically remove itself during 'walking' (Aldred *et al.*, 2013b). However, the uniformity of adsorption observed did not tally with the difference in affinities of the temporary adhesive to surfaces of different charge and wettability observed by Phang *et al.* (2008; 2009) and Guo *et al.* (2014), potentially indicating that the SIPC is not the sole component of the temporary adhesive. Furthermore, Aldred *et al.* (2010) also observed differences in surface affinity between purified SIPC and temporary adhesive footprints directly from cyprids, supporting this hypothesis. This evidence indicates the SIPC is unlikely to comprise the entirety of the cyprid temporary adhesive, leaving the question of the putative remaining components unanswered.

1.3.3.2. Anatomy and Ultrastructure

While the cyprid temporary adhesive is directly responsible for adhesion, this adhesive must be synthesised and delivered to the surface of the attachment disc (Nott and Foster, 1969; Walker and Yule, 1984; Høeg, 1987; Yap *et al.*, 2017). On the disc surface, in the spaces amongst the villi, are secretory pores, from which the temporary adhesive is secreted during exploration (Walker and Yule, 1984).

Presently, while the temporary adhesive (1.3.3.1) is widely believed to act as the primary form of attachment for the cyprid during exploration, the function of the cuticular villi is not fully understood. It is posited that they may increase the surface area of the disc, allowing the retention of more adhesive (Nott, 1969). Alternatively, that they protrude through the secreted adhesive, displacing the surrounding water, and splitting contact with the substratum, distributing stress and increasing adhesion strength in a manner akin to a gecko's foot pad (Phang *et al.*, 2008; Kamperman *et al.*, 2010). The adhesion strength during surface exploration is mediated behaviourally, with continual movement of the disc resulting in weak attachment, or depression and spreading to attach more strongly (Aldred *et al.*, 2013b). Meanwhile, the muscles in the third segment are oriented in a circular pattern, allowing the cyprid to deform the disc on the edge, which assists it when attempting to detach from a surface (Nott and Foster 1969; Aldred *et al.*, 2013b).

The temporary adhesive is transported from the glands to the secretory pores via a system of ducts (Nott and Foster, 1969; Høeg, 1987; Yap *et al.*, 2017). In the third antennular segment, these ducts become oriented around the disc periphery and take on a unique structure, with two distinct sections (Nott and Foster, 1969; Yap *et al.*, 2017). The outer section is comprised of a protective sheath cell and supporting rod-like structures, while the inner section contained the temporary adhesive in homogenous vesicles, amongst a network of longitudinally oriented microtubules (Nott and Foster, 1969; Yap *et al.*, 2017). While the duct system in the attachment disc has been relatively well documented, the location of the temporary adhesive glands is less clear. Originally, the distal region of the second antennular segment of *S. balanoides* was hypothesised to contain unicellular temporary adhesive glands (Nott and Foster, 1969; Høeg, 1987) (figure 1.7a). However, a recent study on the cyprid of the stalked barnacle species *Octolasmis angulata*, described a pair of multicellular temporary adhesive glands in the anterior mantle of the cyprid, near the compound eye and permanent cement gland, and that the 'glands' described in the antennules of *S. balanoides* are merely collecting ducts (figure 1.7b). In this description of the *O. angulata* adhesive system, temporary adhesive proteins are synthesised within these glands, then packaged into small vesicles, which aggregate and coalesce to form larger vesicles (Yap *et al.*, 2017). These vesicles are transported to the third

antennular segment via branching ducts, which are extensions of the gland cells themselves, and subsequently delivered to the disc surface (Yap *et al.*, 2017).

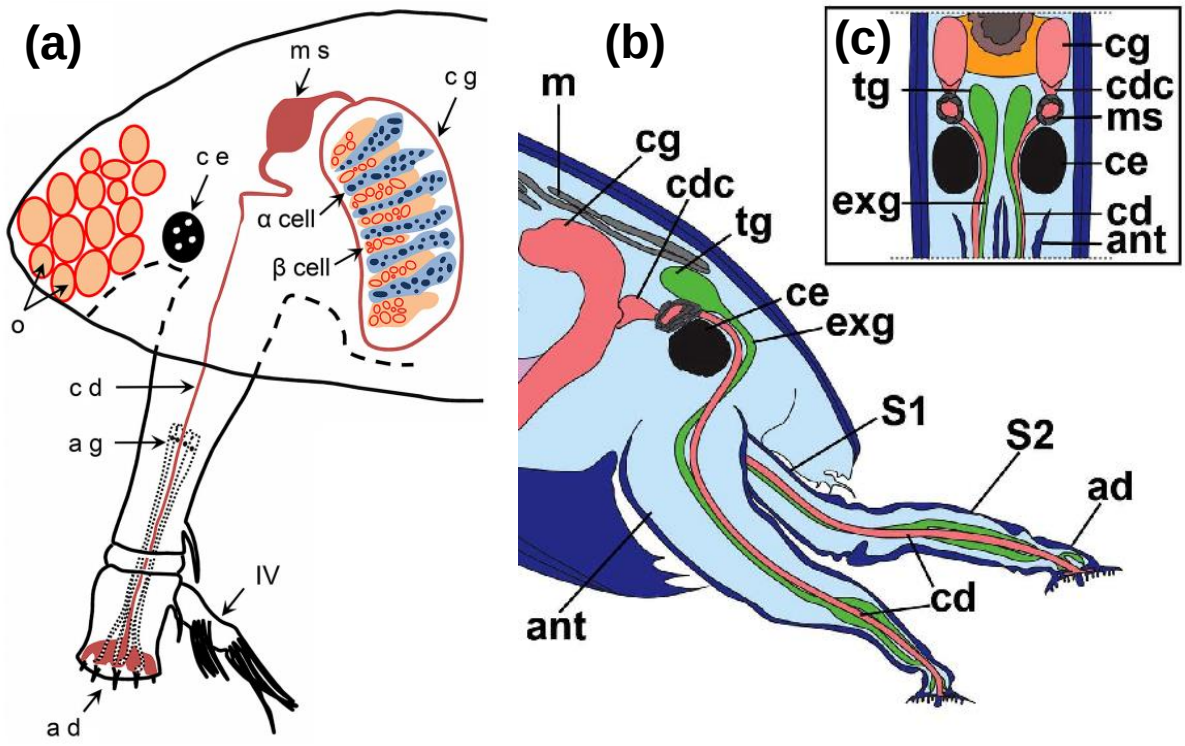

Figure 1.7. Two proposed models of the barnacle cyprid temporary and permanent adhesive systems. **(a)** = Lateral cross section of the cyprid anterior, depicting the originally hypothesised lcoation of the temporary adhesive glands in the second antennular segment (Nott and Foster, 1969; Høeg, 1987). Figure adapted from Walker (1981). **(b,c)** = Lateral and dorsal, respectively, cross sections of the cyprid anterior, depicting the newly observed location of the temporary adhesive glands in *Octolasmis angulata*, behind the eye, anterior to the permanent cement gland. Figure adapted from Yap *et al.* (2017). ad = attachment disc; ag = temporary adhesive gland; cd = permanent cement duct; ce = compound eye; cg = permanent cement gland; ms = muscular sac; o = oil and lipid storage; S1 = first antennular segment; S2 = second antennular segment; ant = antennule; tg = temporary adhesive gland; exg = temporary adhesive gland extension; ce = compound eye; cdc = collecting duct cell; ms = muscular sac; m = muscle.

Despite the taxonomic distance between the two species in which these temporary adhesive systems were described, the possibility remains that the isolated TEM images collected by Nott and Foster (1969) were not comprehensive enough to capture the full temporary adhesive system in *S. balanoides*, and that the 'glands' were misidentified, as suggested by Yap *et al.* (2017). Additional research into the temporary adhesive systems of acorn barnacles is needed to determine whether this is the case.

1.4. Present Study

1.4.1. Motivations

The focus of this study was twofold. The primary aim was to characterise the temporary adhesive, as there is evidence within the currently available literature that, whilst containing the SIPC, it is not composed entirely of it (1.3.3.1). Historically, the major obstacle to characterisation of the temporary adhesive material has been the low quantities available for study. Deposits on surfaces are only nanometres thick (Phang *et al.*, 2008; Phang *et al.*, 2010; Di Fino, 2015), and no methodology for effective dissolution and retrieval has been published, unlike for the adult cement (Schultzhaus *et al.*, 2019). However, the sensitivity of modern 'omics technologies allow the characterisation of materials even at these abundances, making it feasible to now attempt to elucidate the nature of the temporary adhesive material.

Secondly, the recent evidence suggesting a novel location of the temporary adhesive glands in barnacle cypris larvae inspired the aim to clarify this in acorn barnacles. Previous explorations of the temporary adhesive system have been hampered by the time-consuming and patchy nature of TEM imaging, in addition to the search for glands being effectively blind. Serial block face scanning electron microscopy (SBF-SEM) systems allow for rapid and comprehensive image capture of entire organisms, with subsequent three-dimensional reconstruction of the internal structures, making documenting novel biological systems substantially easier.

1.4.2. Aims and Objectives

The overall aim of the project was to improve the understanding of temporary adhesion in prevalently fouling acorn barnacle species. *B. amphitrite* was chosen as the primary target due to its nature as a prolific fouling barnacle species and tendency to gregarious settlement. Furthermore, it has been widely studied and is the species from which the SIPC was first characterised. Additionally, any information gathered on cyprid adhesion will be widely applicable to future literature and antifouling technologies. Where available and relevant, other acorn barnacles will also be included in the work. These include *Megabalanus coccopoma*, *and B. improvisus*. *M.*

coccopoma is an invasive, fouling barnacle species (Crickenberger and Moran 2013). Thus, the data obtained will again be beneficial to future measures developed to combat its biofouling tendencies, as well as providing a close comparison to *B. amphitrite*. *B. improvisus*, on the other hand, has valuable omics resources available for the interrogation of differential expression patterns (Abramova *et al.*, 2019b).

The primary objectives of this study were as follows: determine the location and nature of the temporary adhesive gland(s); characterise the acorn barnacle cyprid temporary adhesive protein(s); determine the spatial and ontogenetic protein expression patterns of the temporary adhesive protein(s); and investigate whether the SIPC is a component of the isolated temporary adhesive.

To characterise the temporary adhesive, a methodology to collect sufficient material for analysis had to be devised. Preliminary analysis was performed using SDS-PAGE and western blotting, and following this, characterisation was attempted using a combination of mass spectrometry and transcriptomics. Candidate proteins were screened for spatial and temporal expression patterns by in qPCR, RNA-seq differential expression analysis, and in-situ hybridisation. To correlate with the spatial expression data, a morphological study of the temporary adhesive system was undertaken using serial block face scanning electron microscopy, to construct three dimensional models of the system and locate the glands.

Chapter 2. Anatomy and Ultrastructure of the Cyprid Temporary Adhesive System in Two Species of Acorn Barnacle

*NB. This chapter was published in the Journal of Marine Science and Engineering Special Issue: "Larval Settlement on Marine Surfaces: The Role of Physico-Chemical Interactions" on November 25th 2020. The content has not been changed other than formatting to meet Newcastle University guidelines.

2.1. Abstract

Acorn barnacles are sessile as adults and select their settlement site as a cypris larva. Cyprids are well adapted to exploring surfaces in dynamic environments, using a temporary adhesive secreted from the antennules to adhere during this process. The temporary adhesive and the secretory structures are poorly characterized. This study used serial block-face scanning electron microscopy and three-dimensional modelling to elucidate the anatomy related to temporary adhesion. The temporary adhesive glands of two acorn barnacle species, *Balanus amphitrite* and *Megabalanus coccopoma,* were located in the proximal region of the first antennular segment, contrary to previous descriptions that placed them in the more distal second segment. The temporary adhesive systems of these acorn barnacles are therefore similar to that described for the stalked barnacle, *Octolasmis angulata*, although not identical. Knowledge of the true location of the temporary adhesive glands will underpin future studies of the production, composition and secretion of the adhesive.

2.2. Introduction

Barnacle cypris larvae use a proteinaceous adhesive secreted from their paired antennules to temporarily attach to the substratum, allowing them to effectively explore dynamic environments (Crisp, 1976; Walker and Yule, 1984). This adhesive is secreted via pores on the third antennular segment and contains the settlement-inducing protein complex (SIPC), or an analogue (Dreanno *et al.*, 2006a). Temporarily adhered cyprids detach via mechanical forces, twisting their antennule and leaving

behind a “footprint” of adhesive material (Walker and Yule, 1984, 4. Phang *et al.*, 2008; 2010; Aldred *et al.*, 2013; Guo *et al.*, 2014). Neither the temporary adhesive nor the structures related to its synthesis and secretion have been fully characterised in acorn barnacles.

The temporary adhesive system is distinct from the permanent adhesive used by the cyprid at the point of fixation. The morphology of the cyprid permanent adhesive system has been well characterised (Walker 1971; Okano *et al.*, 1996; Ödling *et al.*, 2006), although only basic compositional data have been obtained. The permanent adhesive is produced and stored in a pair of glands situated behind the compound eyes, with each gland serving a single antennule. When secreted, the cement is transported to the attachment disc by a single duct, which radiates at the surface to numerous pores, spreading it over a wider area.

Details regarding the composition and morphology of the temporary adhesive system are equally scant. The first description of the temporary adhesive system and its associated structures was provided by Nott and Foster (1969) for *Semibalanus balanoides*; a boreo-arctic, intertidal, acorn barnacle (Cirripedia, Balanomorpha). They noted that the distal region of the second antennular segment contained numerous unicellular glands, arranged around the circumference of the appendage, and postulated that these may be responsible for producing the temporary adhesive (Nott and Foster, 1969).

These putative glands extended into ducts that fed into pores on the surface of the third antennular segment (the attachment disc, figure 2.1). Supporting rod structures and a sheath cell encapsulated the ducts in places, while the interior of the gland contained the adhesive material packed within vesicles, and numerous microtubules oriented longitudinally (figure 2.1). However, these putative glands were only 1–2 µm in diameter and did not appear to contain any of the cellular structures related to protein synthesis or vesicular packaging.

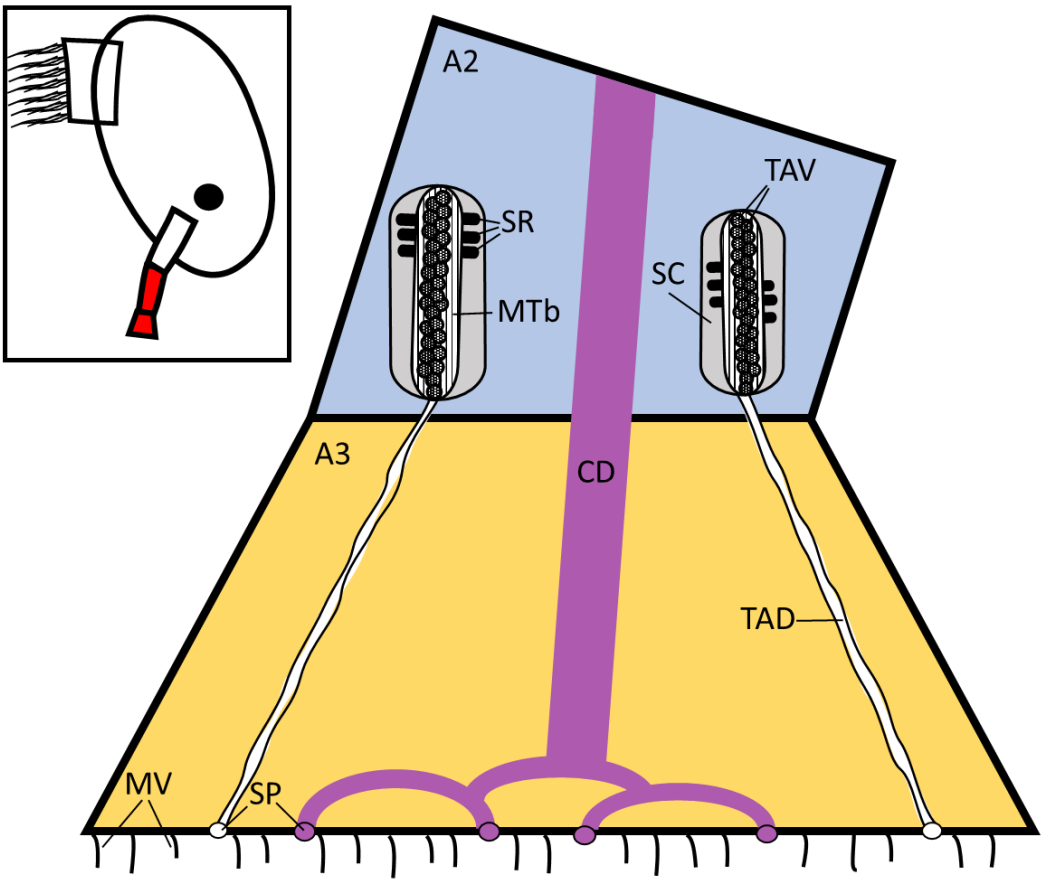

Figure 2.1. Schematic diagram of the temporary adhesive system located in the distal second antennular segment as proposed by Nott and Foster (1969) Not to scale. The region detailed in the schematic is highlighted in red on the inset. A2 = second antennular segment; A3 = third antennular segment (attachment disc); CD = cement duct; TAV = temporary adhesive vesicle; TAD = temporary adhesive duct; SR = supporting rod; MTb = microtubules; SP = secretory pores; SC = sheath cell; MV = microvilli.

A more recent study on the epibiotic stalked barnacle *Octolasmis angulata* (Yap *et al.*, 2017) provided evidence of different anatomy. While many aspects of the descriptions of the two species were similar, a major difference was that the temporary adhesive glands of *O. angulata* were located in the anterior mantle of the cyprid behind the compound eyes, rather than in the antennules. The glands (~20 × 25 µm) comprised large, multicellular secretory cells, which contained vesicles. Ducts from the glands extended down the length of the antennules, through which the putative adhesive-containing vesicles were transported to the surface of each attachment disc (Yap *et al.*, 2017).

As proposed by Yap et al. (2017) it is conceivable that the “glands” described by Nott and Foster (1969) for *S. balanoides* corresponded to the unicellular gland extensions observed in the distal second and third antennular segments of *O. angulata*. There is,

therefore, the possibility that the anatomies of the adhesive systems of the two species are comparable. Certainty over the location of the adhesive glands in acorn barnacles is essential if molecular (e.g., in situ hybridisation) and immunohistochemical techniques are to be successfully applied in studies of adhesive composition.

To address this question, the present study used serial block face-scanning electron microscopy (SBF-SEM) to obtain a comprehensive series of images of the antennule, and to track the temporary adhesive system on its route from the disc surface back to the glands. In addition, the image series allowed for three-dimensional reconstruction and modelling of the cyprid anatomy in the Microscopy Image Browser (MIB) (Belevich *et al.*, 2016). Using these techniques, this study explored the temporary adhesive system of two acorn barnacle species, *Balanus amphitrite* (= *Amphibalanus amphitrite*) and *Megabalanus coccopoma*, in order to provide a basis for future investigations into the composition and secretion of the adhesive material.

2.3. Materials and Methods

2.3.1. Organism Acquisition

The cypris larvae of two species, *Balanus amphitrite* and *Megabalanus coccopoma,* were prepared for SBF-SEM. Larval production required the culturing of adult populations.

Adult broodstock of *B. amphitrite* was obtained from Duke University Marine Laboratory (DUML), Beaufort, North Carolina (USA). Adults were maintained in ~33 ppt artificial seawater (ASW, Tropic Marin) at 28^{o}C with aeration. Barnacles were fed daily with freshly hatched *Artemia* sp. (Varicon Aqua Solutions Ltd.) nauplii supplemented with the diatoms *Tetraselmis suecica* and *Isochrysis galbana* algae at weekends. The water was also changed, and the barnacles cleaned daily.

Hatching and release of *B. amphitrite* nauplii were stimulated by removing the adults from water overnight and reintroducing water the following morning. They were kept in the dark, with a single source of illumination to attract the released nauplii. The nauplii were periodically collected by pipette and pooled in beakers containing *T. suecica*. When their number was sufficient, the nauplii were added to aerated buckets

of artificial seawater at a density of no greater than 1000 larvae per litre and cultured at 28ºC on a 16 h:8 h L:D cycle. The nauplii were fed 50 mL per litre of culture of *T. suecica* (~1.3 × 10^6 cells mL^{-1}) and *I. galbana* (5 x 10^6 cells mL^{-1}) in a 3:1 ratio initially and after three days. The nauplii developed to the cyprid stage in five to six days under these conditions. Cyprids were collected from cultures by filtration with a 250 µm mesh, then transferred to dishes of ASW for storage at 4ºC until required.

Adult broodstock of *M. coccopoma* was also acquired from DUML and maintained as described for *B. amphitrite.* For the collection of larvae, buckets containing the adult *M. coccopoma* were checked each morning for the presence of nauplii. Nauplii were collected and cultured in the same manner as *B. amphitrite*. The nauplii developed to the cyprid stage in seven to eight days under these conditions. The larvae were filtered from the cultures and returned to clean buckets with fresh ASW and algal feed after four or five days. Cyprids were extracted from cultures by filtration with a 250 µm mesh. Cyprids retained on the mesh were transferred to dishes containing ASW and stored at 4ºC until required.

2.3.2. Sample Preparation

Cyprids of each species, (*B. amphitrite*, n = 6; *M. coccopoma*, n = 2) were fixed overnight in 2% glutaraldehyde (Agar Scientific) in 0.1 M sodium cacodylate buffer. Once fixed, the samples were processed using a heavy metal staining protocol adapted from Deerinck et al. (2010). Samples were incubated in a series of heavy metal solutions, rinsing three times for five minutes each in distilled water between steps: 3% potassium ferrocyanide in 2% osmium tetroxide for one hr, 10% thiocarbohydrazide for 20 min, 2% osmium tetroxide for 30 min, 1% uranyl acetate overnight at 4ºC, and finally lead aspartate solution (0.02 M lead nitrate in 0.03 M in aspartic acid, pH 5.5) for 30 minutes at 60ºC. The samples were then dehydrated through a graded series of acetone to 100% and then impregnated with increasing concentrations of Taab 812 hard resin, with three changes of 100% resin. The samples were embedded in 100% resin and left to polymerise at 60ºC for a minimum of 36 h.

The resin blocks were trimmed to approximately 0.75 mm by 0.5 mm and glued onto an aluminium pin. To reduce sample charging within the SEM, the block was painted

with silver glue and sputter-coated with a 5 nm layer of gold using a Polaron SEM coating unit.

2.3.3 Serial Block Face-Scanning Electron Microscopy

The pin was placed into a Zeiss Sigma SEM incorporating the Gatan 3view system with DMGMS3 software, which allows sectioning of the block in situ and the collection of a series of images in the z-direction. Multiple regions of interest were imaged at variable magnification, pixel scan, section thickness and pixel resolution depending on the species (table 2.1).

In the resulting z-stacks, the areas of interest were identified and segmented manually using Microscopy Image Browser (MIB, University of Helsinki) (Belevich *et al.*, 2016). The segmentations were imported into Amira (FEI) for the construction of the 3-D models. The *B. amphitrite* antennule and *M. coccopoma* third antennular segment overlay models used 3090 and 114 sections, respectively.

Table 2.1. Details on the parameters selected for image capture using the Gatan 3view system. 'Series' refers to the z-stack of images collected and compiled for three-dimensional model reconstruction, while 'Stills' are the images collected for two-dimensional presentation.

Species	Magnification	Pixel Time	Section Thickness	Pixel Resolution
Balanus amphitrite	Series: 1290–1880× Stills: 898–4000× as required	Series: 20 µs Stills: 20 µs	Series: 100 nm Stills: 100 nm	Series: 20 nm, 2000 × 2000–3500 × 3500 Stills: 10 nm 4000 × 4000
Megabalanus coccopoma	Series: 646× Stills: 157–6700x as required	Series: 20 µs Stills: 20 µs	Series: 100 nm Stills: 100 nm	Series: 25 nm, 3000 × 3000 Stills: 5.6 nm–478.5 nm, 2000 × 2000

2.4. Results

2.4.1. Balanus amphitrite

Cyprids of *B. amphitrite* were serially sectioned in the transverse plane. This orientation allowed for the best opportunity to identify the temporary adhesive ducts and track them through the antennule from the gland to the disc. However, the orientation of mounting and curvature of the antennules resulted in some sections being taken at an oblique angle. The temporary adhesive gland (one of a pair) was located in the proximal region of the first antennular segment and can be observed in figure 2.2a,b.

The gland was formed of a cluster of 10–15 cells. The gland and component cells were roughly spherocylindrical in shape. The gland was ~40 µm, by 10 µm overall, while individual cells were 8–12 µm by 4–5 µm. Therefore only a few cells sat in parallel. A summary of the dimensions of key structures is presented in table 2.2.

Table 2.2. Summary of the dimensions of the cyprid species imaged, and the key structures of their temporary adhesive systems (± standard deviation). TAV = temporary adhesive vesicle; TAD = temporary adhesive duct; TAG = temporary adhesive gland; A1 = first antennular segment; A2 = second antennular segment; A3 = third antennular segment.

Species	TAV Diameter	TAD Diameter	TAG Cells	TAG	Cyprid Length	A1 Length	A2 Length	A3 Diameter
Balanus amphitrite	~250 nm (±89)	~0.5 µm (±0.11)	~4.5 × 4.5 × 10 µm	~10 × 10 × 40 µm	~400 µm	~90 µm	~80 µm	~20 µm
Megabalanus coccopoma	~400 nm (±104)	~0.8 µm (±0.26)	~5 × 5 × 25 µm	~25 × 25 × 50 µm	~500 µm	~150 µm	~140 µm	~35 µm

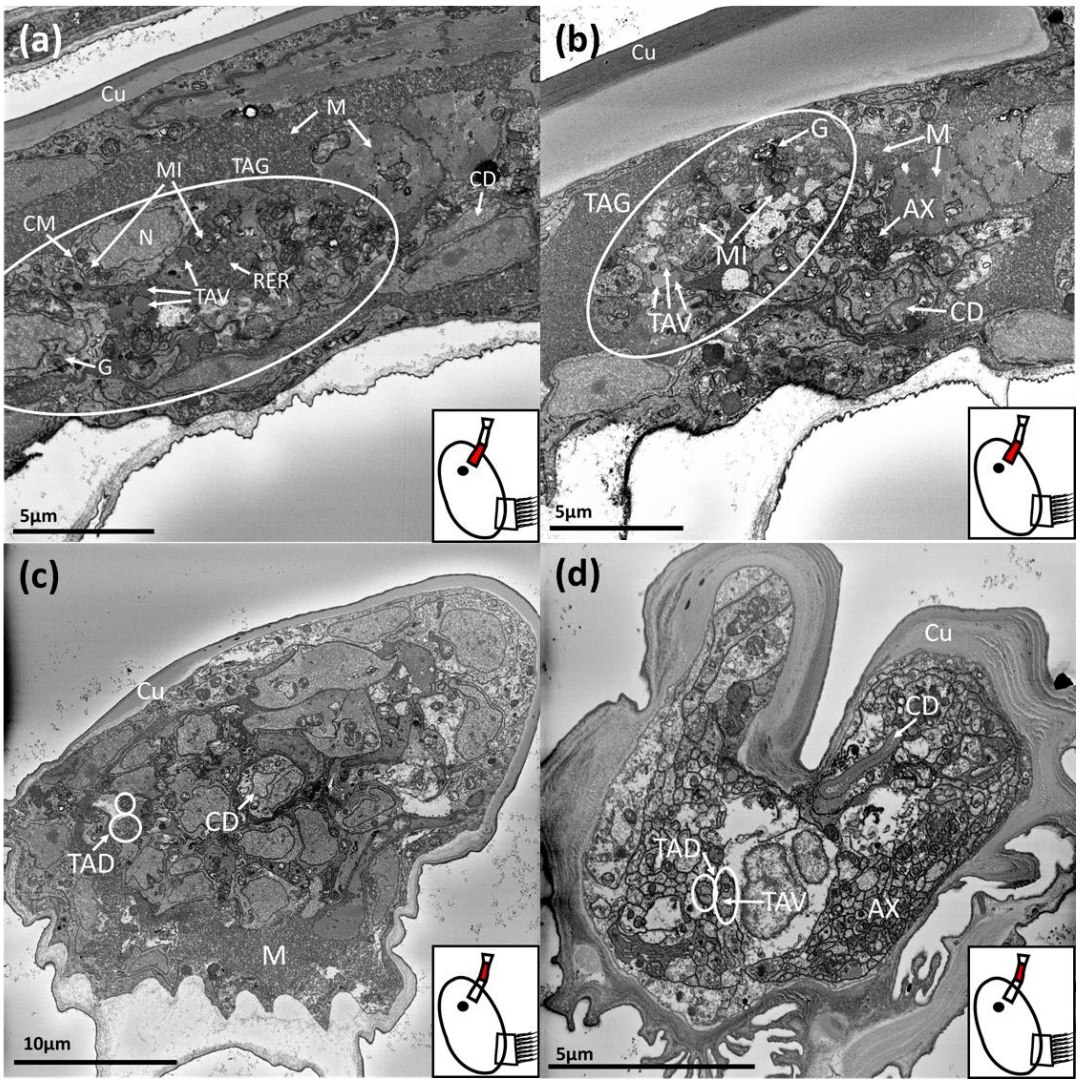

Figure 2.2. SBF-SEM images of a *Balanus amphitrite* cyprid temporary adhesive gland and ducts. The region where the image was captured is highlighted in red on the schematic inset: **(a,b)** = proximal first antennular segment, **(c)** = proximal second antennular segment, **(d)** = distal second antennular segment. TAG = temporary adhesive gland; TAV = temporary adhesive vesicle; TAD = temporary adhesive duct; N = nucleus; MI = mitochondria; G = Golgi body; AX = axons; CM = cell membrane; RER = rough endoplasmic reticulum; M = muscle; CD = cement duct; Cu = cuticle.

The components for protein production and packaging were present in the gland cells (figure 2.2a,b). Rough endoplasmic reticulum and Golgi bodies were clearly visible, along with mitochondria. In a number of these cells, newly formed vesicles (50–200 nm) could be observed prior to their transportation down the antennule (figure 2.2a,b). While the contents of the vesicles were homogenous in appearance, their size was more variable compared to those observed distally in the first and second antennular segments (figure 2.2c,d). Much of the proximal first antennular segment was filled with muscle tissue, in various orientations, and the temporary adhesive gland was surrounded by muscle. The cement duct was also evident in this region and was

distinct from the temporary adhesive gland as it proceeded proximally into the cephalon where the cement gland was located (figure 2.2a,b). Finally, the bundled axons comprising the antennular nerve were observed, which would eventually connect with the antennular soma cluster and brain if followed proximally (figure 2.2b).

Proceeding distally down the first antennular segment, the temporary adhesive gland cells transitioned into narrow ducts. The morphology of the temporary adhesive ducts remained relatively constant through the first and second antennular segments (figure 2.2c,d). The temporary adhesive ducts did occasionally vary in width, however, depending on the number of vesicles contained within. For the individual illustrated, the ducts contained few vesicles for much of their length and remained narrow as a result (figure 2.2c,d). The cement duct remained similar in size but became flattened as it approached the junction of the second and third antennular segments (figure 2.2c,d). The axons of the antennular nerve followed a similar path through these segments, remaining clustered (figure 2.2d).

The ducts then entered the third antennular segment, or attachment disc. Here the temporary adhesive ducts expanded noticeably, becoming larger spherocylindrical structures ~1–1.5 µm in diameter with two distinct regions (figure 2.3). The inner region seemed to be the transporting duct and contained numerous homogenous vesicles, each ~200 nm in diameter. These vesicles were surrounded by numerous peripheral microtubules (figure 2.3b,c). The outer section was identifiable by the presence of supporting rods (figure 2.3b,c). The ducts and associated elements did not appear to contain any of the cellular components required to produce and package the temporary adhesive. The number of ducts correlated with the number of cells in the temporary adhesive gland. Towards the disc surface, secretory ducts lost the supporting outer section (figure 2.3a) and the secretory pores for both the temporary adhesive and cement duct could be seen terminating among the microvilli that cover the surface of the attachment disc (figure 2.3a).

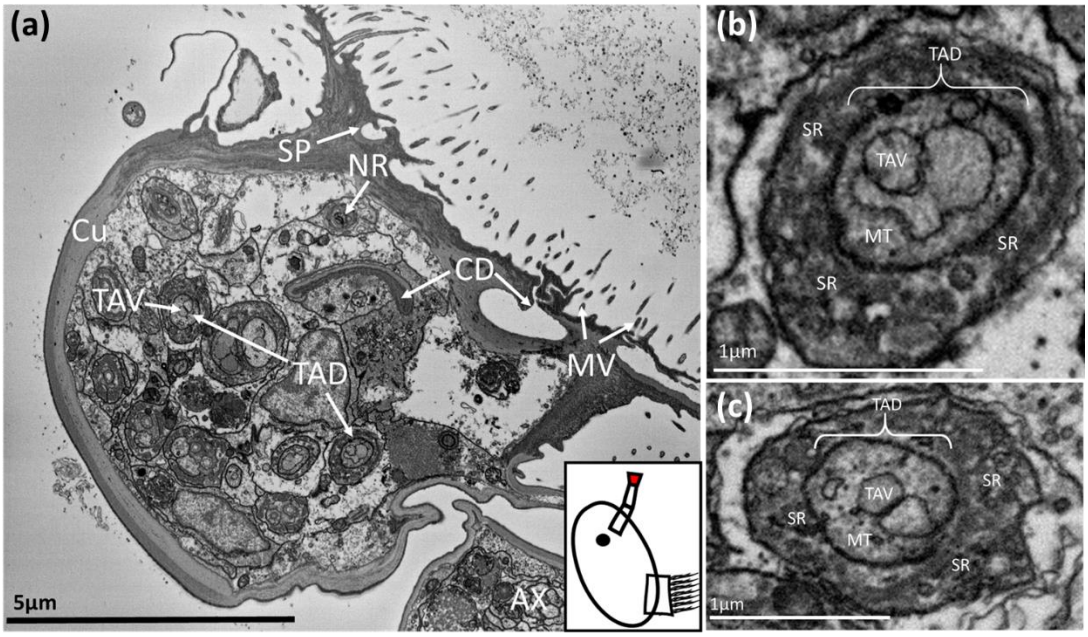

Figure 2.3. SBF-SEM image of a *Balanus amphitrite* cyprid: **(a)** = third antennular segment, **(b,c)** = temporary adhesive ducts within the third antennular segment. The region where the image was captured is highlighted in red on the schematic inset. TAD = temporary adhesive duct; TAV = temporary adhesive vesicle; SP = secretory pore; CD = cement duct; NR = neurone; AX = axon; MT = microtubules; SR = supporting rods; MV = microvilli.

The cement duct remained flattened as it extended into the third antennular segment. As the specimen in figures 2.2-3 had not begun the process of permanent adhesion, the duct was empty and appeared to have narrowed to a slit of ~3 x < 0.5 µm. Presumably, this slit would stretch and open during secretion of the permanent cement (figure 2.3a). At the disc surface, this singular permanent cement duct diverged into many smaller channels to dispense the adhesive over a larger area.

Finally, the axons comprising the antennular nerve connected to neurones serving sensilla on the third and fourth antennular segments (figure 2.3a).

The two-dimensional images (figures 2.2-3) allowed for detailed ultrastructural observation of sections of the cyprid adhesive systems. However, the morphology of the complete system is not easy to visualise from two-dimensional sections alone. To this end, a three-dimensional reconstruction of the systems described for *B. amphitrite* was produced (figure 2.4). Here the division of the singular cement duct into the smaller channels across the disc surface was visible, as was the position of the cement gland behind the eye. Also modelled were two of the 10–15 temporary adhesive ducts, which led back to the temporary adhesive gland in the proximal first segment, where the widening and elongation of the cells could be seen.

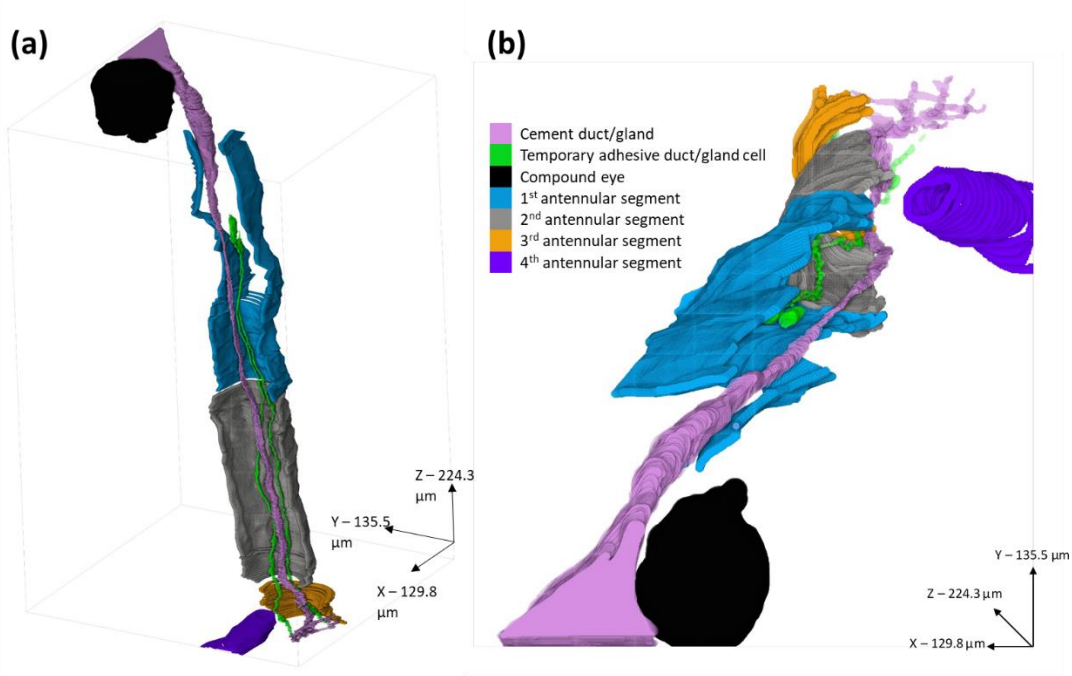

Figure 2.4. 3-D models of *B. amphitrite* antennule and adhesive systems, reconstructed from an SBF-SEM series. **(a)** = lateral view; **(b)** = dorsal view. The antennular segments were left open to allow viewing of the interior. Lilac = cement duct/gland; green = temporary adhesive duct/gland cell; black = compound eye; blue = 1st antennular segment; grey = 2nd antennular segment; yellow = 3rd antennular segment; purple = 4th antennular segment.

2.4.2. Megabalanus coccopoma

It seemed likely that the adhesive systems of *B. amphitrite* and *M. coccopoma* would be similar, however confirmation of the new observations in a second acorn barnacle species was nevertheless important. Since the temporary adhesive gland of *B. amphitrite* had already been located, the sectioning of *M. coccopoma* cyprids was changed from transverse to longitudinal to observe the structures from an alternate angle.

The initial longitudinal sections revealed the core structures, namely the antennule, the brain and oil cells within the anterior cephalon, and the thoracic appendages within the thorax (figure 2.5a). The temporary adhesive gland was not visible in the initial imaging; however, deeper sectioning revealed its location to be consistent with that of *B. amphitrite*, in the proximal region of the first antennular segment (figure 2.5a,b).

The temporary adhesive gland was approximately 25 × 50 µm, roughly prolate spheroid in shape and comprised of ~12 elongated cells surrounded by muscle (figure 2.5b,c). A summary of the dimensions of key structures is presented in table 2.2. A closer view of the gland revealed the cells to be full of homogenous vesicles of 300–400 nm in diameter (figure 2.5c,d). These cells were up to 5 µm wide depending on vesicular content and 20–25 µm long. Additionally, the gland cells contained nuclei, rough endoplasmic reticulum and Golgi apparatus; the cellular structures necessary for protein production and vesicular packaging (figure 2.5d). The vesicles near the Golgi apparatus were smaller and sparsely distributed, in addition to being situated on the right of the images, furthest from the antennule and transporting ducts (figure 2.5c,d).

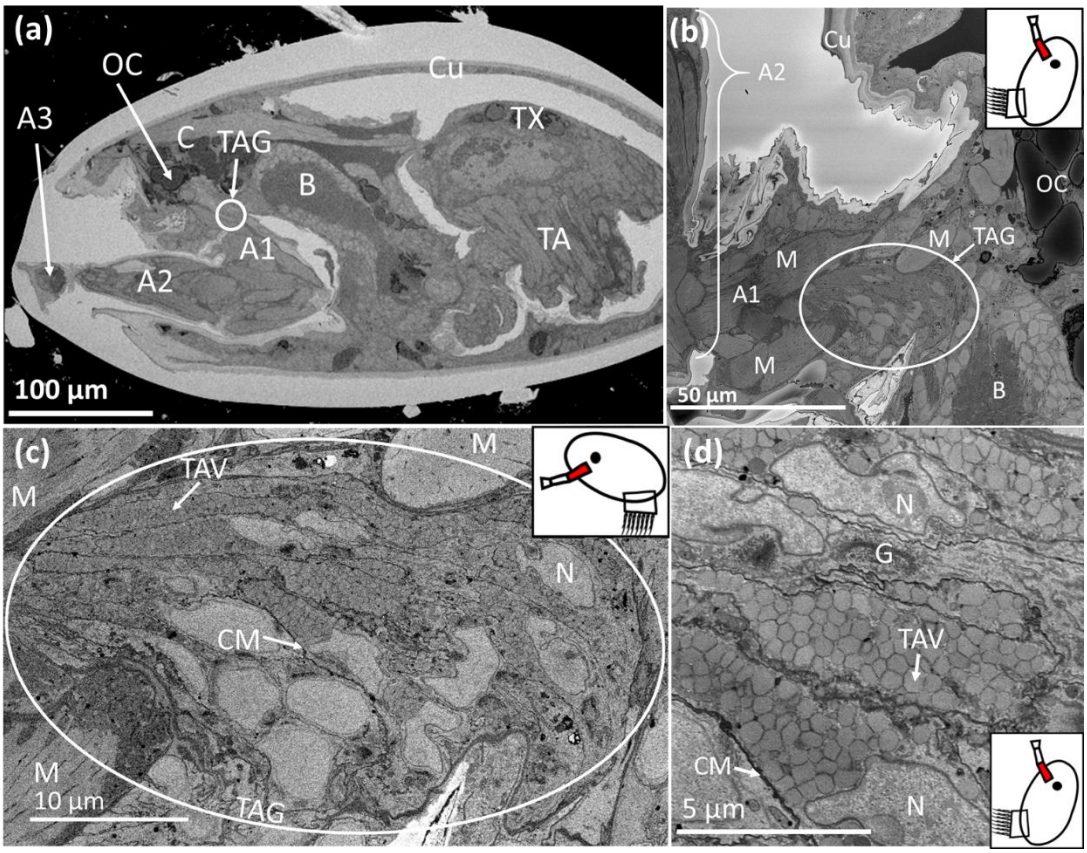

Figure 2.5. SBF-SEM images of *Megabalanus coccopoma*: **(a)** = cyprid; **(b)** = cyprid anterior mantle; **(c)** = temporary adhesive gland; **(d)** = temporary adhesive gland cells. The region where the image was captured is highlighted in red on the schematic inset. C = cephalon; TAG = temporary adhesive gland; TAV = temporary adhesive vesicle; OC = oil cell; A1 = first antennular segment; A2 = second antennular segment; A3 = third antennular segment (attachment disc); Cu = cuticle; TX = thorax; TA = thoracic appendages; M = muscle; B = brain. CM = cell membrane; N = nucleus; G = Golgi body; RER = rough endoplasmic reticulum.

As was the case in *B. amphitrite*, the gland cells of *M. coccopoma* transitioned into ducts as they proceeded distally, narrowing to ~0.5–1 µm (figure 2.6a). The duct diameter appeared to be correlated with the abundance of vesicles, with fewer vesicles resulting in a narrower duct. Other than this, the morphology of the ducts remained constant through the first and second antennular segments (figure 2.6a).

Once the temporary adhesive ducts reached the third antennular segment, they expanded into larger, spherocylindrical structures on the periphery of the disc close to the surface (figure 2.6b). These structures were over 1.5 µm in diameter and formed of two major sections, the vesicle-filled duct at the centre, and the supporting sheath around the outside (figure 2.6b). In addition, these structures numbered approximately 12; as for the gland cells (figure 2.6b,c). The temporary adhesive ducts were filled with the homogenous vesicles originally observed within the temporary adhesive gland cells. However, no vesicles were present between the spherocylindrical structures and the disc surface, where the ducts narrow and feed into secretory pores (figure 2.6b). In contrast to the peripheral, singular, temporary adhesive ducts, the cement duct split into multiple sub-channels and opened out into the centre of the disc (figure 2.6b).

Reconstructing the temporary adhesive ducts using three-dimensional modelling reveals that the “collecting structures” occurred in parallel pairs and were peripheral to the cement duct (figure 2.6b). Unlike in *B. amphitrite,* the ducts took a circular route immediately following the putative collecting structures (figure 2.6c) and surrounding muscle tissue.

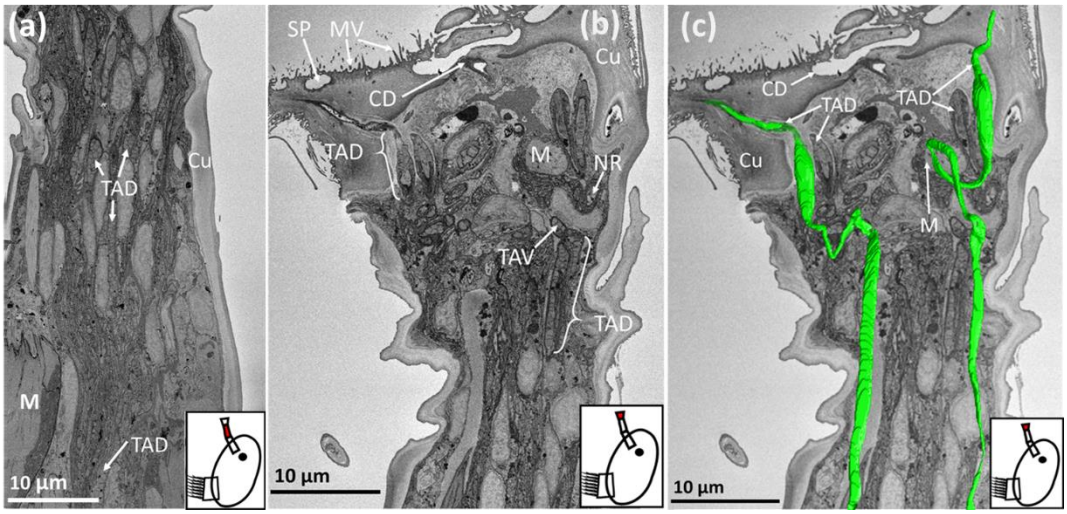

Figure 2.6. SBF-SEM images of *Megabalanus coccopoma*: **(a)** = second antennular segment; **(b)** = third antennular segment.; **(c)** = third antennular segment overlaid with a 3-D model of temporary adhesive ducts (green). The region where the image was captured is highlighted in red on the schematic inset. TAD = temporary adhesive duct; TAV = temporary adhesive vesicle; M = muscle; SP = secretory pore; MV = microvilli; CD = cement duct; Cu = cuticle; NR = neurone.

2.5. Discussion

This study provides new evidence for the location of the temporary adhesive glands in acorn barnacle species and gives greater insight into the temporary adhesive system. Contrary to the findings of Nott and Foster (1969), the temporary adhesive glands of *Balanus amphitrite* and *Megabalanus coccopoma* were not situated in the second antennular segment, but in the first (figure 2.2a,b, 2.4, 2.5b and 2.7). Instead, the ultrastructure of the acorn barnacles appeared more consistent with that of the stalked barnacle *Octolasmis angulata* (Yap *et al.*, 2017), though there were some key differences.

The temporary adhesive glands of *B. amphitrite* and *M. coccopoma* possessed similar morphology and location. The glands were located in the proximal region of the first antennular segment (figure 2.2a,b figure 2.5b). Each gland is comprised of ~10–15 elongated cells filled with homogenous vesicles containing the packaged temporary adhesive, and the organelles needed for protein synthesis and secretion (figure 2.2a,b and 5c,d). Smaller vesicles were observed in the glands of both species, situated in the vicinity of Golgi apparatus. These vesicles may have been undergoing the process of aggregation, coalescence and condensation described by Yap et al. (2017). In *M.*

coccopoma, these smaller and more sparsely distributed vesicles were located at the furthest possible point from the ducts leading to the antennule, indicating an organisation of the cells within the gland to produce and transport the adhesive in a single direction (figure 2.5c,d). The glands were roughly spherocylindrical or prolate spheroid in shape, with the overall size correlated to the size of the cyprid of each species (table 2). However, the glands did not appear to have the morphology of a typical “exocrine gland”, as each cell fed a single duct, and these ducts did not combine or diverge as they extended towards the third antennular segment (Noirot *et al.*, 1974; Talbot *et al.*, 1993; Quennedey, 1998; Freeman *et al.*, 2020). As Yap et al. (2017) described in the temporary adhesive system of the stalked barnacle, *Octolasmis angulata*, the ducts that carry the temporary adhesive to the disc surface are simply extensions of the gland cells themselves. In both cases, the glands were surrounded by muscle tissue in various orientations. Antennule locomotion is likely the primary function of these muscles, as described by Lagersson and Høeg (2002), however, contraction of these muscles may apply pressure to the gland and aid in the secretion of the adhesive (Yap *et al.*, 2017).

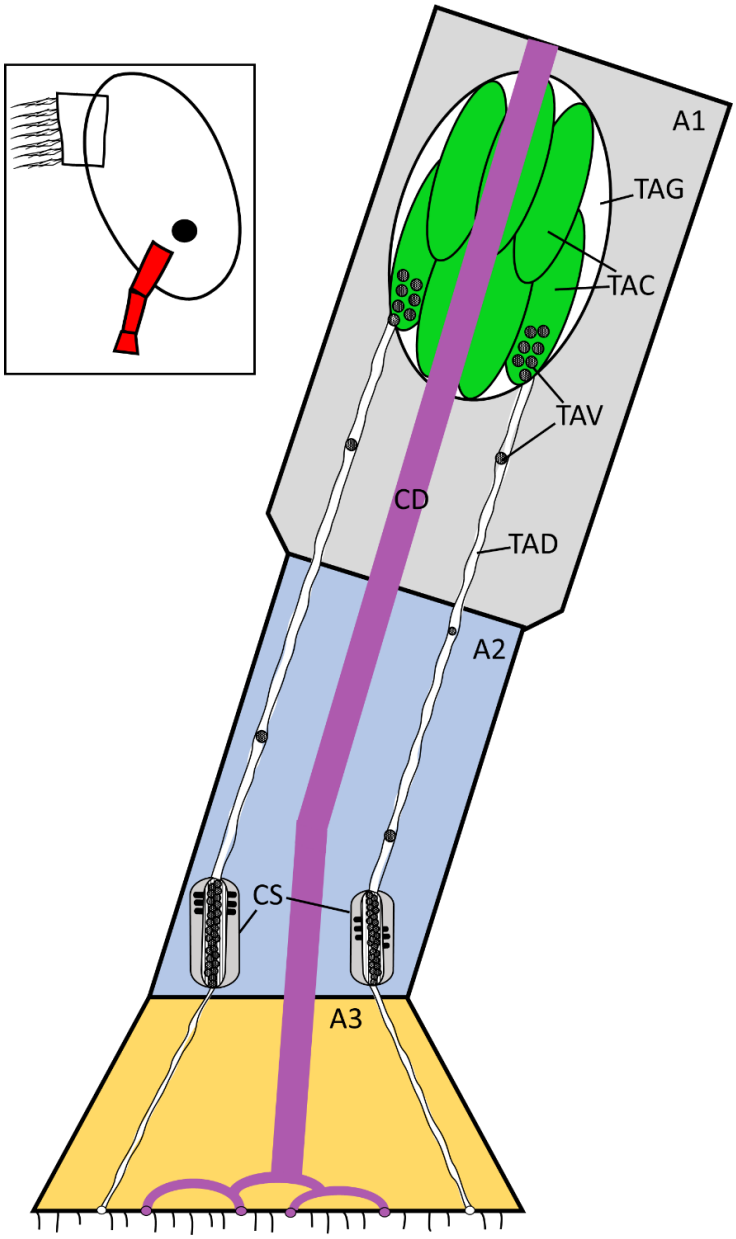

Figure 2.7. Updated schematic diagram (figure 2.1) of the temporary adhesive system, with the gland located in the proximal first antennular segment. Not to scale. The temporary adhesive gland contains numerous cells for the synthesis and packing of the temporary adhesive and each cell feeds one duct. The region detailed in the schematic is highlighted in red on the inset. A1 = first antennular segment; A2 = second antennular segment; A3 = third antennular segment (attachment disc); CD = cement duct; TAG = temporary adhesive gland; TAC = temporary adhesive gland cell; TAV = temporary adhesive vesicle; TAD = temporary adhesive duct; CS = putative collecting structures, previously proposed to be the temporary adhesive gland by Nott and Foster (1969).

Following synthesis and vesicular packaging in the temporary adhesive gland, the vesicles containing the proteinaceous adhesive were transported to the third antennular segment via narrow ducts (figure 2.2c,d and 2.6a). Like the gland cells, the diameter of the ducts and the abundance of vesicles were correlated to the size of the cyprid species (table 2). These vesicles were homogenous in electron density and

shape, suggesting that unlike the permanent cement, the temporary adhesive is a single component, or a mixture of components, secreted as a singular phase.

Close to the surface of the disc, the ducts widened into a spherocylindrical shape, gaining a supportive outer sheath filled with rod-like structures (figure 2.3a–c and 2.6b). These structures were similar to those previously described by Nott and Foster (1969). which were interpreted as unicellular glands and the origin of the temporary adhesive. As their ultrastructural descriptions are in close accord with this study, it is proposed that these duct expansions are “collecting structures” for on-demand secretion. The same interpretation was made by Yap et al. (2017) for *O. angulata*. In addition, these “collecting structures” appeared to be arranged in parallel pairs, peripheral to the central cement duct. The reason for this is unknown (figure 3a and 6b). The abundance of these “collecting structures” was consistent with the number of cells observed in the temporary adhesive gland, further indicating that the ducts did not diverge. Finally, between the “collecting structures” and the secretory pores on the disc surface, the ducts lost the outer sheath, contained no vesicles and did not branch (figure 2.3a and 2.6b). Interestingly, 3-D modelling of the ducts revealed that those of *M. coccopoma* encircled a region of muscle tissue in the centre of the third antennular segment, while those of *B. amphitrite* did not, suggesting potential species-specific differences (figure 2.4a,b and 2.6c). Whether this muscle is simply related to articulation of the third and fourth antennular segments, or functions to aid secretion of the temporary adhesive, is unknown.

Although similar in many respects, there are notable differences in the temporary adhesive system in the two acorn barnacle species compared to that of the stalked barnacle *O. angulata* (Yap *et al.*, 2017) Primarily, the glands were observed in the proximal region of the 1st antennular segment in the acorn barnacles, as opposed to behind the eye in *O. angulata*. Secondly, no merging or diverging of the temporary adhesive ducts was observed in the acorn barnacles, while in the stalked barnacle some was described (figure 2.4a,b). Finally, Yap et al. (2017) observed no difference in the content of the glands in relation to cyprid age, implying that production is constitutive throughout the cyprid stage. Cyprids of different ages were not compared here, however, the gland and ducts of the *B*. *amphitrite* specimens contained considerably fewer vesicles than the *M. coccopoma* specimens, implying either a species-specific difference or that unknown factors can influence temporary adhesive

production. It is possible that these differences are attributed to the distance in the evolutionary relationships between stalked and acorn barnacles (Pérez-Losada *et al.*, 2004; Ewers-Saucedo *et al.*, 2019).

In conclusion, this study has corrected a decades-old description of the location and structure of the temporary adhesive glands in acorn barnacle cyprids. Furthermore, variations were identified between individuals of the acorn barnacles studied here and the prior observations for *O. angulata*. The importance of these apparent variations will only be determined by further investigation of the ultrastructure of these, and a broader spectrum of barnacle species. Such information would allow for improved future studies of the temporary adhesive systems of barnacle larvae, via both morphology, as some aspects remain unclear still, and molecular biology, as isolation of the gland, will allow for the easier characterisation of the still-unidentified temporary adhesive protein(s).

Chapter 3. Footprint Collection and Preliminary Characterisation

3.1. Abstract

Cypris larvae use a proteinaceous temporary adhesive when exploring surfaces, detaching mechanically and depositing footprints of the adhesive material. These footprints share some homology, based on cross reactive antibodies, with the settlement-inducing protein complex (SIPC), but otherwise are uncharacterised. The low abundance of available material has historically made collection and characterisation challenging. A batch collection method was developed to collect working quantities for SDS-PAGE and western blot analyses, and the material investigated using these techniques. Antibodies raised against the C-terminal of the SIPC reacted with footprint extracts, but on proteins of a different mass, indicating that the SIPC, as it exists in cyprids adults, was not present in the footprints. Mannose residues, common on the SIPC, were not found on all the bands which reacted with the SIPC antibody, suggesting they were not fragments of the same protein. The four bands which reacted with the SIPC antibody were put forward for characterisation by multi-omics.

3.2. Introduction

As discussed in chapter 1.3.3., acorn barnacle cyprids utilise an adhesive secreted from their third antennular segment to temporarily adhere to the substratum during exploration. The adhesive allows the larva to select a suitable settlement location, even in highly dynamic environments, without being removed (Nott, 1969; Nott and Foster 1969; Aldred et al., 2013). Although given only cursory attention compared to the adult cement, evidence supports a proteinaceous temporary adhesive (Walker and Yule, 1984) comprised of nanofibrils (Phang *et al.*, 2008; Phang *et al.*, 2010), and containing the settlement-inducing protein complex (SIPC), or an analogue (Dreanno *et al*., 2006a). Most importantly, however, the temporary adhesive is deposited on surfaces when the cyprid detaches, leaving behind an adhesive 'footprint' (Yule and Walker, 1984; Clare *et al.*, 1994; Phang *et al.*, 2008; Phang *et al.*, 2010; Aldred *et al.*,

2013). Surfaces that have a general affinity for protein, such as nitrocellulose membrane, bind the footprints (Dreanno et al. 2006a).

Given that *B. amphitrite* deposits have an estimated volume of 0.5-10.1 μm^3 depending on the surface, previous attempts have found collecting sufficient material challenging. Furthermore, despite the footprint protein(s) binding with SIPC antibodies (Dreanno et al. 2006a), the SIPC also occurs widely in the rest of the cyprid, thus preventing an immunoprecipitation approach to material collection, as it would be difficult to determine which proteins are relevant (Dreanno *et al*., 2006b).

Here, a method of batch collection using nitrocellulose membrane is outlined. The method is based on comparisons between actively exploring cyprids, and those rendered inactive by a magnesium chloride solution iso-osmotic with sea water. Footprint proteins should only be deposited by the actively exploring cyprids, thus making identification of candidates easier when compared by SDS-PAGE. This was followed by sample combination and concentration to generate workable quantities for western blotting. Western blots testing reactivity against SIPC antibodies and D-mannose/glucose-binding lectins were performed, based upon the known affinity of SIPC antibodies for deposited footprints (Dreanno *et al*., 2006a), and the importance of D-mannose residues on the SIPC molecule (Pagett *et al.*, 2012). Candidates identified through these preliminary investigations were carried forward to candidate selection and expression studies in chapters 4 and 5, respectively.

3.3. Experimental procedures

3.3.1. Larval culture

Balanus amphitrite larvae were cultured as described in 2.3.1.

For culturing new adult *B. amphitrite*, the filtered cyprids were introduced to a new vessel along with algal feed as described above and left undisturbed for six days. Following this, the water was gently changed, and fresh algal feed added. *B. amphitrite* were then fed and water changed every 3-4 days. Once the juvenile settled barnacles were visible, a small brush was used to gently clean any algal buildup that had accumulated on the organisms.

3.3.2. Footprint collection

To collect footprint material for analysis of the temporary adhesive, cyprids were allowed to explore and deposit material on protein-binding nitrocellulose membranes, from which the protein was then extracted. This process, described below, is also outlined in figure 3.1.

Strips of nitrocellulose membrane were cut to fit and lay flat inside 1ml Eppendorf tubes, such that ~50% of the interior surface was covered (~0.5 x 2cm). These tubes were divided into three sets of 40. To the first set (active), 20-30 active cyprids were added to each tube, which were then filled to the brim with artificial sea water (ASW; Tropic Marin) and sealed. The second set (inactive) was filled with 20-30 cyprids that had been rendered inactive with 7.14% w/v magnesium chloride hexahydrate ($MgCl_2$) in distilled water, to a final salinity of 33 ppt. The tubes were filled to the brim with the same $MgCl_2$ solution. Finally, the third set (blank) was filled only with ASW, and no cyprids. These tubes were oriented horizontally and incubated in racks overnight at 28°C, allowing time for the cyprids to explore, but not settle in abundance.

Following incubation, the membranes were removed, rinsed in ASW, and the areas where any cyprids had settled were cut off. The membranes were then washed briefly in Milli-Q water (18.2 MΩ) and incubated in 1ml of 8M urea in Eppendorf tubes, at 10 membranes per ml for three hours at room temperature. The membranes were agitated constantly to solubilise proteins adsorbed to the membrane.

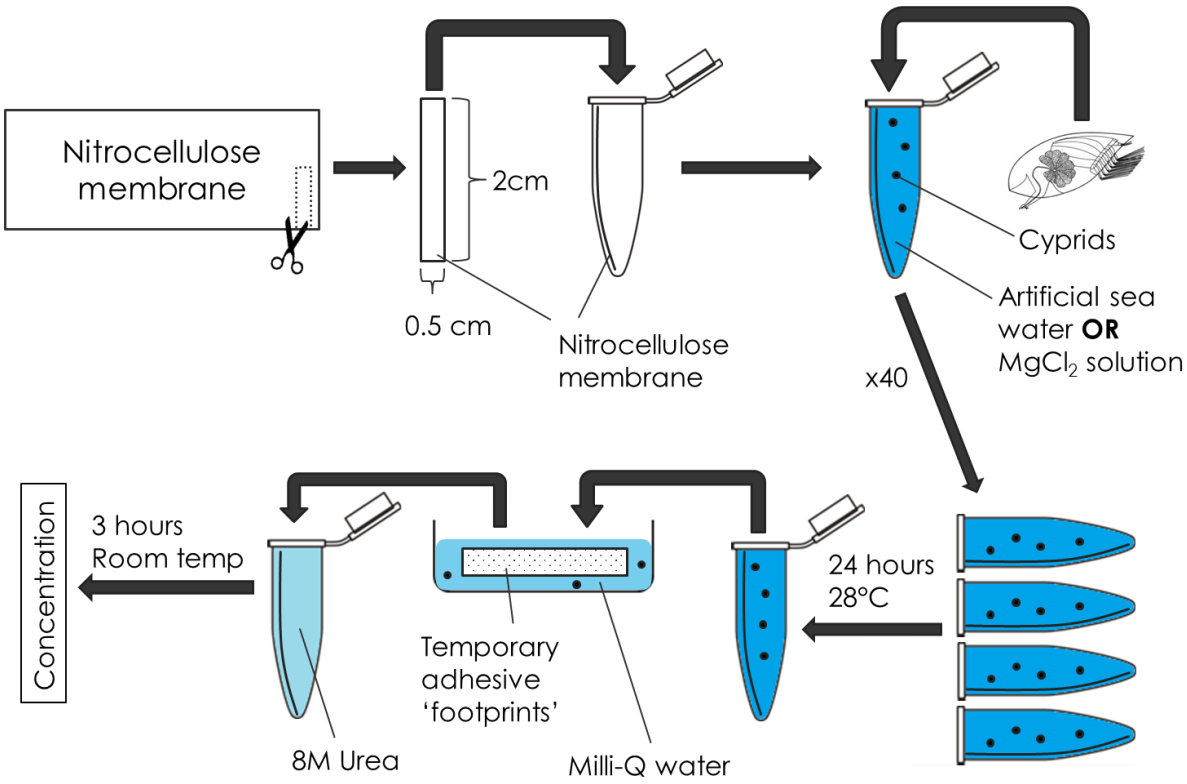

Figure 3.1. Schematic diagram of the temporary adhesive material collection process.

The urea, containing any solubilised proteins, was then transferred to Amicon® Ultra-4 10 kDa centrifugal concentrators, with the extracts from the active, inactive, and blank treatments kept separate. The urea solutions were spun at 4000 x g for 30 minutes at 4°C to concentrate proteins. The final concentrates (~50-100µl) were removed from the filter and frozen at -20°C until use with downstream SDS-PAGE.

In the case where the collected protein solutions were to be used downstream with western blotting, the protein from a single collection and concentration was too dilute to visualize effectively. As such, multiple collection batches (3-4) were combined and concentrated in Amicon® Ultra-4 10 kDa centrifugal concentrators to achieve a final volume of ~50-100 µl.

3.3.3. SDS-PAGE

Thirteen µl of protein extract were mixed with 5 µl 4x LDS sample buffer and 2 µl 10x reducing agent (500mM DTT) to a total volume of 20µl. The solution was denatured at 70°C for 10 min, then loaded into the gel wells (NuPAGE™ 4-12% Bis-Tris Protein

Gels, 1.0 mm thickness) along with 20 µl of protein marker in one well (Novex Mark12™ Unstained Standard), either diluted 1/2 for gels to be western blotted, or by 1/20 for silver staining. The gels were run at 200V, 120mA for one hour, or until the dye ran off the bottom of the gel. Gels were then either silver stained, or western blotted.

For silver staining, gels were immediately stained using Pierce Silver Staining kit. Gels were rinsed twice for five minutes each in Milli-Q water, fixed for 30 minutes in 30% ethanol:10% acetic acid solution, replacing the solution after 15 min, washed (2 x 5 min) in 10% ethanol solution, and again in Milli-Q water (2 x 5 min). Next, the sensitizer working solution was added (1 part Pierce Silver Stain Sensitizer with 500 parts Milli-Q water), in which the gels were incubated for 1 minute. The gels were then rinsed in Milli-Q water twice for 1 minute each. Gels were then stained for five minutes in silver stain working solution (1 part Pierce Silver Stain Enhancer with 50 parts Pierce Silver Stain), rinsed twice in Milli-Q water for 20 seconds each, and then developed in developer working solution (1 part Pierce Silver Stain Enhancer with 50 parts Pierce Silver Stain Developer) until bands were visible. Development was stopped once the desired band intensity had been reached by adding 5% acetic acid in place of the developer solution. The gels were then photographed with an Azure Biosystems c280 imaging system.

3.3.4. Western blotting

Proteins were transferred from unstained gels to nitrocellulose membranes via a Bio-Rad transblot turbo cell. The gel, nitrocellulose membrane, and six pieces of western blotting filter paper, all cut to the same size, were soaked in NuPAGE® transfer buffer for five minutes before being stacked on the anode plate of the cell in the following order: three sheets of filter paper, the nitrocellulose membrane, the gel and finally three more sheets of filter paper. The cathode plate was placed on top and the blot was run at 1A and 25V for 30 min.

3.3.5. Antibody staining

The western blotted proteins on the nitrocellulose membrane were stained with polyclonal antibodies raised against the C-terminal of the SIPC (peptide sequence: PEERNIQEYELT, Dreanno *et al.*, 2006, Aviva Systems Biology) of *Balanus amphitrite*. The membrane was washed in 0.22 µm filtered TBST (20mM Tris-HCl, 0.5M NaCl, 0.05% Tween20) for 10 min, then incubated in 0.22 µm filtered blocking buffer (Blocker^{TM} Casein, ThermoFisher Scientific, 1% w/v casein in TBS) overnight at 4°C. Following this, the membrane was incubated in 1:5000 solution of antibody buffer (blocking buffer diluted in TBS 1:2) and primary antibody (SIPC-C) for one hour at room temperature. The membranes were then rinsed in TBST, then washed again for 20 min, changing the TBST every 5 min. Next, the membranes were incubated in 1:10000 solution of antibody buffer and secondary antibody (Anti-Rabbit IgG – HRP, produced in goat, Sigma) for 1 hr. Finally, the membranes were rinsed in TBST and washed for 15 min, changing the TBST every 5 min. The buffer was then removed and a 1:1 mix of Azure Radiance chemiluminescent substrate reagents was applied to the membrane surface for 2 min. Excess reagent was then removed and the blot imaged.

3.3.6. Lectin Staining

Proteins were western blotted as described above, then stained as described for the antibody staining, with the following differences: 2% BSA in TBST as the blocking buffer, lens culinaris agglutinin (LCA) biotinylated lectin (Vector) instead of the primary antibody, and horseradish peroxidase (HRP) streptavidin as the secondary antibody.

3.3.6. Cyprid protein extraction

Crude cyprid protein extracts were collected by lysing the organisms into 8M urea using Qiagen PowerBead Tubes Garnet (0.7mm) on ice. The lysate was centrifuged at 4°C for ten minutes at 10000 x G to remove cellular material.

3.4. Results

3.4.1. Active vs inactive

The initial step to characterising the temporary adhesive protein(s) was to identify candidates via comparison of differential protein deposits (footprints) made by *B. amphitrite* cyprids during surface exploration. The SDS-PAGE gels comparing these deposits are displayed in figure 3.2 and analysed in table 3.1.

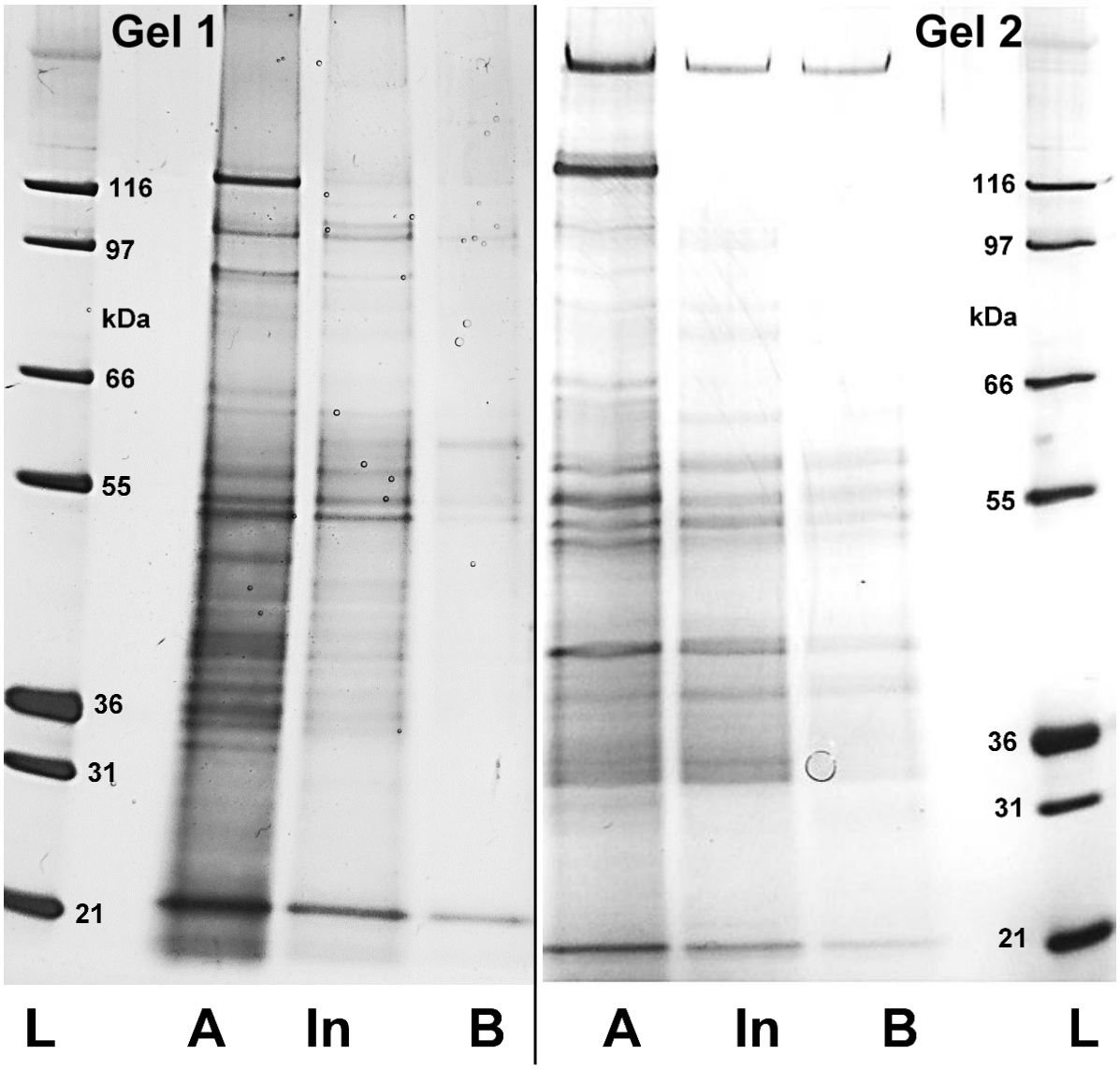

Figure 3.2. SDS-PAGE comparing protein extracts collected from nitrocellulose membranes exposed to assorted treatments: A = Active *B. amphitrite* cyprids in ASW; In = B. amphitrite cyprids rendered inactive by $MgCl_2$ solution; B = Blank, ASW with no cyprids. L = Ladder, protein standard, 21-200 kDa mass. Gel 1 and Gel 2 were different extract samples collected from different batches of cyprids. Images have been adjusted for colour, contrast, and brightness to best highlight the bands. Images were processed in GelAnalyzer 2010 software to isolate the bands. Outputs are displayed in table 3.1.

Table 3.1. GelAnalyzer outputs estimating molecular weight (kDa) of detected protein bands from figure 3.2, compared between treatments and gels. Proteins have been aligned and colour coded based on their occurrence patterns: Green = present in at least one active sample, and none of the controls; orange = present in at least one active sample, and at least one inactive control; red = resent in at least one blank control.

figure 3.2	Gel 1			Gel 2		
Ladder	A (Active)	In (Inactive)	B (Blank)	A (Active)	In (Inactive)	B (Blank)
	127			131		
	123	123		125		
116		114				
	105	105		103	102	
	102	101	101	98	97	
97	90	89		90		
	81	80		80	80	
	79					
	75	74		75	74	
66		64		64		
	62			61		
	59	59		59	59	60
55	53	54	54	52	52	53
	50	51		48	48	49
	47	47	47	46	46	47
	46	46	45	44	45	45
	42			42		
	40	40				
	39	39				
	38	38		38		
	37	37		36	37	37
36	36			35		
	35	35		34	34	35
	35	35				
	34	34		33	33	
	33	33		32	33	
	32	32		32	32	
31	31					
	31					
	30	30		31	31	31
	30			30		
	29	29				
	28	29				
21	27	27	27	27	27	27

The band pattern between the two gels was broadly similar, though the intensity of staining suggested that more protein was isolated from membranes that were actively explored by cyprids (figure 3.2). Overall, the GelAnalyzer detected 34 bands between the two gels. Of these, eight bands were exclusive to the active samples (green), a further 15 were deposited in both active and inactive samples (orange), while the remaining 11 appeared in the blank samples and thus were assumed to be contaminants (red) (table 3.1). For selection of temporary adhesive protein candidates, those bands appearing exclusively in extracts from actively explored membranes were prioritised (table 3.1). However, in the case of the ~123 kDa band, which occurred in both the active and inactive samples, the abundance was considerably higher in the active sample, thus it was also considered a candidate temporary adhesive protein.

3.4.2. Temporary adhesive or permanent cement

To ensure the proteins extracted were from the temporary adhesive footprint deposits, and not permanent cement secreted by settling cyprids, a comparison between nitrocellulose membranes which had been washed of settled cyprids and membranes where settled cyprids had been cut off was performed. In theory, the membranes which were only washed would have had permanent cement from settling cyprids remaining on them, while the cut membranes would not. Thus, any differences in band patterns would identify proteins to exclude as candidate components of the temporary adhesive.

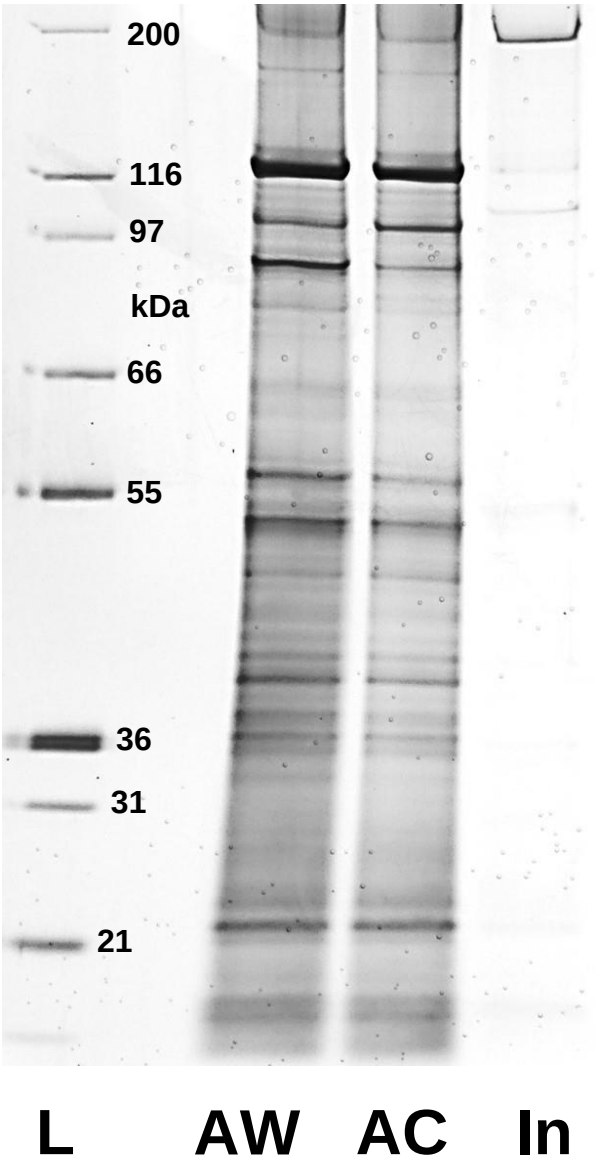

Figure 3.3. SDS-PAGE comparing protein extracts collected from nitrocellulose membranes exposed to assorted treatments: AW = Active *B. amphitrite* cyprids in ASW, subsequently washed in MQ-water; AC = Active *B. amphitrite* cyprids in ASW, subsequently cut to remove settled cyprids; In = *B. amphitrite* cyprids rendered inactive by $MgCl_2$ solution. L = Ladder, protein standard, 21-200 kDa mass. Images have been adjusted for colour, contrast, and brightness to best highlight the bands. Images were processed in GelAnalyzer 2010 software to isolate the bands. Outputs are displayed in table 3.2.

Table 3.2. GelAnalyzer outputs estimating molecular weight (kDa) of detected protein bands from figure 3.3, compared between treatments. Proteins have been aligned and colour coded based on their occurrence patterns: Green = present in both washed and cut active samples, and none of the controls; orange = present in both washed and cut active samples, and at least one inactive control; pink = present in only one washed or cut active sample, and none of the controls; red = present in none of the active samples, and at least one inactive control.

figure 3.3 Ladder	AW (Active Washed)	AC (Active Cut)	In (Inactive)
200	193	191	191
	172	170	
	131	129	
	123	121	124
116	116	115	
	112	111	
	104	102	108
97	95		
	91	90	
	81	82	
66	64	63	
55	51	50	
			47
	46	45	
	41	40	
	37	37	
36	36	36	
	35	34	
	33	33	
31	31	31	
		30	
	30	30	30
	29	28	
	27	27	
	26	26	
	25	25	
	24	24	24
	23	23	23
21	22	22	22

The two active samples had similar band patterns (figure 3.3). Analysis revealed that of the 26 protein bands present in the active samples, 24 of them co-occurred, indicating that few, if any, of the proteins extracted were components of the permanent cement (table 3.2). The candidate proteins identified from the initial investigation in table 3.1 were all present among the co-occurring bands here, thus none were eliminated.

3.4.3. Reduced vs non-reduced

Given that the SIPC may be a native homodimer (Matsumura *et al.*, 1998; Ferrier *et al.*, 2016; Zimmer *et al.*, 2016), its putative presence in the temporary adhesive (Dreanno *et al.*, 2006a), and the bundled nanofibrillar formation of the temporary adhesive observed by AFM (Phang *et al.*, 2010), protein extracts were compared under reducing and non-reducing conditions in order to determine if any protein-protein interactions were occurring amongst the candidates identified.

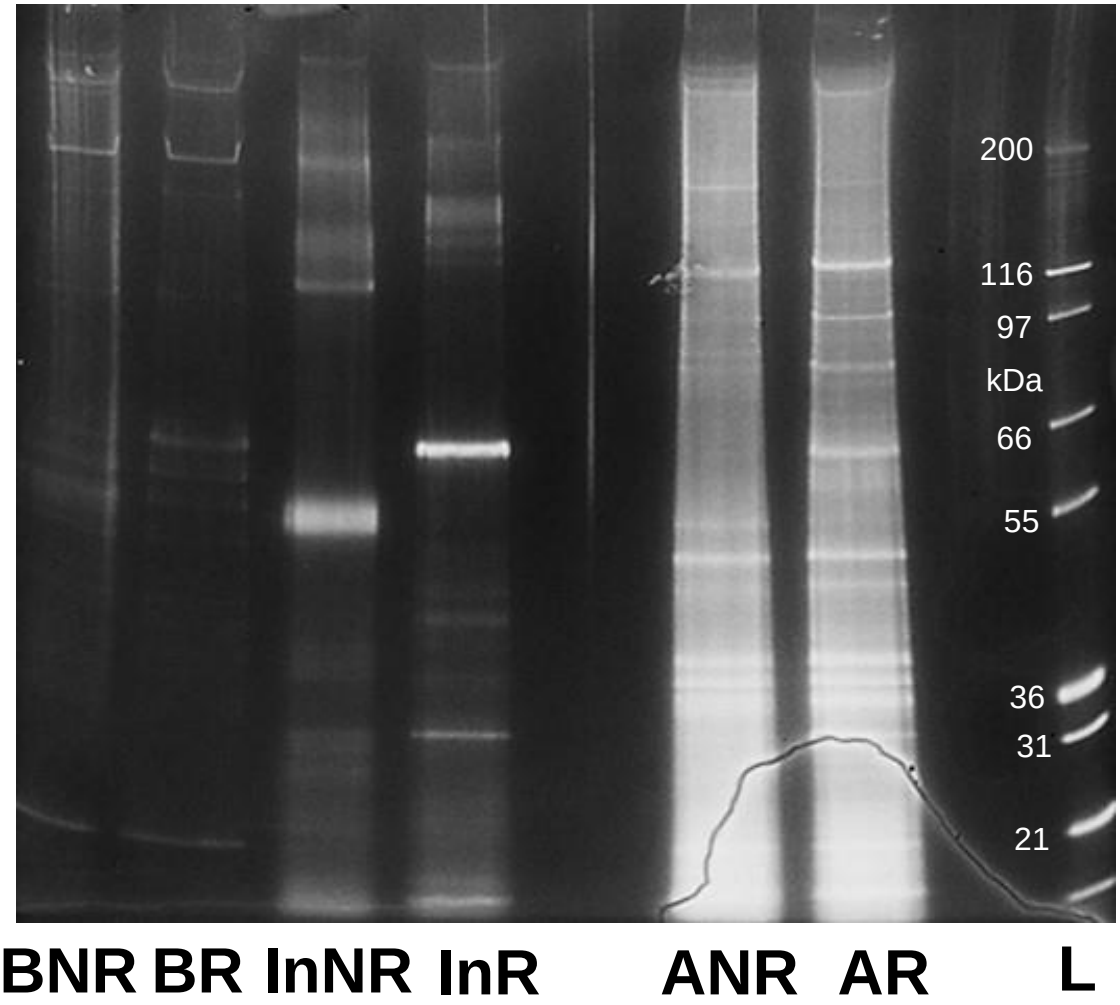

Figure 3.4. SDS-PAGE comparing protein extracts collected from nitrocellulose membranes exposed to assorted treatments: A = Active *B. amphitrite* cyprids in ASW; In = B. amphitrite cyprids rendered inactive by MgCl2/ASW solution; B = Blank, ASW with no cyprids; R = Protein sample reduced with 10nM DTT; NR = protein sample not reduced. L = Ladder, protein standard, 21-200 kDa mass. Images have been adjusted for colour, contrast, and brightness to best highlight the bands. Images were processed in GelAnalyzer 2010 software to isolate the bands. Outputs are displayed in table 3.3.

Table 3.3. GelAnalyzer outputs estimating molecular weight (kDa) of detected protein bands from figure 3.4, compared between treatments. Proteins have been aligned and colour coded based on their occurrence patterns: Dark green = present in both reduced and non-reduced active samples, and none of the controls; light green = present in only the non-reduced active sample; orange = present in both reduced and non-reduced active samples, and at least one inactive control; yellow = present in only the non-reduced active sample, and at least one inactive control; red = present in a blank control, or only an inactive control.

figure 3.4 Ladder	AR (Active reduced)	ANR (Active non-reduced)	InR (Inactive reduced)	InNR (Inactive non-reduced)	BR (Blank reduced)	BNR (Blank non-reduced)
		278	282	288		
						266
		263				
					258	253
	251	249				
200			203			
				185	189	197
	172	166				
					163	165
			151			
			134	134		
	122	116	124			
116				110	107	111
97	98	97				
		86				
	82	81				
66					62	63
	60		60			59
55	54				56	53
					51	
		47		48		48
	43	42				
	40	39				
36			36			
	32	32		33		
31	31	31	31			
	30	30				
				32		
				31		
	28		27	27		
				27		
				26		
	23	23	22		23	24
21	22	21	21	21	21	21

Both the active and inactive extracts displayed some differences in band pattern between the reduced and non-reduced samples, while the blank extracts did not (figure 3.4). When analysed, protein bands previously identified as unique to, or dominant in, the active extracts (tables 3.1 and 3.2) were still present in both reduced and non-reduced active extracts, namely: five bands in the 30-45 kDa range, one at ~80 kDa, one at ~120 kDa, and one at ~170 kDa. The protein band at ~60 kDa, which had been a candidate initially (table 3.1), also occurred in the inactive and blank controls, and thus was rejected. The bands at ~98 kDa and ~250 kDa had not been previously observed but were unique to the active extracts and were considered to be potential candidates (table 3.3). Three proteins occurred only in the non-reduced active extracts, at 278 kDa, 263 kDa and 86 kDa, indicating they may be composed of other, smaller proteins observed in the reduced active extracts.

3.4.4. Western Blots – the SIPC and LCA

The footprint extracts were tested for reactivity against SIPC antibodies, and mannose-binding lectin, to determine whether the putative SIPC observed in cyprid footprints (Dreanno *et al.*, 2006a) was similar to the SIPC found in the rest of the cyprid.

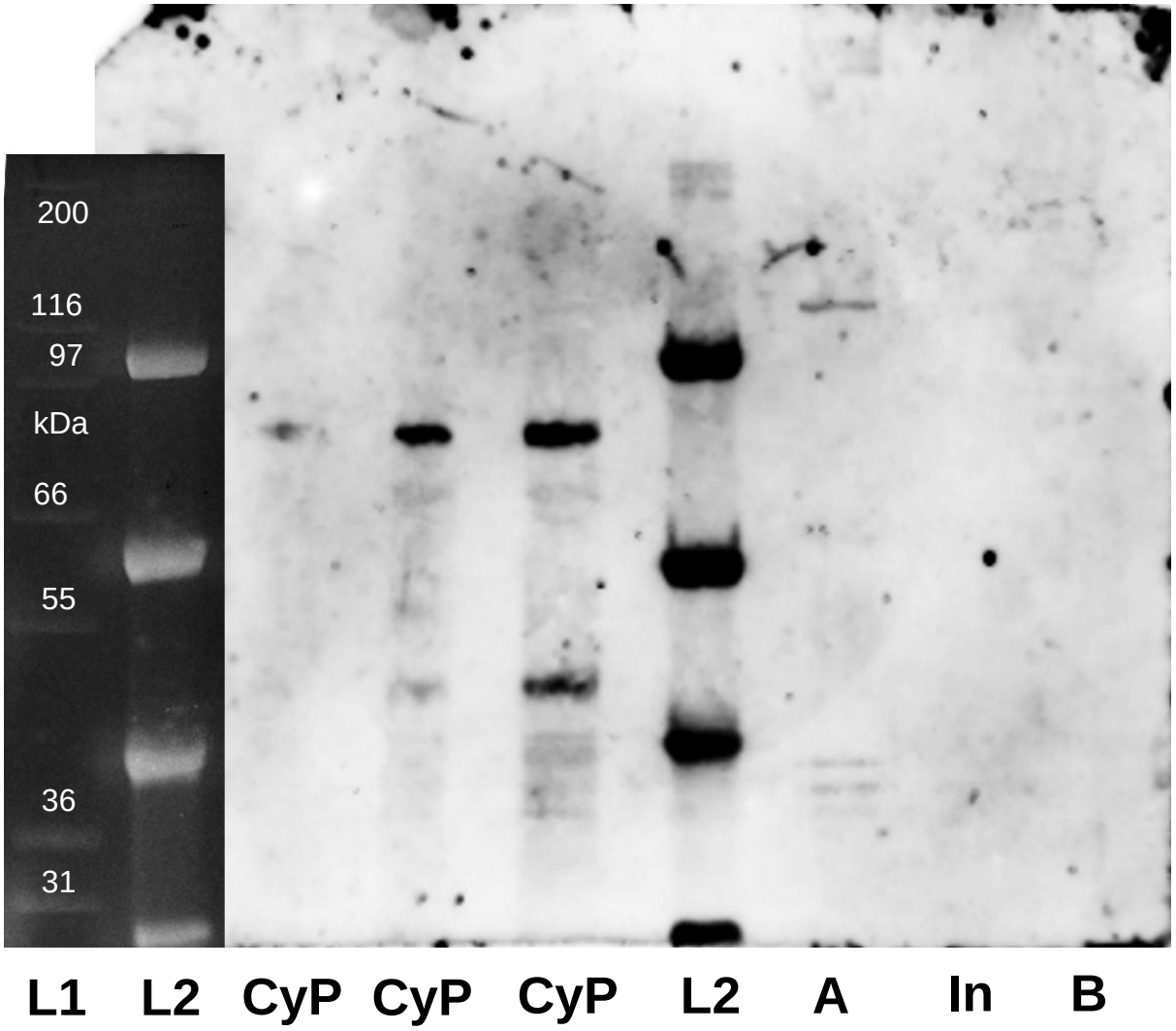

Figure 3.5. Western blot of SIPC antibody reactivity to *B. amphitrite* cyprid protein samples. CyP = whole cyprid proteome, 20%; 50% & 100%, respectively; A = nitrocellulose membranes exposed to active cyprids in 33ppt artificial seawater (ASW); In = nitrocellulose membranes exposed to cyprids rendered inactive by 7% $MgCl_2$ solution; B = Blank, nitrocellulose membranes exposed to 33ppt ASW with no cyprids. L1 = Ladder, protein standard; 31-200 kDa mass, L2 = Ladder, protein standard 27-110 kDa. Images have been adjusted for colour, contrast, and brightness to best highlight the bands. Images were processed in GelAnalyzer 2010 software to isolate the bands.

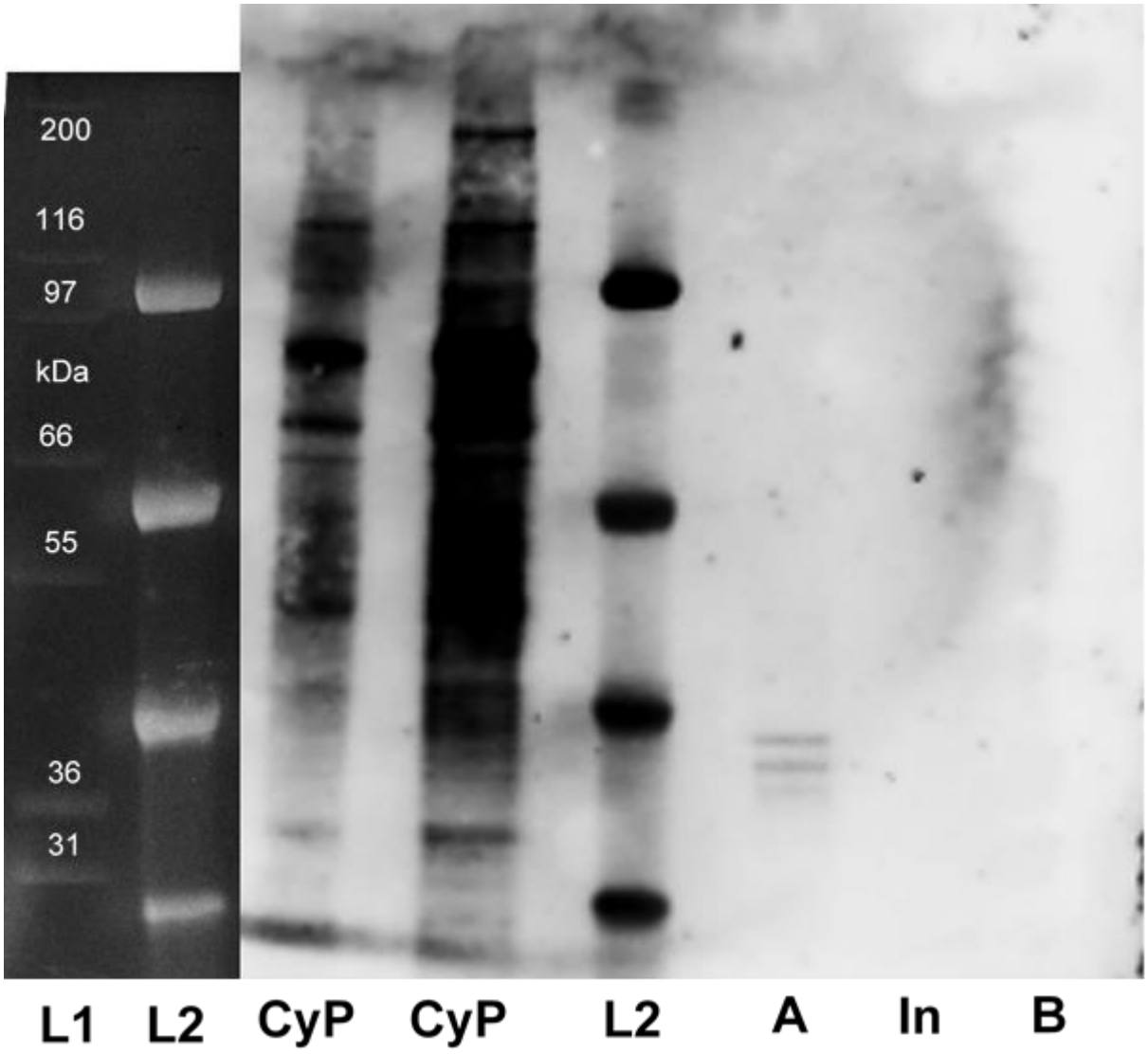

Figure 3.6. Western blot of lens culinaris agglutinin (LCA) reactivity to *B. amphitrite* cyprid protein samples. CyP = whole cyprid proteome, 50% & 100%, respectively; A = nitrocellulose membranes exposed to active cyprids in 33ppt artificial seawater (ASW); In = nitrocellulose membranes exposed to cyprids rendered inactive by 7% MgCl2 solution; B = Blank, nitrocellulose membranes exposed to 33ppt ASW with no cyprids. L1 = Ladder, protein standard; 31-200 kDa mass, L2 = Ladder, protein standard 27-110 kDa. Images have been adjusted for colour, contrast, and brightness to best highlight the bands. Images were processed in GelAnalyzer 2010 software to isolate the bands.

Table 3.4. GelAnalyzer outputs estimating molecular weight (kDa) of detected protein bands from figures 3.4 and 3.5, compared between treatments. Proteins have been aligned and colour coded based on their occurrence patterns: Dark green = stained positive for SIPC and mannose residues in both active footprint and whole cyprid extracts, and none of the controls; light green = stained positive for only SIPC in both active footprint and whole cyprid extracts, and none of the controls; orange = stained positive for only SIPC in only active footprint samples, and none of the controls; pink = stained positive for SIPC and mannose residues in only whole cyprid extracts, and none of the controls; red = stained positive for only SIPC or only mannose in only whole cyprid extracts, and none of the controls.

	figure 3.5	SIPC			figure 3.6	LCA		
Ladder	A (Active)	CyP (Cyprid whole proteome)	In (Inactive)	B (Blank)	A	CyP	In	B
	287							
	266							
	254							
200						184		
						135		
	132	129						
						120		
116						114		
97		86				91		
		72				74		
66						67		
						59		
55						53		
						50		
						46		
		43						
						38		
36	36	37			35	34		
	34	34			33	33		
31	33	33			32	33		
						29		
21						25		

Two major bands stained positively for the SIPC in the whole cyprid proteome, at 86 kDa, and 72 kDa, approximating the 88 and 76kDa subunits of the SIPC (Dreanno *et al.*, 2006c) (figure 3.5). However, these bands were absent from the footprint extracts. Three of the previously identified candidate proteins occurring between 30 and 45 kDa also reacted with the SIPC antibodies in both the active footprint extracts, and the whole cyprid proteome, along with the ~125 kDa band. In addition, three proteins >250 kDa stained positively for the SIPC, matching the trio of bands observed in the non-reduced active extracts discussed previously. These bands were absent in the whole

cyprid proteome (table 3.4). Of the proteins which tested positively for the SIPC in the active footprint extracts, only the three 33-37 kDa proteins also tested positively for LCA (figure 3.6). The two bands observed in the whole cyprid proteome at 86 kDa, and 72 kDa, believed to be SIPC subunits, co-occurred in the LCA blot. None of the inactive or blank extracts stained positively in either assay. There was also no staining in the region of ~80 kDa or 170 kDa for either active footprint extract, where candidate bands had been previously observed (figure 3.6, table 3.4).

3.5. Discussion

The temporary adhesive of barnacle cypris larvae has received little attention compared with the well characterised adult cement. The evidence presented here documents the first steps in developing a collection methodology to provide sufficient material for study, candidate temporary adhesive proteins for further analysis, and insight into the nature of the SIPC as it relates to the temporary adhesive.

The low abundance of temporary adhesive available material has, until now, been a major hurdle to obtaining sufficient material for analysis, as the volume of a single footprint deposit has been estimated to be ~0.5-10 μm^3 depending on the adsorbing surface (Phang et al., 2008; Phang et al., 2010; Di Fino, 2015). The solution was to allow many cyprids to explore nitrocellulose membrane, a substrate known to retain footprint material (Dreanno *et al*., 2006a), and then pool the retained material. The high density of cyprids per Eppendorf was used to stimulate gregarious behaviours, as *B. amphitrite* cyprids are well known to increase their exploration and settlement in the presence of conspecific cyprids, thus depositing a higher volume of footprint material for collection (Clare *et al.*, 1994; Head *et al.*, 2003; 2004; Elbourne *et al.*, 2008).

The second issue was that of extraction. Criteria for selecting an appropriate solvent were limited given the paucity of information on the protein composition of the temporary adhesive. The use of 8M urea, a strong denaturant widely used for solubilising proteins (Herbert, 1999), was guided by the partial success of using this solvent to solubilise adult barnacle cement proteins (He *et al.*, 2013; 2018; Schultzhaus *et al.*, 2019). It is worth noting that as the comparison between reduced

and non-reduced protein extracts (table 3.3, figure 3.4) indicated the presence of several high molecular mass proteins (250-290 kDa), which were potentially broken down by the reducing process, the inclusion of reducing agents in the extraction buffer may improve extraction process. Low concentrations of DTT in urea buffers have also been documented to assist in the solubilisation of adult cement proteins (He *et al.*, 2013; 2018). The resulting protein extracts from a single batch collection could not be visualised following SDS-PAGE by traditional Coomassie staining (data not shown) but were by more sensitive silver staining (figure 3.2). Combining different batches of footprints served to concentrate the protein content to a sufficient level for Coomassie visualisation, western blotting (figure 3.5) and mass-spectrometry analysis.

The primary aim of this chapter was to identify temporary adhesive protein candidates to carry forward for further analysis. The cyprid temporary adhesive, or at least the footprint deposits, have been documented as predominately proteinaceous by way of histochemical staining and protease degradation (Walker and Yule, 1984; Aldred *et al.*, 2008). By using SDS-PAGE to compare the proteins which occurred in extracts from membranes on which cyprids had explored and those which had not, initial identification of candidate proteins was possible (figure 3.2). Of the candidates identified in the initial investigation, none correlated with previously reported adult cement proteins by way of molecular mass, though there was some similarity to the permanent cement protein composition reported by Al-Aidaroos *et al.* (2016). The permanent cement was reported to be composed of several small proteins between 20-43 kDa, with an additional one at 66 kDa, compared to the candidate proteins observed here being 30-42 kDa, with an additional one at 62 kDa (Al-Aidaroos *et al.* (2016). Other temporary adhesive candidates were, however, observed at higher molecular masses, ~79 and ~125 kDa, so it remains unlikely that the materials are the same. These candidate proteins are not components of the permanent cement, as all co-occurred in extracts from membranes which had been cut to remove permanent cement deposits, and those which had not (table 3.3). In fact, these two extracts displayed a band similarity of over 92%. It is possible that the 8M urea used to extract the proteins from the nitrocellulose was not capable of solubilising the permanent cement without addition of further reducing or denaturing agents.

When comparing the reduced and non-reduced extracts to those not reduced, the ~60 kDa protein was also observed in the inactive and blank controls and was thus

discounted as a candidate temporary adhesive protein. However, the remaining candidates previously observed were all present in both the reduced and non-reduced extracts, indicating it is unlikely they take on a quaternary structure. However, several new candidates were observed at ~98 kDa, ~170 kDa and >250 kDa. The protein at ~170 kDa may be a trace of the SIPC. The SIPC and MULTIFUNCin have been reported occurring at ~180 kDa (Dreanno *et al.*, 2006c; Ferrier *et al.*, 2016; Zimmer *et al.*, 2016).

To narrow down the candidate proteins further, the known homology of the temporary adhesive to the SIPC was used, by testing footprint extracts for reactivity with antibodies raised against the SIPC (Dreanno *et al.*, 2006a). This revealed seven proteins in the footprint extract, which shared homology with the SIPC: three bands at 30-35 kDa, one at ~125 kDa and three faint bands at >250 kDa, all of which matched previously identified candidates. The low abundance of the three >250 kDa proteins precluded further analysis. However, the identity of the remaining four bands was subsequently examined by peptide mass fingerprinting (Chapter 4)

In addition to identifying candidate temporary adhesive proteins for further study, these investigations also provided some novel insight into the temporary adhesive proteins themselves. Notably, two of the three proteins of >250 kDa were more prominent in the non-reduced sample (table 3.3), suggesting that the reduction of their disulphide bonds causes disassociation into subunits. The candidate at ~125 kDa was approximately half the molecular mass of these proteins, so it might occur natively as a dimer, despite its appearance in both reduced and non-reduced active extracts (table 3.3). There is a precedent for the formation of dimers by barnacle proteins, as the SIPC and MULTIFUNCin are hypothesised to form homodimers as a quaternary structure (Matsumura *et al.,* 1998; Ferrier *et al.*, 2016; Zimmer *et al.*, 2016), and the known homology that the temporary adhesive protein(s) share with the SIPC lends further credence to this theory (Dreanno *et al.*, 2006a). Furthermore, both the ~125 kDa protein, and the >250 kDa proteins reacted with SIPC antibodies, indicating they share at least some structural commonalities (table 3.4). It is also noteworthy that the ~125 kDa protein, stained intensively with silver staining. Given the known affinity of silver stains for Asp, Glu, His, Cys and Lys residues, this may indicate a high content of these amino acids within this protein. This would parallel the structure of the 20 kDa adult cement protein, which is also rich in these charged amino acids (Mori *et al.*, 2007;

Kamino *et al.*, 2016). Cys, in particular, forms disulphide bonds, the reduction of which in the active extracts resulted in the absence of some of the >250 kDa proteins, lending further support to the hypothesis that these are in fact a disulphide-bonded quaternary structure of the ~125 kDa protein.

While the >250 kDa, ~125 kDa and three 30-35 kDa proteins shared some homology with the SIPC by antibody reactivity (figure 3.5), there was no evidence of the putative SIPC subunits, which were observed in the whole cyprid proteome extracts (at 72 and 86 kDa), in the footprint extracts (table 3.4) (Dreanno *et al.*, 2006c). The C-terminus antibody used was that shown to have affinity for footprint deposits by Dreanno *et al.* (2006a). This suggests that the temporary adhesive proteins may not include the full molecule of the SIPC, as described from adult tissues, but may contain an epitope. The ability of footprints to stimulate conspecific gregarious settlement behaviours has been documented consistently (Walker and Yule, 1984; Clare et al. 1994; Head *et al.*, 2003; 2004; Elbourne *et al.*, 2008). However, it appears that the full SIPC molecule isolated from adults is not required to elicit this response, thus the active portion(s) is able to be included in the temporary adhesive, while altering the remainder of the protein structure. This concept was demonstrated by Kotsiri *et al.* (2018), whereby certain fragments of recombinant adult SIPC could stimulate settlement in *B. amphitrite*.

In addition to the SIPC, the footprint extracts were tested for reactivity against LCA, a lectin that reacts with D-mannose and D-glucose residues (Matsumura *et al.*, 1998). In the whole cyprid extracts, bands are present concurrent with those of the SIPC 88 and 76 kDa subunits (figure 3.6, table 3.4). Mannose residues of the SIPC are reported to be involved in stimulating gregarious behaviours, as blocking the residues leads to settlement inhibition (Matsumura *et al.*, 1998; Khandeparker *et al.*, 2002; Pagett et al., 2012). Thus, given that footprint deposits stimulate settlement, mannose residues present a potential mode of action on the that the temporary adhesive protein(s). Interestingly, while seven proteins from the footprint extracts reacted with SIPC antibodies, only three, the 30-35 kDa bands, reacted with LCA (figure 3.6, table 3.4). The difference in mannose residue occurrence between these proteins indicates they are distinct, and that the temporary adhesive is formed of a mix of proteins, perhaps each with unique functions.

In conclusion, this work presents novel information on the nature of the temporary adhesive protein of *B. amphitrite* cyprids, in particular the relationship to the SIPC. Furthermore, it presents four candidate protein bands for characterisation, at ~125, and ~30-35 kDa, and outlines a collection methodology for future temporary adhesive collection.

Chapter 4. Multi-omics for candidate selection

4.1. Abstract

The application of combined omics workflows to material characterisation are powerful and widely used and have been previously successful in identifying cyprid adhesive proteins. This approach was taken with the aim to identify candidate adhesive proteins. Peptide mass fingerprinting was performed on the protein bands which reacted with the settlement-inducing protein complex (SIPC) C-terminal antibody. A *Balanus amphitrite* cyprid-specific larval transcriptome was generated and used in conjunction with existing multi-stage transcriptomic data as a library for peptide mass fingerprinting. Transcriptome cross referencing and homology searches were used to narrow down candidates. A total of nine candidates were carried forward to expression studies. Interrogation of the candidates and transcriptomes revealed no mRNA sequence coding for the antibody peptide targets that were unrelated to the SIPC, indicating a potentially greater difference between the SIPC and temporary adhesive than previously thought.

4.2. Introduction

Multi-omics is a powerful approach for materials characterisation, having been utilised across a wide variety of marine organisms and proteins, including barnacles (Guerette *et al.*, 2013; 2014; Aldred *et al.*, 2020). This approach involves the cross-referencing of proteomic data with RNA-seq or genomic datasets in order to identify the transcripts relevant to the biological question and serves as an effective means to narrow down the potentially gargantuan datasets that omics provides to manageable levels. The more selective the omics data inputs, by collecting from a specific spatial region or ontogenetic stage for instance, the more streamlined this process becomes, as irrelevant data are excluded before the analysis begins. Aldred *et al.* (2020) demonstrated the efficacy of these principles in barnacle larvae in their analysis of the cyprid permanent cement, and the involvement of chitin. By selecting for proteins extracted from the cyprid cement gland, which also reacted with wheat germ agglutinin (WGA), a chitin-binding lectin, they were able to narrow candidates down to two bands

for peptide mass fingerprinting. To match the peptides, two transcriptomes were used, one covering all stages of *Balanus amphitrite* (= *Amphibalanus amphitrite*), and the other only the cement gland of *Megabalanus rosa*. By cross referencing these datasets, a single putative chitin-containing cement protein was identified and confirmed via immunostaining (Aldred *et al.*, 2020).

The current state of barnacle genomic and transcriptomic data availability is relatively strong. A reference genome for *B. amphitrite* is available (Kim *et al*., 2019), along with several published transcriptomic datasets for *B. amphitrite* and other acorn barnacles (De Gregoris *et al.*, 2011; Al-Aqeel *et al.*, 2016; Abramova *et al.*, 2019b). The transcriptomic data are available for all larval stages (Al-Aqeel *et al.*, 2016) and individual stages for *B. amphitrite* (De Gregoris *et al.*, 2011), and even differing behaviours within a larval stage for *Balanus improvisus* (Abramova *et al.*, 2019). In addition to these cyprid-specific ontogenetic datasets, some spatial data are also available for the antennule and permanent cement glands of *B. improvisus* and *M. rosa*, respectively (Abramova *et al.*, 2019a; Aldred *et al.*, 2020).

The availability of proteomic data is a little weaker, however. While there are just over 4000 entries in the NCBI database for proteins related to '*Balanus'*, the majority of previous work has focused on the adult cement proteins (Kamino et al., 1996; 2000; Mori et al., 2007; Urushida et al., 2007; Kamino, 2013; 2016). Nevertheless, important information for the identification of the temporary adhesive protein(s) is available, namely the reactivity of antibodies raised against the settlement-inducing protein complex (SIPC) with footprint proteins deposited by cyprids during exploration (Dreanno *et al.*, 2006).

This chapter aimed to take a multi-omics approach using currently available proteomic and transcriptomic data, in conjunction with the data generated in chapter 3, to identify, through a process of elimination, candidate transcripts relating to the temporary adhesive protein(s). The resulting candidate transcripts could then be utilised for expression analyses. The process consisted of peptide mass fingerprinting, multiple stage specificity transcriptome matching and cross referencing, homology searches, and interrogation for SIPC N- and C-terminal sequences concurrent with the antibody-targeted residues in 3.3.4.

4.3. Experimental procedures

4.3.1. RNA extraction

Barnacle larvae were cultured as described in 2.3.1 until they reached the desired stage, RNA was then extracted using a Qiagen RNeasy plus mini kit. Larvae were filtered from culture buckets using 250 µm mesh for cyprids or 300 µm mesh for nauplii. These filtration steps were preceded with filters of a larger mesh size to remove other particulate matter. Larvae were transferred from the mesh to a dish with autoclaved artificial sea water (aASW) by rinsing the reverse side of the mesh, then washed with aASW twice to clean the larvae of debris and microalgae. Washed larvae were allowed to recover at 28°C for one hour before being transferred to RNase AWAY™-treated baskets in 1.5ml sterile, RNase-free tubes. The larvae were washed briefly in DEPC-treated Milli-Q water, before being transferred into lysis buffer (supplied with the kit) and lysed by Qiagen PowerBead Tubes Garnet (0.7mm) in 600 µl of the buffer. From this point, RNA was extracted, and gDNA removed, as per the manufacturer's instructions. The resulting RNA was frozen at -80°C until use in library preparation.

4.3.2. Library preparation, sequencing and transcriptome assembly

Library preparation, sequencing and transcriptome assembly were performed as described by Guerette *et al.* (2013; 2014).

Briefly, 5 µg of total cyprid RNA was used to construct the RNA-seq library. Enrichment of poly-A messenger RNA (mRNA) was performed using oligo dT beads (Invitrogen). Enriched mRNA was prepared into a paired end library using ScriptSeq mRNA-Seq library kit v1 (Illumina). Final library amplification was performed for 12 cycles using Phusion PCR polymerase (Thermo Scientific). The resulting library was cleaned with a MinElute PCR purification kit (Qiagen) and checked with an Agilent 2100 Bioanalyzer for quality and quantity. The library, diluted to 8 pM, was used to generate clusters on paired-end flow cells on an Illumina cBot. The library was then sequenced using an Illumina GAIIx, collecting 2 x 76 bp paired end reads. Illumina Offline Base Caller was used to convert the reads to FASTQ format. The transcriptome was assembled *de*

novo using Trinity (Grabherr *et al.*, 2011) set to default parameters and used in downstream applications (hereafter referred to as the 'NTU transcriptome').

In addition to the NTU transcriptome, the publicly available transcriptome for stage 2 and 6 *B. amphitrite* nauplii, and cyprids, generated by Al-Aqeel *et al.* (2016) (NCBI SRX661927) was used. This will be referred to as the 'KAUST transcriptome'.

4.3.3. Mass spectrometry

The four bands that the SIPC C-terminal antibody reacted with (3.3.4, figure 3.5) were excised for mass spectrometry analysis and peptide mass fingerprinting, with two replicates for each band.

SDS PAGE bands were excised with a clean scalpel (wiped with lint free tissue after each cut). Each band was diced into 1 mm^3 cubes and transferred to a clean microcentrifuge tube. Gel pieces were destained by the addition of excess 50mM ammonium bicarbonate: 50% acetonitrile. The destaining buffer was removed and exchanged 3 times, or until the gel pieces were clear. A molecular weight marker band was also excised as a digest control. Proteins were reduced with 10 mM dithiothreitol for 30 minutes at 60˚C to break disulphide bridges. This was followed by alkylation with 50 mM iodoacetamide for 30 minutes, at room temperature, in the dark, to prevent disulphide reformation. Gel pieces were washed in 50 mM ammonium bicarbonate and then dehydrated with 3 washes of 100 μL of acetonitrile. Residual moisture was removed from gel pieces in a vacuum drier. Proteins were digested by the addition of trypsin at a ratio of 30:1 (protein:trypsin), buffered with 50 mM ammonium bicarbonate and incubated for 16 hours at 37 ˚C. The digest was stopped by the addition of 10% TFA to a final concentration of 0.5% and shaken for 30 minutes. The liquid containing hydrophilic peptides was transferred to a fresh microcentrifuge tube. Acetonitrile (80%) with 2% TFA was then added to the gel pieces and shaken for 30 minutes at 750 rpm. This dehydrates the gel pieces and removes hydrophobic peptides from the gel. The solution containing hydrophobic peptides was pooled with the hydrophilic peptide mix. The peptide solution was dried in a centrifugal evaporator and peptides were dissolved in 3% acetonitrile, 0.1% TFA. The resulting peptide solutions were desalted using self-

packed C18 stage tips (Rappsilber *et al.*, 2007). The sample was dissolved in 50 μL of 3% acetonitrile, 0.1% TFA giving the final concentration of ~1 μg/μL.

A 1 μg protein digest samples were separated with a 97-minute nonlinear gradient (3-40%, 0.1% formic acid) using an UltiMate 3000 RSLCnano HPLC. Samples were first loaded onto a 300μm x 5mm C18 PepMap C18 trap cartridge in 0.1% formic acid at 5 μl/minute and passed on to an in house made 75μmx25cm C18 column (ReproSil-Pur Basic-C18-HD, 3 μm, Dr. Maisch GmbH) at 400 nl per minute. The eluent was directed to an Ab-Sciex TripleTOF 6600 mass spectrometer through the AB-Sciex Nano-Spray 3 source, fitted with a New Objective FS360-20-10 emitter.

For data-dependent data acquisition (DDA), MS1 data were acquired within a range of 400-1250 m/z (250ms accumulation time), followed by MS2 of top 30 precursors with charge states between 2 and 5 (total cycle time 1.8 s). Product ion spectra (50ms accumulation time) were acquired within a range of 100-1500 m/z, using rolling collision energy for precursors, which exceed 150 cps. Precursor ions were excluded for 15 s after one occurrence.

The acquired DDA data were searched against the KAUST transcriptome, translated into amino acids in all six reading frames using EMBOSS Transeq (EMBL-EBI) on Ubuntu Linux v18.04 LTS, then concatenated to the Common Repository for Adventitious Proteins v.2012.01.01 (cRAP, ftp://ftp.thegpm.org/fasta/cRAP), using TheGlobalProteome Machine (GPM). The parameters used were cysteine alkylation: iodoacetamide, digestion enzyme: trypsin, parent mass error of 20ppm, fragment mass error of 30ppm.

4.3.4. Transcriptome and genome interrogation

Interrogation of the transcriptomes was performed on the public server at usegalaxy.org (Jalili *et al.*, 2020). Unless otherwise stated, the BLASTn tool (Altschul *et al.*, 1990) was used with default parameters.

Identification of the mRNA sequences on the SIPC which coded for the peptides against which the C- and N-terminus antibodies were raised, used expasy.org (Gasteiger *et al.*, 2003). The SIPC mRNA sequence (ENA: AY423545.1) was

translated to its amino acid sequence, the correct reading frame selected and the peptide sequence against which the antibody was raised was manually located. The mRNA coding sequences for these peptides were recorded and verified through BLASTn short read optimised searches of the transcriptome, which identified transcripts aligned to the SIPC in the correct regions.

Interrogation of the *B. amphitrite* genome (NCBI: PRJNA549550) was performed using the online 'BLAST Genomes' function with default parameters.

4.4. Results and discussion

4.4.1. Candidate selection

The mass spectrometry peptide mass fingerprinting identified 51 candidates from the KAUST transcriptome over the four protein bands carried forwards from chapter 3. Some of these candidates occurred in multiple bands in the 30-35 kDa range, but there was no overlap between the 125 and the 30-35 kDa band candidates. The number of candidates needed to be reduced to allow for targeted expression studies.

The first step to eliminating candidates was cross referencing between the multiple stage KAUST and cyprid only NTU transcriptomes, to ensure all candidates were expressed at the cyprid stage. A cut-off of 80% coverage and identity was used to confirm parity between the two datasets. This is below the combined per base and mutated sequence error rate of ~7% proposed by Pfeiffer *et al.* (2018). The lower threshold was chosen to allow for differences in geographical population, assembly methods, and transcripts not overlapping. This removed almost 50% of candidates. BLAST searches of the rejected candidates revealed that the majority did not have homology with known arthropod nucleotide records, and those that did were of low homology. Others were identified as contaminating organisms, such as *Vibrio owensii*, a crustacean pathogen (Cano-Gómez *et al.*, 2010). The remaining candidates are presented in table 4.1.

Table 4.1. Transcriptome cross-referencing. Candidate transcript matches (>80% cover and identity) between the KAUST and NTU transcriptomes, as identified by BLASTn sequence alignment. 'Gel band' indicates which SDS PAGE gel band the transcript is associated with from those put forward for peptide mass fingerprinting.

Query sequence (KAUST)	Subject sequence (NTU)	Cover	Identity	e value	bitscore	gel band (kDa)
k85_1865598	NODE_6813	100%	97.424%	0	1125	125
k45_6243571	NODE_12522	93.4%	81.377%	0	924	125
k45_1194892	NODE_16940	99.4%	99.375%	4.42E-165	580	32.5
k45_6229312	NODE_11739	100%	96.315%	0	981	30-32.5
k45_6236322	NODE_1719	88%	97.684%	0	2150	35
k45_6245999	NODE_5445	100%	100%	0	2248	32.5
k55_4432846	NODE_26764	100%	93.123	1.78E-144	512	35
k55_4766728	NODE_15688	100%	97.889	0	1552	35
k55_4809949	NODE_26814	100%	97.885	0	1146	30-35
k65_2820919	NODE_67014	100%	98.551	0	732	32.5
k65_3283434	NODE_42329	99.3%	94.276	2.58E-127	455	35
k65_3642173	NODE_1889	100%	97.211	0	850	30
k65_3659377	NODE_4268	100%	98.039	0	798	35
k65_3660540	NODE_2621	100%	99.537	0	4715	30
k75_2466758	NODE_29304	82%	94.136	0	1428	30-35
k75_2476289	NODE_5283	100%	96.774	1.02E-161	569	30
k75_2496648	NODE_5654	100%	96.875	0	804	35
k75_2505784	NODE_3504	100%	98.806	0	1194	35
k75_645919	NODE_13780	100%	99.412	3.57E-176	617	32.5

k85_1827598	NODE_119290	100%	100	2.63E-160	568	30
k85_1841077	NODE_21781	100%	96.595	0	926	35
k85_1857937	NODE_8120	100%	98.597	0	883	35
k85_1859180	NODE_897	100%	98.423	0	1116	30
k85_1877424	NODE_7520	100%	99.722	0	660	35
k85_1882426	NODE_33480	89%	96.933	5.15E-155	547	35
k85_1893376	NODE_6717	100%	98.3	1.03E-176	619	35
k85_1830366	NODE_21933	99.9%	96.336	0	1700	30

The cross-referenced candidates were subjected to a generic BLAST homology search, with the aim of rejecting candidates which exhibited high homology with known, non-adhesive, records. The settlement-inducing protein complex (SIPC) of *B. amphitrite* shares 63–76% homology of its predicted amino acid sequence with other acorn barnacle species (Yorisue *et al.*, 2012), so a cut-off in the middle of this range was selected; 70% cover and identity. None of the candidates displayed high homology with known adhesive proteins. The homologies are presented in table A1.

The highest quality peptide fingerprinting matches were selected from the remaining candidates following the BLAST homology search. The quality was determined by the number of peptide matches, a log(e) value of -2 or below, and/or occurrence in multiple gel bands. This selection was based on the occurrence of the SIPC C-terminal activity in all four bands submitted to peptide mass fingerprinting, indicating an analogous or shared region. This provided six candidates (table 4.2.)

Table 4.2. Peptide mass fingerprinting quality. The six highest quality candidate transcripts based on their corresponding mass spec peptide matches. Log(I) = sum of raw spectrum intensities; rI = number of peptides found; log(e) = expectation of finding the protein stochastically. 'Gel band' indicates which SDS PAGE gel band the transcript is associated with from those submitted for peptide mass fingerprinting.

Sequence Identifier	log(I)	rI	log(e)	Gel band (kDa)
k85_1865598/ NODE_6813	2.99	2	-8	125
k45_6229312/ NODE_11739	3.12	1	-1.5	30-32.5
k65_3660540/ NODE_2621	4.02	1	-2	30
k65_3283434/ NODE_42329	3.23	1	-2	35
k75_2466758/ NODE_29304	4.37	2	-10	30-35
k45_6236322/ NODE_1719	3.25	1	-2.3	35

In addition to the highest quality peptide fingerprinting matches, candidates from the BLAST homology search were subjected to an additional search limited to only the top 20 NCBI nucleotide database entries for the genera *Balanus*, *Megabalanus*, *Amphibalanus*, and *Semibalanus*. From these results, five candidates shared some homology with either an SIPC analogue or a known acorn barnacle adhesive protein and were added to the candidate list. Two of these overlapped with the highest quality peptide fingerprinting selected candidates. However, while the sequence identities were universally over 80% among the matches, the cover was extremely low, indicating that the SIPC analogues and cement proteins do not share significant structural similarities. These candidates are presented in table 4.3.

Table 4.3. Acorn barnacle cement/SIPC homology search. BLASTn sequence alignments found in the top 20 NCBI nucleotide database entries for acorn barnacles of the genera *Balanus, Megabalanus, Amphibalanus, and Semibalanus.* Results curated for entries containing known adhesive, cement, or SIPC analogue sequences.

Name	Best Assignment (Blastn)	Cover	Identity	E value	Total Score	Accession	Gel band (kDa)
k45_6236322/ NODE_1719	*Balanus improvisus* SIPC mRNA for settlement inducing protein complex, partial cds	1%	88.46%	0.013	34.6	AB695618.1	35
k85_1859180/ NODE_897	*Chthamalus fissus* MULTIFUNCin mRNA, complete cds/ *Amphibalanus improvisus* waterborne settlement pheromone-like protein 2 mRNA, complete cds	5%/ 0.1%	82.86%/ 87.5%	0.011/ 2e-04	37.4/ 41	KC152473.1/ MK275630.1	30
k75_2466758/ NODE_29304	*Amphibalanus amphitrite* CP52-like cement protein 3 mRNA, partial cds	2%/ 2%	82.35%/ 84.38%	0.005/ 0.006	35.6/ 36.5	KY285989.1	30-35kDa
k65_2820919/ NODE_67014	*Amphibalanus amphitrite* CP19-like cement protein 4 mRNA, partial cds	5%/ 3%	91.30%/ 91.30%	0.007/ 0.011	33.7/ 33.7	KY285987.1	32.5kDa
k85_1830366/ NODE_21933	*Megabalanus volcano* cement protein 113k mRNA, complete cds	2%/ 5%	87.10%/ 87.10%	0.001/ 6e-04	35.6/ 35.6	MK336236.1	30kDa

The final candidate selection stage was performed based on the occurrence of antibody residues. The protein bands used for peptide mass fingerprinting had reacted with SIPC C-terminal antibodies (3.3.4), and footprint deposits react with SIPC antibodies raised against both the C- and N-terminals (Dreanno *et al.*, 2006a). As such, the candidates which had passed the BLAST homology search were queried for the reverse translated nucleotide sequences associated with the peptides against which the antibodies were raised (table 4.4). None of the candidates contained either antibody sequence, but no candidates were eliminated based on this finding as transcripts do not necessarily represent complete mRNA sequences. Therefore, the C- and N-terminal antibody sequences may be situated in a region that was not covered. Additionally, the antibodies may have reacted to a region of the footprint deposit protein(s), which was similar enough to the SIPC to cause cross-reactivity, but was comprised of a different peptide and mRNA coding sequence.

Table 4.4. Candidate SIPC antibody search. Peptide, and corresponding reverse translated mRNA sequences against which SIPC C- and N-terminal antibodies were raised. The reverse translated mRNA sequences were not present in any candidate sequence identified by peptide sequencing.

Antibody terminal	Peptide sequence	Reverse translation	Short read optimised Blastn hits
C	PEERNIQEYELT	cctgaggagaggaacattcaggagtacgagctgact	0
N	STHKKYESHVKTEF	agcacacacaagaagtacgagtcgcacgtgaagaccgagttc	0

As no matches to the antibody-recognised sequences were found among the candidates from peptide fingerprinting, the full KAUST and NTU transcriptomes were searched for the C- and N-terminal mRNA sequences. A total of 35 matches were found, 34 of which aligned with the *B. amphitrite* mRNA sequence with over 80% coverage and identity (BLASTn). The one remaining match (k55_3755605) contained the SIPC C-terminal antibody target and had a high similarity with the SIPC mRNA sequence, but only in a localised region, as the coverage was below 15%. This transcript was added to the candidate list based on the hypothesis that the footprint protein(s) shares an analogous region with the SIPC but is not identical.

Given the potential for transcripts from transcriptome assemblies to provide incomplete sequence coverage, the candidates were aligned to the *B. amphitrite* reference genome (Kim et al., 2019), with the aim of determining if the C- and N-terminal antibody residues occurred on the same transcripts as the candidates and, if

so, in the same region. Three candidate transcripts were found to share a contig in the genome with the C- and N-terminal antibody residues, with one (k55_3755605) located within 5 kb of the C-terminal sequence (table 4.5). Five kb was selected as the localised distance, as it translates to a protein size of ~185 kDa, which is within the size range of the SIPC/MULTIFUNCin (Dreanno et al., 2006b; Ferrier et al., 2016). However, this transcript also shared a local region with the SIPC mRNA sequence. Due to its close proximity to the SIPC gene, this candidate was removed from the final selection (table 4.6).

The absence of any significant homology with the *B. amphitrite* SIPC mRNA sequence amongst the candidates, and the lack of transcripts from either transcriptome or genome containing the C- or N-terminal, which do not align with the SIPC mRNA sequence, suggests that the SIPC molecule characterised by Dreanno et al. (2006b) is not involved in the temporary adhesion process, and the analogue which stimulates footprint mediated gregarious settlement (Clare et al., 1994; Head et al., 2003; 2004; Elbourne et al., 2008) and reacts with antibodies raised against the SIPC (Dreanno et al., 2006a), may be significantly different.

Table 4.5. Final candidate alignments with *Balanus amphitrite* reference genome transcripts containing the SIPC C- and N-terminal antibody sequences. Colours indicate adjacency: red = >5kb away from a SIPC antibody sequence; yellow = <5kb from an SIPC antibody sequence and a SIPC mRNA alignment.

Sequence Identifier	Genome transcript	Alignment start location on transcript (bp)	Cover	Identity	E - value	Total score	Accession
SIPC mRNA	516	215650/ 162897	99%	100%	0	20214	VIIS01001705.1
SIPC mRNA	919	228243	65%	80.65%	2.00E-144	8214	VIIS01002152.1
Anti-SIPC - C	919	228243	55%	100%	0.038	37.4	VIIS01002152.1
Anti-SIPC - C	516	216032/ 163285	100%	100%	0.003	156	VIIS01001705.1
k85_1865598/ NODE_6813	919	270366	73%	66.55%	5e-110	475	VIIS01002152.1
k45_6236322/ NODE_1719	919	214650	2%	78.87%	1e-06	61.7	VIIS01002152.1
k55_3755605	919	230050	55%	100%	0.038	37.4	VIIS01002152.1
k55_3755605	516	215696/ 162944	16%	91.80%	8e-16	176	VIIS01001705.1

In total, the analysis provided nine final candidates to carry forward for expression studies (table 4.6). The process of candidate selection is outlined in figure 4.1.

Table 4.6. The nine final candidates selected for expression studies, aligned with *Balanus amphitrite* SIPC mRNA sequence Colours indicate the source of selection: green = peptide mass fingerprinting quality; yellow = peptide mass fingerprinting quality and acorn barnacle homology; and blue = acorn barnacle homology.

Sequence Identifier	Cover	Identity	E value	Total score	Gel band (kDa)
k85_1865598/ NODE_6813	-/ 0%	-/ 100%	-/ 0.036	-/ 28.3	125
k45_6229312/ NODE_11739	-	-	-	-	-
k65_3660540/ NODE_2621	-	-	-	-	-
k65_3283434/ NODE_42329	-	-	-	-	-
k75_2466758/ NODE_29304	1%/ 1%	90%/ 90%	0.017/ 0.019	28.3/ 28.3	30-35
k45_6236322/ NODE_1719	-	-	-	-	-
k85_1859180/ NODE_897	-/ 0%	-/ 94.74%	-/ 0.017	-/ 31.0	30
k65_2820919/ NODE_67014	-	-	-	-	-
k85_1830366/ NODE_21933	-	-	-	-	-

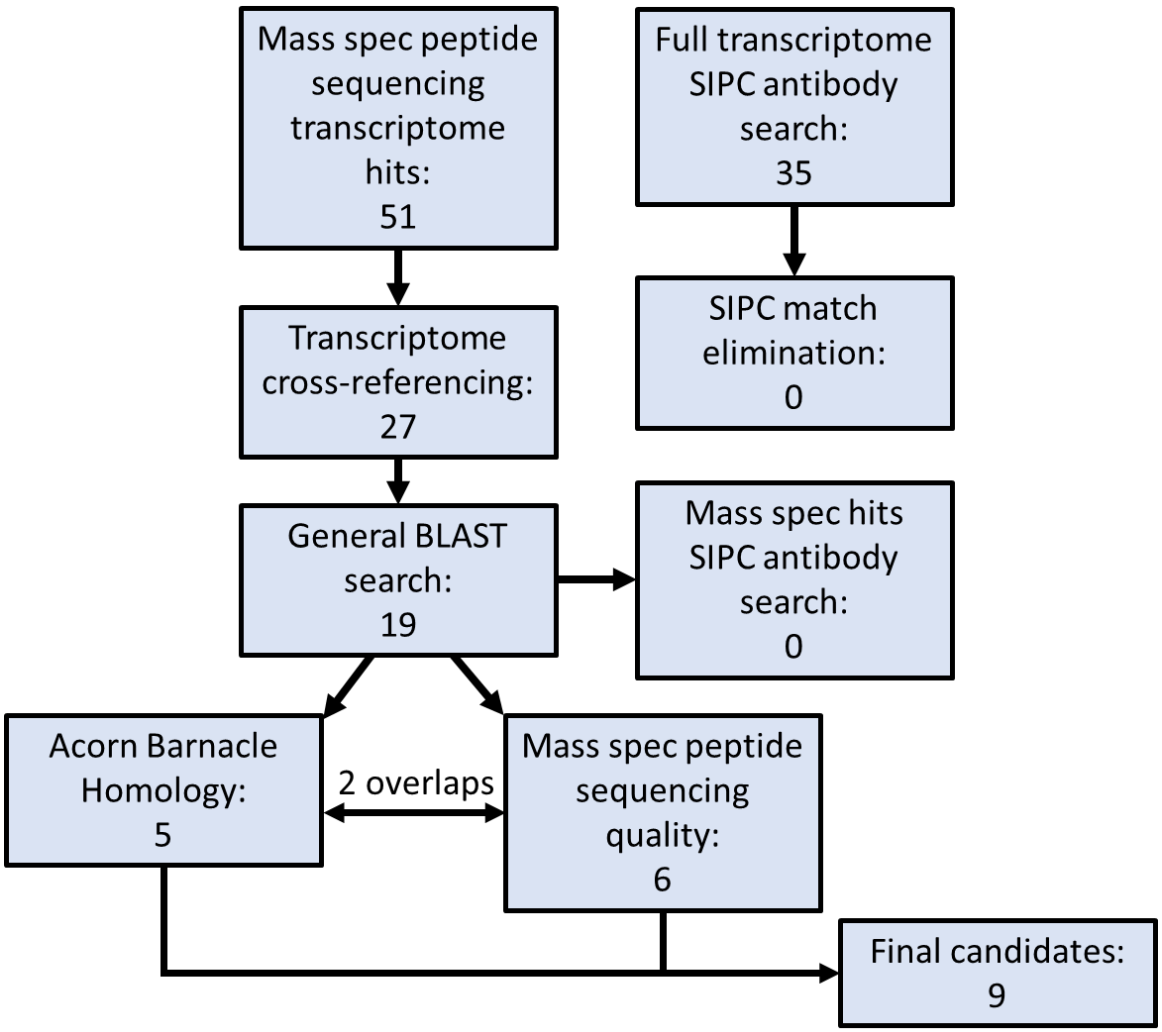

Figure 4.1. Flow chart of the candidate identification processes, and the number of candidate transcripts retained after each step.

4.5. Conclusion

The use of a combined omics approach to candidate selection has identified candidate temporary adhesive proteins from peptide mass fingerprinting and transcriptomic data and narrowed down those candidates to a feasible number (nine) for expression studies. These investigations have also revealed that the SIPC molecule, as it exists in adult and larval cuticles, may not have a high similarity to the protein(s) involved in temporary adhesion. Furthermore, the sequences against which the C- and N-terminal antibodies were raised on the SIPC, are not present on any mRNA captured in the transcriptome that does not align strongly with the SIPC mRNA.

Chapter 5. Spatial and Ontogenetic Expression of Candidates

5.1. Abstract

Studies of mRNA expression in acorn barnacles have used a variety of molecular tools. Prior work on cyprids has often focused on changes in expression associated with pathways involved in metamorphosis, and the tools have been relatively underused to identify adhesives. Here, qPCR, RNA-seq differential expression analyses, and whole mount in-situ hybridisation were applied to the previously selected candidate adhesive proteins. The candidates upregulated in cyprids over stage 6 nauplii and downregulated in permanently attached cyprids and early juveniles were considered to align most closely to the expected expression pattern of a cyprid-specific temporary adhesive. The most promising candidate was not localised to the region of the temporary adhesive gland, and instead was distributed in patches across the carapace. A role in carapace formation and repair was hypothesised for this candidate. The identity of the temporary adhesive protein(s) remains elusive. Some broad-scale expression differences between settlement stages were also highlighted.

5.2. Introduction

The analysis of gene expression patterns has developed drastically over the last three decades, with a range of powerful tools and techniques available depending on the desired purpose. Three of the most common techniques are quantitative PCR (qPCR) (Higuchi *et al.*, 1993), RNA sequencing (RNA-seq) (Stark *et al.*, 2019) and in-situ hybridisation (ISH) (Cassidy and Jones, 2014). All these techniques have been utilised in the study of acorn barnacle larvae.

5.2.1. Quantitative PCR

Quantitative PCR has been applied to all barnacle life stages, and for a range of target genes. The distinct developmental stages of barnacles, and subsequent post-settlement metamorphosis, makes them an ideal target for qPCR as the organisms

can be separated by phenotype and will often display significant differences in expression due to the variable functions of each life stage.

In adult acorn barnacles, qPCR has been used to study the spatial expression of cement proteins (Lin *et al.*, 2014; Wang *et al.*, 2015), improving understanding of the cementing process, and spatial and ontogenetic expression patterns of osmoregulation genes in response to salinity changes, helping to elucidate environmental tolerances (Lind *et al.*, 2013; 2017).

For cyprids, the range of targets investigated by qPCR is even greater, including ontogenetic expression patterns of receptors for mannose, ecdysone, neuropeptide, and sound (Chen *et al.*, 2011; Al-Aqeel *et al.*, 2016; Yan *et al.*, 2017); vitellogenin and neuropeptides (Chen *et al.*, 2011; Yan *et al.*, 2012); nitric oxide signalling pathways related to settlement (Zhang *et al.,* 2012); and a 20 kDa adult cement protein homologue (Chen *et al.*, 2011). Identification and quantification of barnacle larvae in zooplankton samples has also been successfully performed using qPCR (Endo *et al.*, 2010; Gaonkar *et al.*, 2015).

While several studies purport to reveal expression changes relating to the signalling pathways and morphological transitions associated with larval metamorphosis and settlement (Chen *et al.*, 2012; 2014; Al-Aqeel *et al.*, 2016; Yan *et al.*, 2012; 2017), no study thus far has attempted to identify the temporary adhesive protein(s) through expression analyses. Perhaps more surprisingly, the SIPC has been included in only a single qPCR study on the stalked barnacle *Pollicipes pollicipes* (Rocha *et al.*, 2015), despite its importance in the settlement process of barnacle larvae, and the publicly available sequence data for five acorn barnacle species (NCBI). SDS-PAGE comparisons of the SIPC expression patterns in acorn barnacles have been made, however, indicating that expression begins at low levels in stage six nauplii, then increases drastically in the cyprid to adult stages (Dreanno *et al.*, 2006c; Kotsiri *et al.,* 2018). This is contradictory to the findings of Rocha (2015), which indicated that expression of the SIPC in *P. pollicipes* cyprids was lower than in stage six nauplii, juveniles and adults.

5.2.2. RNA sequencing and differential expression analysis

RNA-seq and differential expression analysis have also been powerful tools in understanding the ontogenetic expression patterns of acorn barnacles and have frequently been used in tandem with qPCR to select targets (Chen *et al.*, 2011; Al-Aqeel *et al.*, 2016; Yan *et al*., 2012; 2017). For barnacles, the ontogenetic expression patterns displayed by the two methods are typically similar, though not always identical (Al-Aqeel *et al.*, 2016).

There are several advantages of using RNA-seq over qPCR. First, while qPCR is limited to a few carefully selected targets with well-designed primers and reference genes, RNA-seq can capture the expression levels of millions of potential genes simultaneously. In barnacles, this has allowed for the up and down regulation of entire pathways to be identified (Chen *et al.*, 2011; Lind *et al.*, 2017; Yan *et al*., 2017; Abramova *et al.*, 2019a). This broad application does not preclude the use of RNA-seq and differential expression analysis for the use on a few specific targets, however. The technique has been applied to the identification of cement proteins in both adult and larval acorn barnacles (Lin *et al.*, 2014; Yan *et al.*, 2020).

The other major advantage of RNA-seq analysis is that the raw data are easy to share and can be used for analyses other than that which the original authors intended. Unfortunately, the current state of the publicly available data for acorn barnacles is that the majority are in the format of assembled transcriptomes. While this is excellent for the purposes of material characterisation (chapter 4), it is not for differential expression analysis, as the raw reads per condition are not provided. Nevertheless, raw data are available for *B. improvisus*, divided according to settlement behaviours and stages (Abramova *et al*., 2019b).

5.2.3. In-situ hybridisation

Significantly fewer expression studies are available which utilise ISH in barnacles, however those that do all focus on the larvae (Gibert *et al.*, 2000; Rabet *et al.*, 2001; Dreanno *et al*., 2006c; Chen *et al.*, 2011; Chen *et al.*, 2012). This skewed analysis may be an artefact of the ability to perform whole mount ISH (WISH) on larvae, given

their relatively small size, but not adults. Both whole mount and section-based ISH have been successfully performed on cyprids (Dreanno *et al*., 2006c; Chen *et al.*, 2012). The targets have been diverse, including developmental genes in the vestigial abdomen (Gibert *et al.*, 2000; Rabet *et al.*, 2001), permanent cement proteins (Chen *et al.*, 2011), mannose receptors (Chen *et al.*, 2011) and the SIPC (Dreanno *et al*., 2006c). Expression of the SIPC in *B. amphitrite* was found to be localised to the antennules, thoracic appendages, and cuticle (Dreanno *et al*., 2006c). ISH has not been used in any attempts to identify the temporary adhesive protein(s) as the mRNA sequence(s) of the protein(s) is not known, and the putative homology with the SIPC may confound the design of specific probes (Dreanno *et al.*, 2006a). The relative unpopularity of ISH hybridisation in barnacle gene expression studies in the last decade may be due to its difficult and time-consuming optimisation process, as each organism and probe often requires unique conditions to achieve the desired results.

This chapter aimed to use a combination of these three methods – qPCR, RNA-seq and ISH to characterise the spatial and ontogenetic expression patterns of the candidates defined in chapter 4, in order to identify the temporary adhesive protein(s). For ease of reading, each cross-referenced transcript candidate pair has been assigned a shorthand tag (table 5.1).

Table 5.2. Recap table of the candidates identified in chapter 4, the shorthand tag, and the associated gel band. Colours and tag letters indicate the source of selection. Green/Q = peptide mass fingerprinting quality, yellow/B = peptide mass fingerprinting quality and acorn barnacle homology, blue/H = acorn barnacle homology.

Sequence Identifier	Tag	Gel band (kDa)
k85_1865598/ NODE_6813	Q1	125
k45_6229312/ NODE_11739	Q2	30-32.5
k65_3660540/ NODE_2621	Q3	30
k65_3283434/ NODE_42329	Q4	35
k75_2466758/ NODE_29304	B1	30-35
k45_6236322/ NODE_1719	B2	35
k85_1859180/ NODE_897	H1	30
k65_2820919/ NODE_67014	H2	32.5
k85_1830366/ NODE_21933	H3	30

5.3. Experimental procedures

5.3.1. Quantitative PCR

RNA extraction was performed on cyprids and stage six nauplii as described in 4.3.1. Larvae were split into three batches of ~300 - 400 individuals prior to extraction to provide replicates. All samples were treated with 1 unit of DNase I recombinant RNase-free (Roche) per 1 µg RNA, for 30 minutes at 37°C, in 1x reaction buffer with 0.05 volumes of Protector RNase inhibitor (Roche). The reaction was stopped with 0.1 volume of 0.2 M EDTA (pH 8.0). Samples were then purified by sodium acetate/ethanol precipitation. 0.1 volume of 3 M sodium acetate, pH 5.2, and 3

volumes of ice-cold absolute ethanol (EtOH) were added to the RNA, incubated overnight at -80ºC, then centrifuged for 15 minutes at 16,000 RCF. The resulting pellets were washed three times in ice cold 75% EtOH, dried and resuspended in 50 µl DEPC water. All precipitation steps were carried out at room temperature. Aliquots of cleaned, DNase-treated total RNA were run on a 1% bleach agarose TBE gel to confirm RNA integrity and absence of gDNA contamination (Aranda *et al.*, 2012). RNA concentrations were checked for purity (260/280 >2.0 and 260/230 2.0-2.2) (NanoDrop One) and the samples stored at -80ºC until used for reverse transcription within two weeks.

Reverse transcription was performed using an Applied Biosystems™ High-Capacity cDNA Reverse Transcription Kit as per the manufacturer's instructions: 20µl reactions, incubated at 25ºC for ten minutes, 37ºC for 120 minutes, and 85ºC for five minutes. Reactions were performed in triplicate and then pooled to account for variation in the reverse transcription reactions, plus one no reverse transcription control, for each biological sample, using 1 µg of total RNA input per reaction. These cDNA libraries were stored at -20ºC until used for qPCR.

Primers for the candidate sequences identified in chapter 4, and *B. amphitrite* SIPC mRNA, were designed using Primer3 software (Koressaar and Remm, 2007; Untergasser *et al.*, 2012; Koressaar *et al.*, 2018). The parameters used were as follows: product size range = 100–250, primer size = min 18, opt 120, max 23, primer Tm = minimum 58ºC, optimum 59ºC, maximum 61ºC, primer GC % = minimum 40, optimum 50, maximum 60, all other parameters were left as the default. Oligonucleotides (synthesized by Eurofins Genomics) were resuspended into stock solutions then aliquoted to a concentration of 10 µM and stored at -20ºC until use. Primer sequences are detailed in table 5.2. Three reference genes identified as being stable between larval stages, *mt-cyb, rplL5* and *ef1a*, (De Gregoris *et al.*, 2009) were used for data normalization.

Table 5.3. Per candidate primer sequences used for qPCR analysis.

Tag	Forward primer	Reverse Primer	Amplicon Length
Q1	TCGGCAACACAGACAACAAG	AGGACCTCGGTAGAAGGCTA	137
Q2	GGTGTTTCTCTCGGCCTACT	TAGATGATGAGGTCGGGCAG	126
Q3	TACATACTAGCGCTCCACCG	CGGAGTCTCACAACCTCGA	217
Q4	CGAGTGAGGCGAGAAGAAGA	AGACGACAGCATCTCCAACA	139
B1	ATCTCTTCCAGTATCGCCCG	CTCCTCTGGGTGTTTCTCCA	195
B2	CATGGAGACGCACAAGATCG	GGAACTGATTGTAGCGCGTC	107
H1	TACAACGTCAATCAGCGCAG	TCGGTGGTGACTTTATGGCT	101
H2	GAGTTCGAGTTCACGGTGGA	GTGAAGTTGTACTGGGCGTG	137
H3	AGACTCTTACCACACGTGCT	TCCACACTCGACTCGTACAG	183
SIPC	CAAGAAGTACGAGTCGCACG	GACGCTGGTAGAAGTCGAGA	174

Reactions for qPCR were prepared using 10 µl SsoAdvanced Universal SYBR Green Supermix 2X (BioRad), 8 µl cDNA diluted 1/80 in DEPC treated milliQ water, and 2 µl forward/reverse primer mix to a final concentration of 500 nM each. Two technical replicates of each biological replicate were prepared, in addition to 'no reverse transcription', and 'no template' controls. Reactions were performed in sealed optical grade 8-strip PCR tubes on a CFX Connect qPCR instrument and analysed using CFX Maestro software (BioRad). Cq was determined by single threshold method above the baseline, auto calculated for SYBR. Primer specificity was determined by melt curve analysis (Appendix, figure A1).

The qPCR thermal profile was set as follows: 95^{o}C for 30 seconds, followed by 40 cycles of 15 seconds denaturation at 95^{o}C, and 30 seconds annealing/extension at

60ºC. Following 40 cycles, melt curves were determined using a temperature ramp from 60 to 95°C, with an increase of 0.5°C per 2 second step.

Calculation of relative-fold change was performed using the delta-delta Cq method (Livak and Schmittgen, 2001). Stage 6 nauplii (n = 6) were used as the control group and cyprids the experiment group (n =6). Data were normalised per sample within biological replicates prior to calculation of the normalised mean-fold change. Two sample t-tests were performed on the $\log_2$ values of normalised expression per sample (Minitab 18).

5.3.2. RNA-seq differential expression analysis

RNA-seq data published comprising four *Balanus improvisus* settlement stages published by Abramova *et al.* (2019b) (NCBI bioproject: PRJNA528777) were used for differential expression analysis. The settlement stages were as follows; free swimming cyprids, close searching cyprids, permanently attached cyprids prior to metamorphosis, and early juveniles no more than 5 days post metamorphosis (Abramova *et al.*, 2019b). A transcriptome assembly comprising all stages was searched for homology with the candidate sequences selected in chapter 4 using BLASTn alignment. The highest scoring match for each candidate was used for the analysis. This process was also performed for *B. amphitrite* SIPC mRNA, and the C- and N- terminal reverse translated antibody sequences (chapter 4).

Paired end raw reads files were loaded into Galaxy (usegalaxy.org) by accession number from the NCBI database (PRJNA528777), and trimmed using Trimmomatic (SLIDINGWINDOW, 4 base average, 20 average quality required). Trimmed reads were pseudo-aligned to a Kallisto index created from the transcriptome assembly master data (Abramova *et al.*, 2019b) and quantified using Kallisto (Bray *et al.*, 2016), including sequence-based bias correction, 100 bootstrap samples, and all other parameters set to default. Kallisto quantification data were analysed and visualised in Sleuth (Pimentel *et al.*, 2017). A measurement error model was fitted, and Wald tests performed per condition to provide expression estimates.

5.3.3. Whole mount in-situ hybridisation (WISH)

DIG labelled probes for WISH were designed as follows: Primers were designed as described for qPCR, with the product size range set to 600-1000. The primer pair for Q4 was outside of this range as no suitable primers were found in the desired range. Primers for *B. amphitrite* SIPC mRNA were also designed as a positive control, as the spatial expression patterns for the SIPC via WISH have been published (Dreanno *et al.*, 2006c).

Table 5.3. Forward and reverse primer sequences, with added SP6 and T7 promoter sequences respectively, used for synthesis of PCR products to be used for RNA probe DIG labelling and synthesis.

Tag	Forward primer	Reverse Primer	Amplicon Length
Q1	ATTTAGGTGACACTATAGTCGGCAACACAGACAACAAG	TAATACGACTCACTATAGGGACAGTCACCGTCCTCATTGT	980
Q2	ATTTAGGTGACACTATAGGGTGTTTCTCTCGGCCTACT	TAATACGACTCACTATAGGGAAACAGACGTCGTGCTTGTC	835
Q3	ATTTAGGTGACACTATAGTACATACTAGCGCTCCACCG	TAATACGACTCACTATAGGGGAACGGGATCAGACACATGC	738
Q4	ATTTAGGTGACACTATAGCCATCGCTTCTTTCGTGACG	TAATACGACTCACTATAGGGAGACGACAGCATCTCCAACA	200
B1	ATTTAGGTGACACTATAGATCTCTTCCAGTATCGCCCG	TAATACGACTCACTATAGGGCGGACCGTCTGTGATGATGA	630
B2	ATTTAGGTGACACTATAGCCCGAGATCAGCATCATCCA	TAATACGACTCACTATAGGGGAGGTGATGTTGAACGGCTG	791
SIPC	ATTTAGGTGACACTATAGCAACATGAAGAGCGGCTACC	TAATACGACTCACTATAGGGGCGGACTGACATCGAAGTTC	887

All forward primers had the SP6 RNA polymerase promoter sequence added to the 5' end (ATTTAGGTGACACTATAG), and all reverse primers had the T7 RNA promoter

sequence (TAATACGACTCACTATAG) added to the 5' end, to enable probe labelling and synthesis.

Sequences were amplified from cDNA libraries prepared as described for qPCR, using the following PCR conditions. Initial denaturation at 95ºC for five minutes, followed by 40 cycles of: 30 seconds denaturation at 95ºC, annealing starting at 61ºC for 1 minute, -0.5ºC per cycle for the first ten cycles to a final annealing temperature of 56ºC, extension at 72ºC for 1 minute. These cycles were concluded with a final extension of 72ºC for five minutes. Reactions were performed in 25 µl volumes using the following mix of New England Bioloabs *Taq* PCR reagents: 2.5 µl 10X Standard Taq Reaction Buffer, 0.5 µl 10 mM dNTPs, 0.5 µl each of 10 µM forward and reverse primers, 0.125 µl Taq DNA polymerase, 1 µl template cDNA, and 19.875 µl DEPC treated Milli-Q water.

Ten microlitres of the amplified PCR products were run on a 1% TBE (Thermo Scientific) agarose gel with 2 µl 6x loading dye (New England Biolabs) (120 mA, 120 V) for 90 minutes. The resultant bands were excised and solubilised in DEPC Milli-Q water, and the PCR repeated using these excised bands in place of the cDNA template, in 50 µl reactions, with the reagents in the same ratios.

The PCR products were cleaned using a Wizard® SV Gel and PCR Clean-Up kit (Promega), the DNA concentration estimated (NanoDrop One), then 1 µg was taken for use in the synthesis of DIG-labelled RNA probes. DIG labelled probes were synthesised using an SP6/T7 RNA labelling kit (Roche), as per the manufacturer's instructions. Synthesised probes were cleaned by sodium acetate ethanol precipitation as previously described, and stored in hybridisation buffer (table 5.5).

Cyprids for WISH were cultured as described in 2.3.1, prepared, and transferred into baskets as described in 4.3.1., with the addition of a 10-minute incubation in relaxation solution following recovery at 28ºC. A full list of reagents and solutions can be found in table 5.5.

Once in baskets, the larvae were washed briefly in DEPC-treated Milli-Q water before being fixed in 4% formaldehyde overnight at 4ºC. Fixed cyprids were washed twice for five minutes in PBST, incubated in 0.75% w/v sodium dodecyl sulphate (SDS) in PBST for 20 minutes, washed once for five minutes in PBST and dehydrated through four, ten-minute washes of increasing concentrations of methanol in PBST

(25%/50%/75%/100%). Cyprids in methanol were removed from baskets, washed three times in methanol, and stored at -20ºC until required. Prepared cyprids were used for WISH, as described in table 5.4.

Table 5.4. WISH protocol for *B. amphitrite* cyprids. Steps marked in grey are overnight (ON). RT = room temperature. Details of solutions are presented in table 5.5.

Step	Duration	Repetitions	Temperature
Cyprids stored in MeOH 100%	n/a	1	-20ºC
MeOH 75% in PBST	10 min	1	RT
MeOH 50% in PBST	10 min	1	RT
MeOH 25% in PBST	10 min	1	RT
PBST	5 min	2	RT
Reduction solution	ON	1	RT
PBST	5 min	3	RT
Proteinase K solution	20 min	1	RT
0.2% Glycine w/v in PBST	5 min	2	RT
PBST	5 min	1	RT
TEA	5 min	2	RT
TEAAA	10 min	2	RT
PBST	5 min	1	RT
4% Formaldehyde	1hr	1	RT
PBST	5 min	3	RT
50% Hybridisation buffer in PBST	10 min	1	RT
100% Hybridisation buffer	2h	1	55ºC
Denature Probes	7 min	1	85ºC
Probes (0.2 µg ml^{-1}) in 100% Hybridisation buffer	ON	1	55ºC
Post-hybridisation buffer 100%	15 min	1	55ºC
Post-hybridisation buffer 66% in 1x SSCT	15 min	1	55ºC
Post-hybridisation buffer 33% in 1x SSCT	15 min	1	60ºC
1x SSCT	15 min	2	65ºC
0.1x SSCT	20 min	2	70ºC
0.1x SSCT+ 1 µg ml^{-1} RNase A	20 min	1	37ºC
0.1x SSCT	20 min	2	70ºC

0.1x SSCT	10 min	1	RT
MABT	10 min	2	RT
Blocking solution	2h	1	RT
Antibody solution	ON	1	4ºC
MABT	15 min	2 6	RT
NTMT	10 min	2	RT
Development solution	5 min – ON	1	RT
PBST	5 min	2	RT
4% Formaldehyde	20 min	1	RT
PBST	5 min	3	RT
Ethanol 33% in PBST	10 min	1	RT
Ethanol 66% in PBST	10 min	1	RT
Ethanol 100%	10 min	1	RT
Clearing solution	ON		4ºC

Following clearing, cyprids were mounted in clearing solution, on washed glass microscope slides, and imaged on a Leica DMi8 using LAS X software.

Table 5.5. Details of solution compositions for the WISH protocol detailed in table 5.4.

Reagent	Contents
Relaxation solution	2.5% w/v anhydrous $MgCl_2$ in DEPC treated Milli-Q. Isosmotic with seawater, 33 ppt.
PBS	1x phosphate buffered saline solution in DEPC treated Milli-Q, pH 7.4.
PBST	1x PBS, 0.1% tween 20, pH 7.4.
4% Formaldehyde	4% w/v paraformaldehyde in PBST, pH 7.4
Reduction solution	50 mM Dithiothreitol (DTT), 1% Triton X100, 0.5% SDS, in PBS
Proteinase K solution	40 µg ml^{-1} Proteinase K in PBST 0.1%, 0.5% SDS.
TEA	Triethanolamine 1% v/v in PBST.
TEAAA	Acetic anhydride 0.3% v/v in TEA.
SSC	Saline Sodium Citrate diluted from 20x stock in DEPC treated Milli-Q, 3M NaCl, 0.3M sodium citrate, pH 7.0.
SSCT	SSC, 0.1% tween 20.
Hybridisation buffer	DI formamide 50% v/v, SSC 5x, tween 20 1% v/v, Dernhardt's Solution 1x, heparin sodium salt 500 µg ml^{-1}, torula yeast RNA 500 µg ml^{-1}, Dextran sulphate 10% v/v, DEPC treated Milli-Q to 100%.
Post-hybridisation buffer	DI formamide 50% v/v, SSC 5x, tween 20 1% v/v, Dernhardt's Solution 1x, heparin sodium salt 50 µg ml^{-1}, torula yeast RNA 500 µg ml^{-1}, DEPC treated Milli-Q to 100%.
MABT	Maleic acid buffer, 0.1 M maleic acid, 0.15 M NaCl, 0.1% tween 20 in DEPC treated Milli-Q, pH 7.4.
Blocking solution	4% w/v blocking reagent (Roche) in MABT.
Antibody solution	1:10000 Anti-Digoxigenin, Fab fragments (Roche) in blocking solution.
NTMT	100 mM NaCl, 100 mM Tris, 50 mM $MgCl_2$, pH 9.5.
Development solution	2% v/v NBT/BCIP Stock Solution (Roche) in NTMT.
Clearing solution	80% glycerol in PBS.

5.4. Results

5.4.1. Quantitative PCR

Changes in expression of the candidate transcripts and the SIPC between stage six nauplii and cyprids were analysed by qPCR.

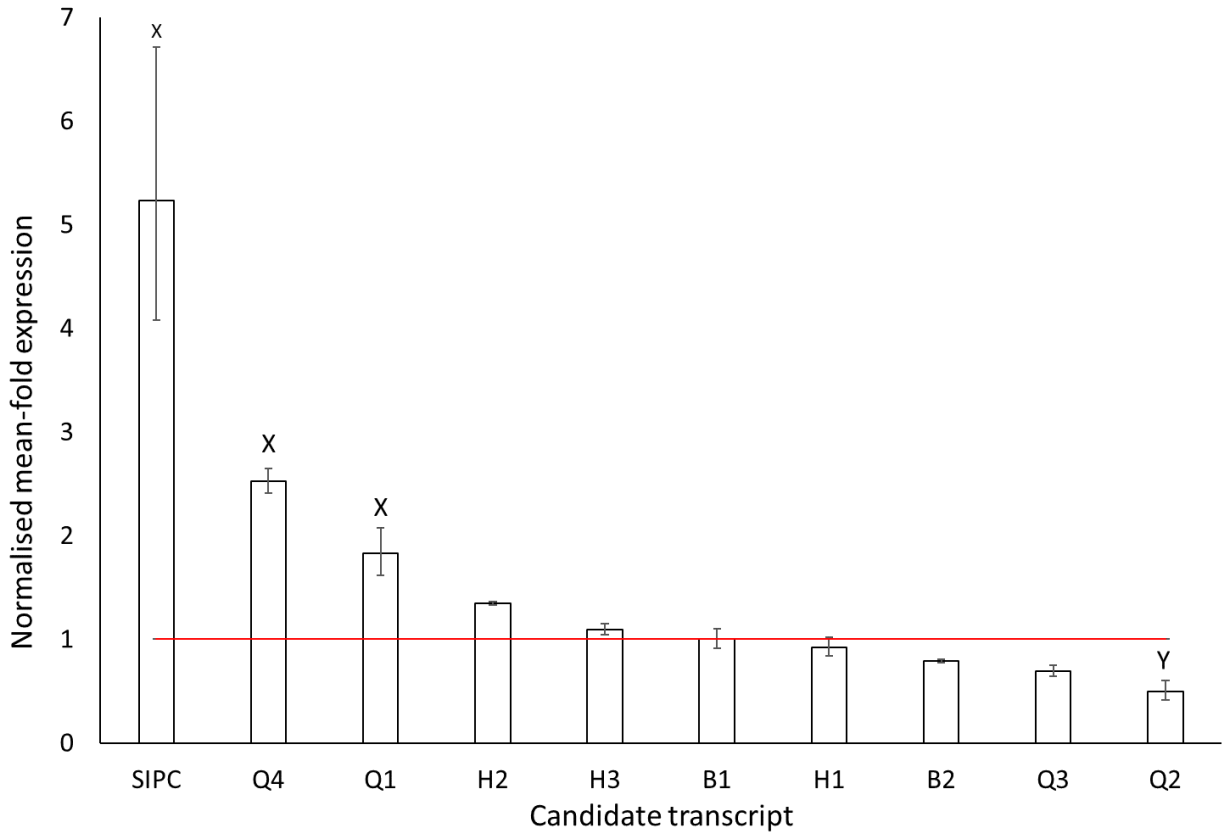

Figure 5.1. Normalised mean-fold expression of candidate transcripts in *Balanus amphitrite* cyprids (table 5.1.) against stage 6 nauplii (red line). Error bars represent standard error. X = significant difference at the 5% level ($p < 0.05$) in $\log_2$ normalised-fold expression of the cyprids (n = 6) and stage 6 nauplii (n = 6)* by two-sample t-test (Appendix, table A2). Y = significant difference at the 10% level ($p = 0.07$) in $\log_2$ normalised-fold expression of the cyprids (n = 6) and stage 6 nauplii (n = 6)* by two-sample t-test (Appendix, table A2). Absence of a letter indicates no significant difference in $\log_2$ normalised-fold expression in cyprids from stage 6 nauplii. *One stage 6 nauplii sample did not amplify in Q3 and was omitted from the analysis (n = 4).

Of the 9 candidates, only two, Q4 and Q1, exhibited significant upregulation in cyprids compared to stage six nauplii with a normalised mean-fold expression of 2.5 and 1.8, respectively (figure 5.1, Appendix, table A2). The SIPC showed the strongest significant upregulation in cyprids of over five-fold. One of the candidates, Q2, was downregulated in the cyprid, but the difference was not significant at the 5% level (p =

0.07). The mean-fold expression of the remaining candidates did not differ significantly from stage 6 nauplii. H2, B2 and Q3 potentially exhibited a small up or down regulation, but the changes were not significant.

5.4.2. RNA-seq differential expression analysis

The RNA-seq data for cyprid settlement stages were only available for *B. improvisus* (NCBI bioproject: PRJNA528777, Abramova *et al.,* 2019b), so the *B. amphitrite* candidate transcripts identified in chapter 4 were first converted to *B. improvisus* homologues (table 5.6). H3 was excluded from the analysis as the homology was low.

Table 5.6. Best BLASTn matches between candidate sequences from *Balanus amphitrite* and subjects in *B. improvisus* transcriptome (NCBI bioproject: PRJNA528777, Abramova *et al*., 2019b).

Candidate sequence (*B. amphitrite*)	**Subject sequence accession (*B.improvisus*)**	**Cover (%)**	**Identity (%)**	**e value**	**bitscore**
Q1	GHIM01064372.1	100/ 100	79.27/ 77.00	5.00E-161/ 0	568/ 1813
Q2	GHIM01046434.1	92/ 60	80.90/ 80.40	5.00E-148/ 0	525/ 1195
Q3	GHIM01061506.1	82/ 82	78.16/ 77.49	0/ 0	1604/ 1928
Q4	GHIM01064919.1	73/ 58	76.47/ 73.62	2.00E-40/ 3.00E-96	165/ 353
B1	GHIM01062846.1	65/ 75	83.13/ 81.89	0/ 0	767/ 926
B2	GHIM01058063.1	90/ 32	80.97/ 82.99	0/ 0	1288/ 1220
H1	GHIM01062567.1	99/ 50	78.90/ 80.37	1.00E-149/ 0	530/ 1862
H2	GHIM01065674.1	99/ 99	84.15/ 82.40	7.00E-125/ 0	447/ 692
H3	GHIM01008429.1/ GHIM01054124.1	21/ 4	78.17/ 77.61	9.00E-46/ 6.00E-06	185/ 54.5
SIPC mRNA	GHIM01064806.1	88	76.17	0	3379
SIPC - C anti	GHIM01064806.1	88	87.50	4.00E-04	41
SIPC - N anti	-	-	-	-	-

Before determining the expression of the individual candidate transcripts per stage, the data were examined for broad differences in expression patterns between settlement stages.

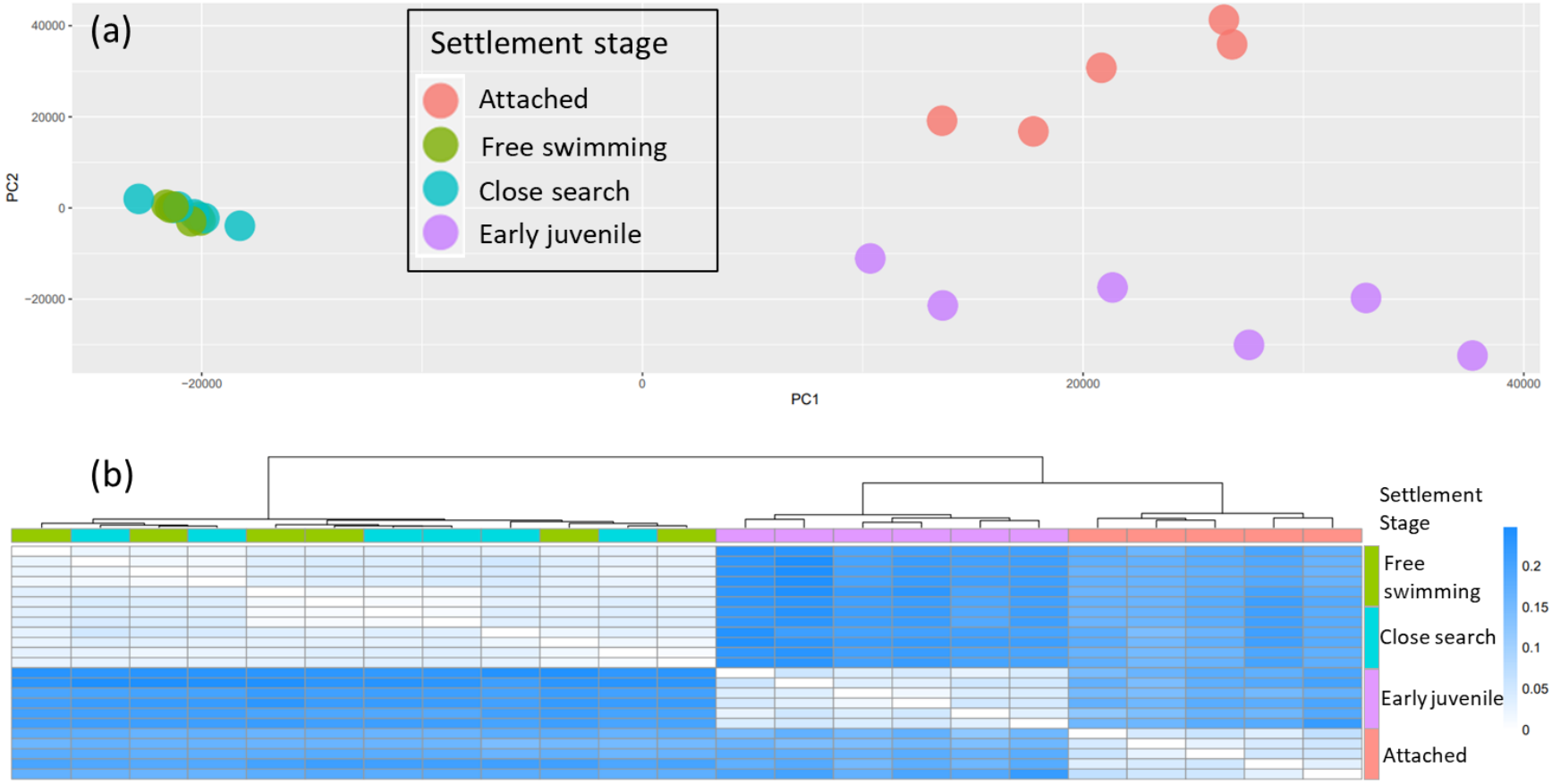

Figure 5.2. (a) Principal component analysis plot of *B. improvisus* cyprids differential expression (tpm) by settlement stage per sample. **(b)** Clustered heat map of *B. improvisus* cyprids differential expression by settlement stage (Jensen–Shannon divergence). The darker the colour, the greater the difference between samples. The cluster tree above the plot indicates the relationship between samples and stages; the closer the branch, the higher the similarity.

In both the principal component analysis (PCA) and clustered heat map analyses, free swimming and close searching *B. improvisus* cyprids exhibited effectively indistinguishable expression profiles, which were also highly consistent (figure 5.2a-b). The attached cyprids and early juveniles displayed expression patterns independent from both the free swimming and close searching cyprids, and each other (figure 5.2a-b). The consistency of expression by PCA of attached cyprids and early juveniles was considerably lower than that of the other two stages, however (figure 5.2a). The expression profiles, by clustering, of attached cyprids and early juveniles were closer to each other than the free swimming or close searching (figure 5.2b).

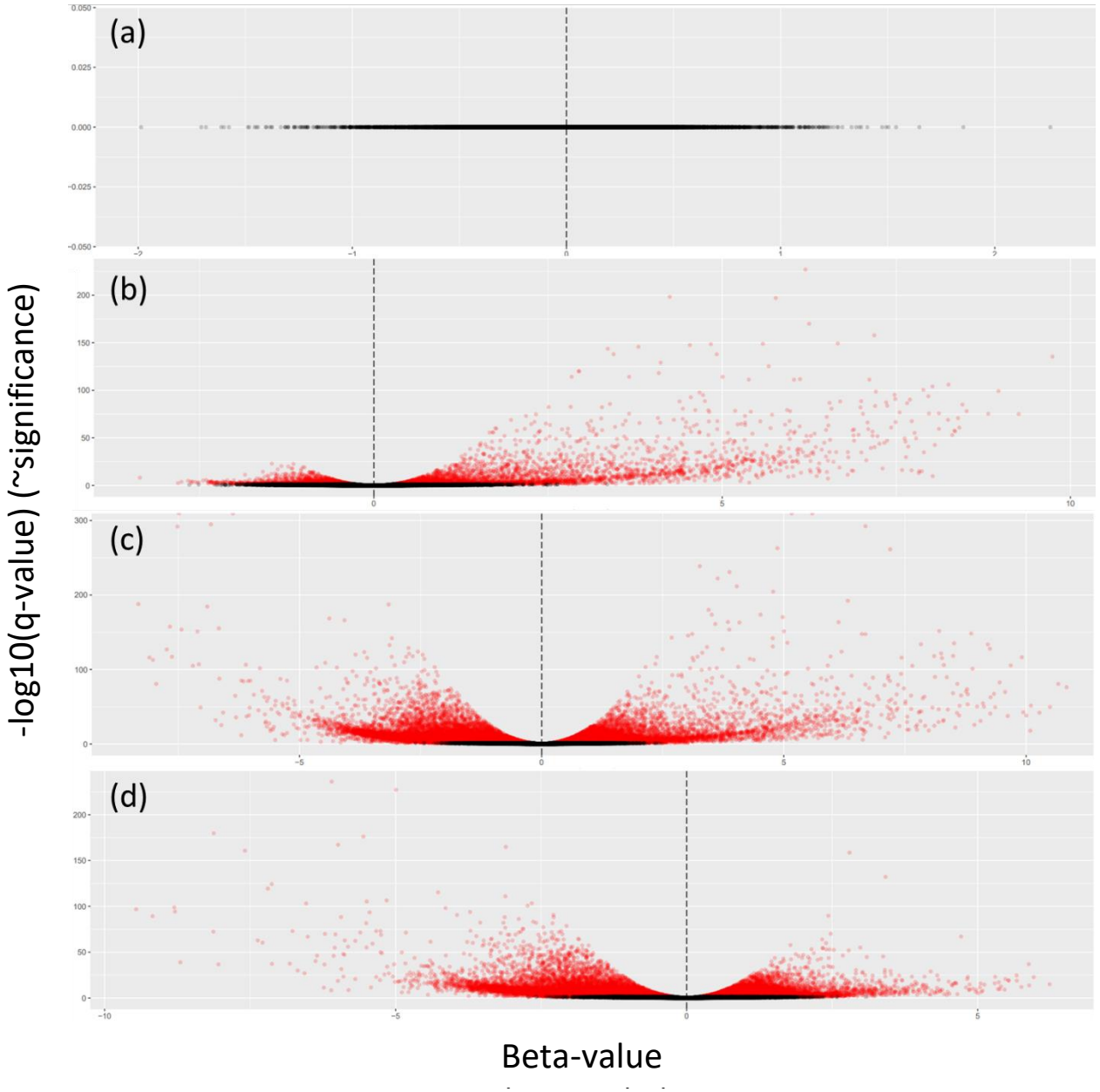

Figure 5.3. Volcano plots indicating distribution and significance of up and down regulated transcripts in *Balanus improvisus* cyprids between settlement stages. Red dots indicate significant differences ($q < 0.05$). The dotted zero line represents the baseline that each stage was compared to, as follows: (**a)** = close search vs free swimming; **(b)** = attached vs free swimming; **(c)** = early juvenile vs free swimming; **(d)** = early juvenile vs attached.

As indicated by the PCA and heat maps (figure 5.3a-b), the free swimming and close searching cyprids again displayed similar expression patterns with no significant differences found between them (figure 5.3a). Attached cyprids displayed a significantly different expression profile from free swimming cyprids, however, with the skew heavily towards upregulation (figure 5.3b). The difference between early juveniles and free swimming cyprids was more balanced - up and down regulation appeared roughly equivalent, with a slight skew towards upregulation (figure 5.3c).

Finally, as the attached cyprids transitioned into the early juvenile stage, a significant number of transcripts were again up and down regulated, with a marginal skew towards downregulated transcripts (figure 5.3d).

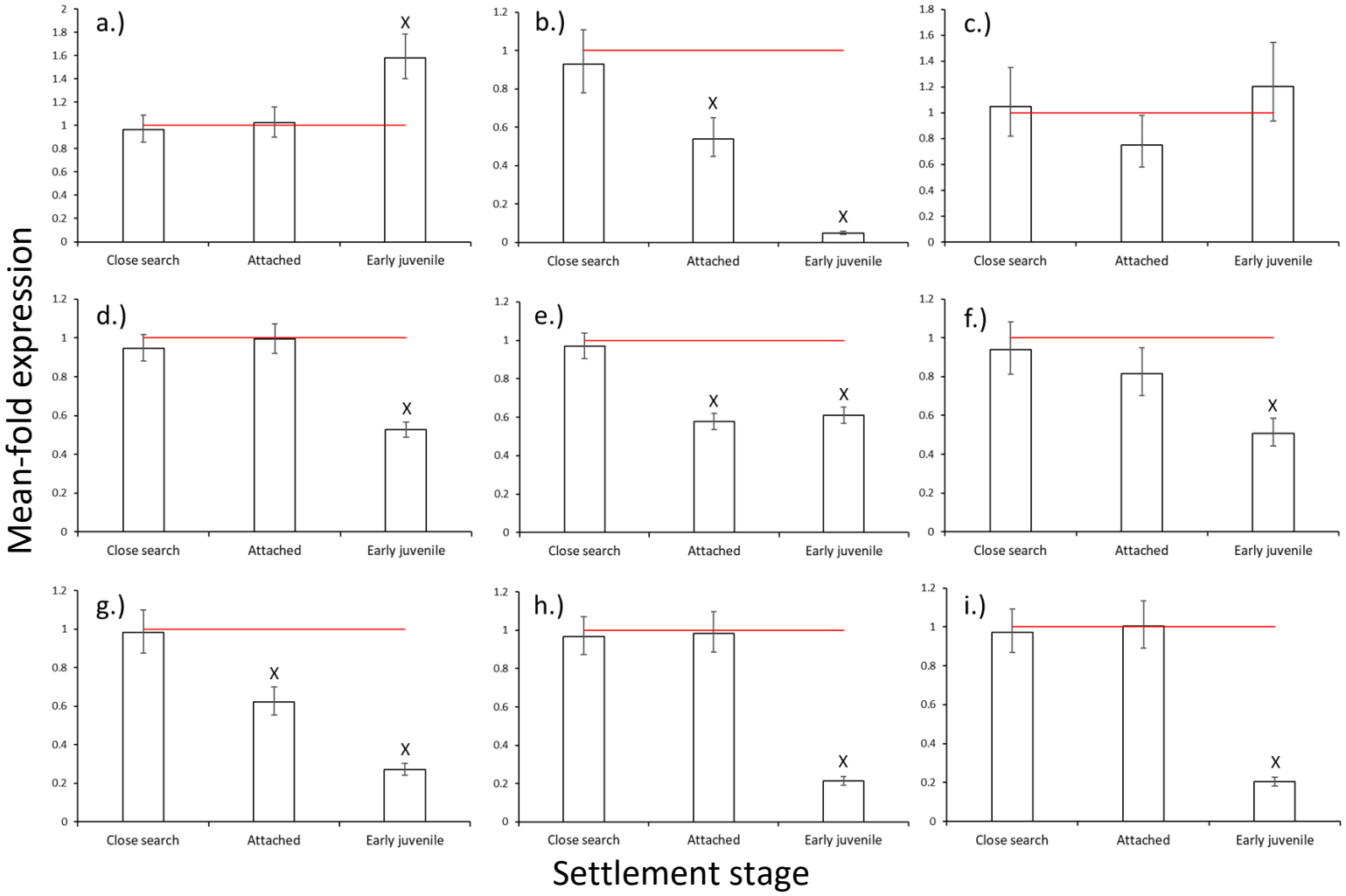

Figure 5.4. Mean-fold expression (± standard error) of the SIPC and *B. improvisus* candidate transcript homologues (table 5.6) by settlement stage against free swimming cyprids (red line). Settlement stages which exhibit a significant difference in expression from free swimming cyprids are denoted by an X (Wald test, $q < 0.05$). **(a)** = SIPC, **(b-e)** = Q1-4**, (f-g)** = B1-2, **(h-i)** = H1-2.

Across all the candidate *B. improvisus* transcript homologues, none differed significantly between close searching and free swimming cyprids (figure 5.4a-i). Three transcripts, Q1, Q4, and B2, were significantly downregulated from free swimming to attached cyprids, and early juveniles (figure 5.4b,e,g). Of these, Q1 and B2 exhibited a continuous decrease through the settlement stages, while the downregulation in Q4 plateaued at the attached cyprid (figure 5.4b,e,g). All remaining candidate homologues except Q2 (Q3, B1, H1-2) exhibited no significant decrease in expression between the free swimming and attached cyprid stages but did at the early juvenile stage (figure 5.4c,d,f,h,i). Expression of Q2 did not differ significantly from the free swimming cyprids in any settlement stage (figure 5.4c). The SIPC meanwhile only showed a significant upregulation between free swimming cyprids and early juveniles (figure 5.4a).

5.4.3. Whole mount in-situ hybridisation

Of the seven prepared probes, only SIPC and Q1 exhibited clear and reproducible staining patterns.

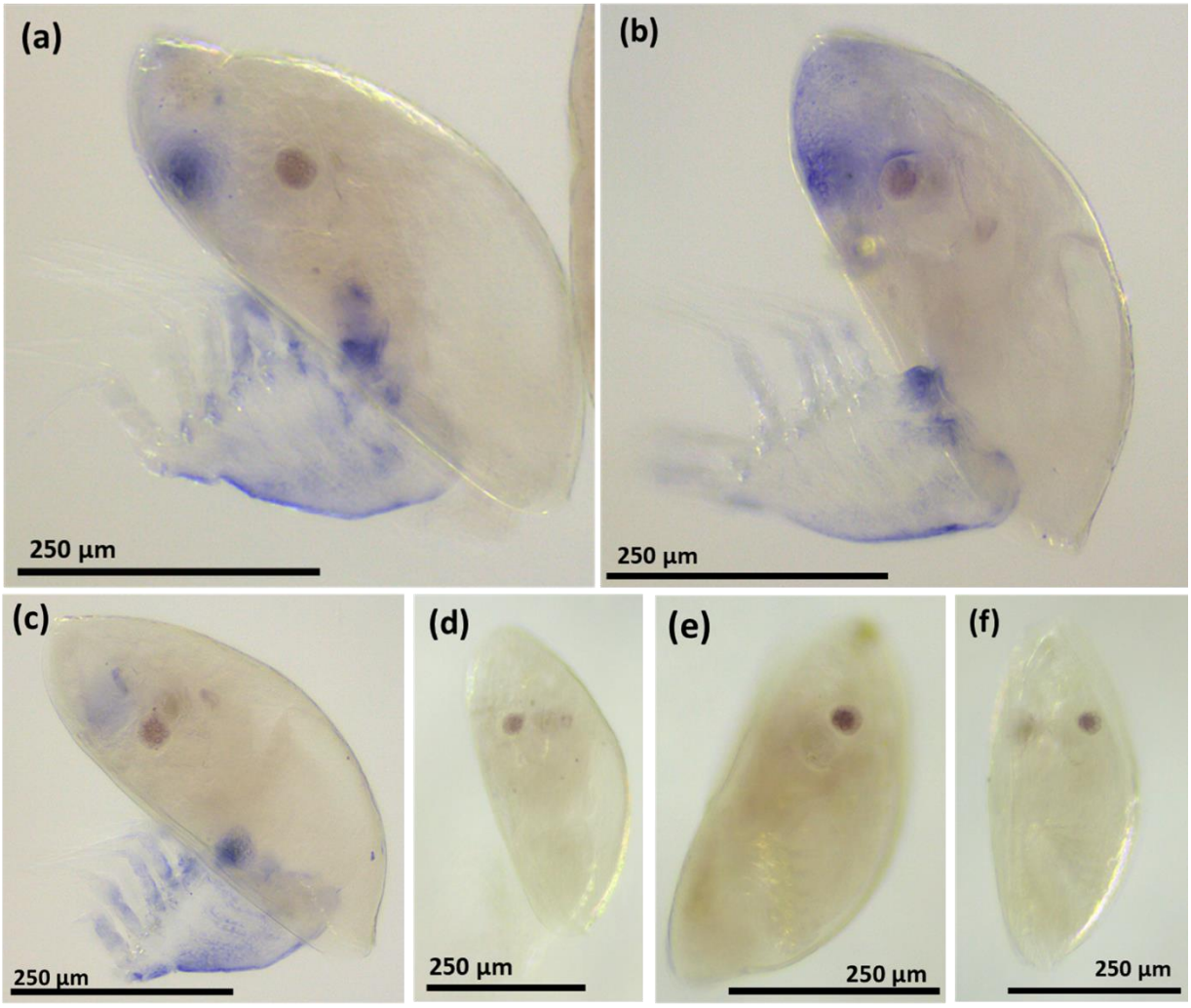

Figure 5.5. WISH images of *Balanus amphitrite* cyprids. Blue staining indicates RNA-RNA hybridisation of DIG-labelled probes, bound to a DIG-alkaline phosphatase secondary antibody, developed by NBT-BCIP. (**a-c) =** antisense probe synthesised from SIPC mRNA, **(d)** = control, sense probe synthesised from SIPC mRNA, **(e)** = control, unrelated DIG labelled RNA, **(f) =** control, no probes.

The expression of the SIPC was focused in the thoracic appendages, anterior mantle in the region of the paired antennules, and the carapace (figure 5.5a-c). The cyprids treated with the controls, sense probes, unrelated DIG labelled RNA and no probes exhibited no staining (figure 5.5d-f).

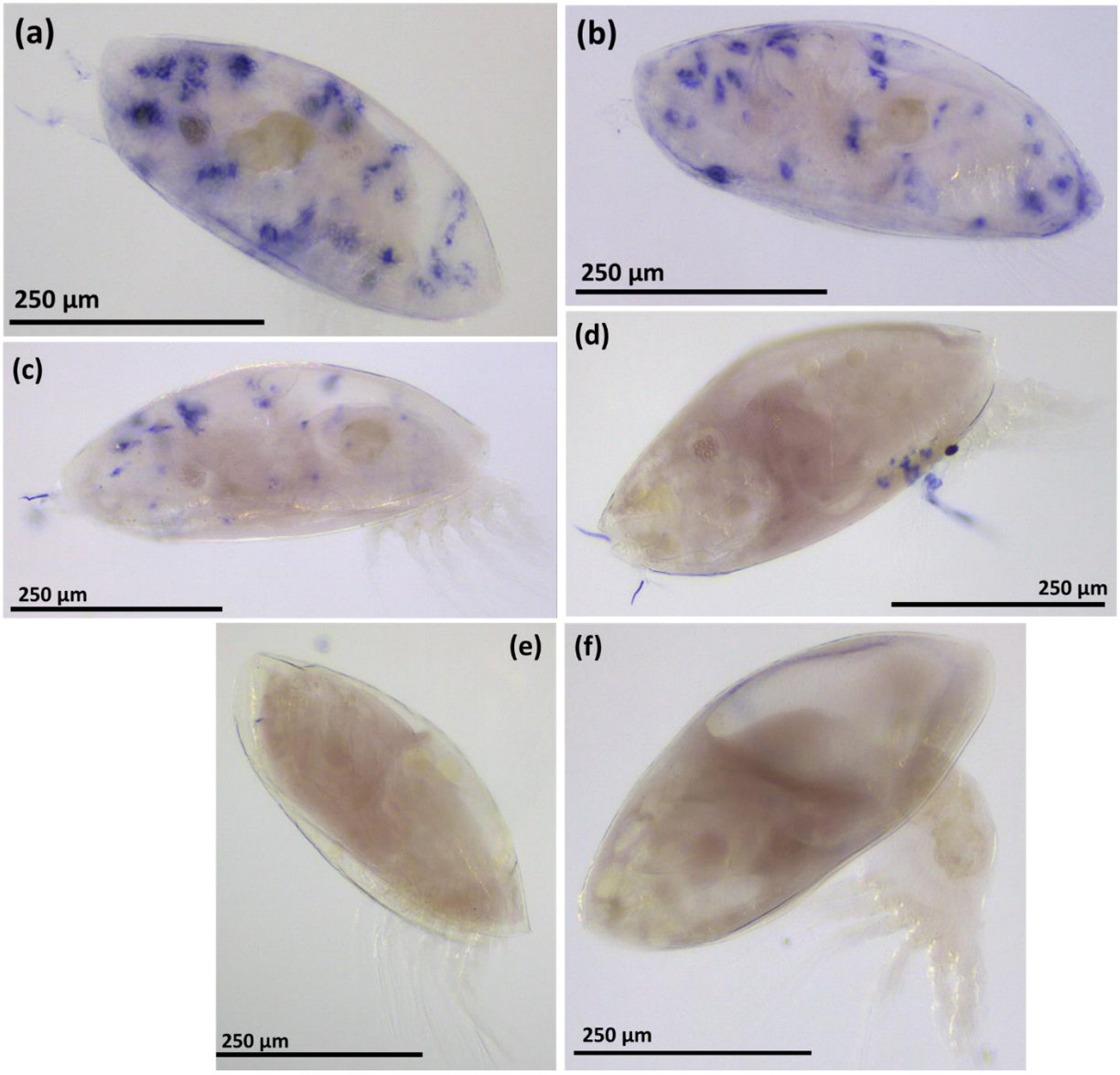

Figure 5.6. WISH images of *Balanus amphitrite* cyprids. Blue staining indicates RNA-RNA hybridisation of DIG-labelled probes, bound to a DIG-alkaline phosphatase secondary antibody, developed by NBT-BCIP. **(a-c) =** antisense probe synthesised from candidate transcript Q1 mRNA, **(d)** = control, sense probe synthesised from candidate transcript Q1 mRNA, **(e) =** control, unrelated DIG-labelled RNA, **(f)** = control, no probes.

Expression of candidate Q1 exhibited a patchy distribution across the carapace of the cyprid, and in the terminal setae (figure 5.6a-c). The patches of staining visible on the carapace displayed low uniformity in size or shape within each cyprid, though generally appeared in linear rather than circular patterns. They did not appear to share a common expression pattern between cyprids (figure 5.6a-c). This is most noticeable in the four regions of expression on the dorsal anterior carapace (figure 5.6a-c) but follows suit for most staining locations. Staining of the sense probe in the terminal

setae suggests that this is non-specific (figure 5.6d), however the carapace staining was not observed for the sense probe, or either of the other controls (figure 5.6d-f).

5.5. Discussion

5.5.1. Quantitative PCR

The SIPC is upregulated significantly in the cyprid over the nauplii, approximately 5-fold (figure 5.1, table A2). This is in accordance with the SDS-PAGE data presented by Dreanno *et al.* (2006c) and Kotsiri *et al.* (2018) in *B. amphitrite*, indicating an increase of SIPC expression in cyprids over stage six nauplii, but contradicts the qPCR expression data of Rocha (2015). While *P. pollicipes* is a stalked rather than an acorn barnacle, it also settles gregariously (Franco *et al.*, 2016), making it unlikely that SIPC expression would be downregulated in the developmental stage most pivotal to settlement. There is little information available, however, on the involvement of SIPC in stalked barnacle settlement.

The temporary adhesive proteins(s) were expected to be upregulated in cyprids above that of stage six nauplii. Of the tested candidates, two were significantly upregulated (figure 5.1, table A2). Both candidates, Q1 and Q4 were selected through peptide mass fingerprinting quality.

From the BLAST homology search, Q1 shares ~60-70% homology with a *P. pollicipes* *'*cell migration-inducing and hyaluronan-binding protein-like' mRNA (XM_037215194.1) (chapter 4, table A1). Hyaluronan, or hyaluronic acid (HA), is a glycosaminoglycan, found in epithelial and connective tissues. In humans, it frequently contributes to the formation of extracellular matrices, aiding in wound healing and cell migration. HA is also known to be a hydrating polymer, associated with fibrosis (Albeiroti et al., 2015), and has even been proposed for use in antifouling surfaces (Yu *et al.*, 2020). Hyaluronan-binding proteins, as the name suggests, have a high affinity for hyaluronan (Knudson and Knudson, 1993). This affinity can function towards matrix assembly of hyaluronan, or depolymerisation (Knudson and Knudson, 1993). Cell migration-inducing and hyaluronan-binding protein (CEMIP, GeneID: 57214) has been related to a wide variety of medical functions, from ossification (Shimoda *et al.*, 2017),

degradation of HA in cartilage (Shimizu *et al.*, 2018), lung disease (Lennon and Singleton, 2011), and cell locomotion (Turley *et al.*, 1991).

The temporary adhesive footprints have been described as fibrillar and porous (Phang *et al.*, 2007), and could feasibly include HA in their assembly. HA has also been incorporated into adhesive hydrogels containing DOPA, a known marine adhesive component used by mussels, for adhesive purposes in medicine (Lee *et al.*, 2006; Koivusalo *et al.*, 2019). Hypothetically, HA polymers could form a component of the barnacle cyprid temporary adhesive matrix, to which Q1 may play a role in binding HA for the formation of that matrix.

Candidate Q4 shared ~50-65% homology with *P. pollicipes* 'serpin B4-like' mRNA (XM_037233051.1) (chapter 4, table A1). Serpins are a family of serine protease inhibitors. Most serpins operate extracellularly and have an irreversible inhibitory effect on the target protease (Law *et al.*, 2006). As a protease inhibitor, Q4 could potentially be secreted with the temporary adhesive to protect it from degradation. While the short duration of contact during temporary adhesion would render protection from enzymatic disruption unnecessary for adhesive purposes, the footprints remain on surfaces post-exploration and act as a settlement cue (Clare *et al.*, 1994; Head *et al.*, 2003; 2004; Elbourne *et al.*, 2008), which could be worth protecting. However, the likely specificity of such a protease inhibitor would render this function questionable.

Some serpins take on a non-inhibitory role, however, functioning as transport proteins and chaperone proteins, which assist in folding and structural assembly of other proteins (Klieber *et al.*, 2007; Mala *et al.*, 2010). As an alternative hypothesis, Q4 may function to assist in the transport and/or assembly of the temporary adhesive protein(s).

Q2 was the only transcript to be significantly downregulated in cyprids compared to stage six nauplii, albeit at a slightly lower significance threshold (figure 5.1 table A2). This downregulation in cyprids suggested that it did not play a part in temporary adhesion, based on the expectations previously outlined. However, this candidate transcript, Q2, shared homology with a *P. pollicipes* 'glycine receptor subunit alpha-2-like' mRNA (XM_037227351.1) (chapter 4, table A1). Glycine is a demonstrated settlement promotor and inhibitor molecule, depending on concentration (Mishra and Kitamura, 2000) and glycine-binding sites have been identified in cyprid ionotropic

receptors (Abramova *et al.*, 2019a), so it is unusual that it was downregulated from the naupliar stage. However, while downregulated in cyprids, it was still present, and information on the sensory repertoire of the naupliar stages is comparatively sparse. Therefore, glycine sensing may be more important to nauplii than cyprids but is still present in both stages.

The temporary adhesive is synthesised in the cyprid stage (Yap *et al.*, 2017; Raine *et al.*, 2020), but there is no evidence that gland formation and initial temporary adhesive synthesis does not begin in stage six nauplii, as many other cyprid processes do (Chen *et al.*, 2011). Upregulation in the cypris larvae over stage six nauplii cannot be taken as a sole indicator of which candidates may be temporary adhesive protein(s).

5.5.2. RNA-seq differential expression analysis

The RNA-seq analysis of the settlement stage-separated *B. improvisus* data identified both broad differences in expression patterns and the specific expression of the *B. amphitrite* temporary adhesive candidate homologs.

Using the RNA-seq data for *B. improvisus* divided by settlement stage published by Abramova *et al.* (2019b) for the original purpose of identifying waterborne settlement pheromones, an overview of ontogenetic shifts in general expression pattern was performed. Broadly, free swimming and close searching cyprids exhibited almost identical expression patterns (figures 2a-b, 3a). The extreme similarity between these two settlement ‘stages’ can likely be attributed to their transient, interchangeable nature, unlike attachment and metamorphosis into a juvenile (Crisp 1976; Aldred *et al*., 2018). This is in accord with the analysis of Abramova *et al.* (2019b), who observed no significant differences between the expression of any of pheromone candidates between free swimming and close searching cyprids. Additionally, the low variation between samples in both these stages suggested that the cyprid expression pattern was relatively consistent among a population, up until the point of attachment (figure 2a). The attached cyprids and early juveniles displaying dissimilar expression patterns to each other and non-attached cyprids is expected, as each of these stages has a distinct primary function. The role of swimming and exploring cyprids is to locate a suitable settlement site, while an attached cyprid must prepare for metamorphosis,

and an early juvenile would likely favour feeding and growth (Anderson, 1993, Høeg and Møller, 2006). This theory is supported by the pairwise comparisons presented in the volcano plots (figure 3a-d). The attached cyprids skewed heavily in favour of upregulating transcripts which were lowly expressed in free swimming cyprids (figure 3b); presumably those relevant to metamorphosis as highlighted in other RNA-seq studies (Chen *et al.*, 2011). The early juvenile displayed a more even spread of up and downregulated transcripts, however, with a slight positive skew (figure 3c). Here the organisms were potentially reducing expression relating to cyprid-specific processes, e.g., surface sensing, temporary adhesive production, and increasing expression of factors relevant to growth. When comparing early juveniles to attached cyprids, the pattern of differential expression instead skewed slightly negative (figure 3d). This may imply that the upregulation of processes integral to juveniles began in the attached cyprid stage, prior to metamorphosis, and that the cessation of cyprid-specific expression did not occur until post metamorphosis. It is notable that the attached cyprids and early juveniles displayed greater inter-sample variation than the non-attached cyprids (figure 3a), potentially indicating that larvae do not diverge greatly prior to settlement, whereupon their expression patterns change to suit individual needs. However, this variability could be an artefact of the sampling method of (Abramova *et al.*, 2019b), whereby all organisms were collected after four to five days of incubation. Therefore, the attached cyprids and early juveniles were potentially of different ages, having settled and metamorphosed at different times, while all non-attached cyprids were in a more concurrent state.

When comparing the expression levels of the candidate transcript homologs for the purpose of temporary adhesive identification, two main assumptions were made. First, synthesis of the temporary adhesive is purportedly constitutive in cyprids (Yap *et al.*, 2017; Raine *et al.*, 2020), thus no difference in expression was expected between the free swimming and close searching stages. Second, once permanently attached, the temporary adhesive would no longer be required, therefore a decrease in expression at the attachment stage was expected. However, considering the inference from the broader expression patterns that downregulation of cyprid-specific transcripts may not fully occur until the early juvenile stage, this may not be the case, and a decrease in expression could be observed later than expected. Regardless, expression of

temporary adhesive was assumed to have stopped following metamorphosis to the early juvenile stage.

Of the two candidate transcripts identified by qPCR that were significantly upregulated in cyprids over nauplii, Q1 and Q4 were both significantly downregulated from the free swimming cyprid to the attached cyprid and early juvenile stages (figure 4b, e). However, the expression of Q1 decreased dramatically from attached cyprids to the early juveniles, while Q4 expression was consistent between them (figure 4b, e). Of these two, given the assumptions, Q1 appeared the more likely candidate for the temporary adhesive.

Among the other candidates, B2 and H1 and 2 (figure 4g-i) also displayed a shift in expression pattern through the settlement stages expected of the temporary adhesive, with all three lowly expressed in the early juvenile stage. The remaining candidates, except for Q2, were all significantly downregulated from the free swimming cyprid to the early juvenile, albeit to a lesser degree, and could not be discounted either. The expression of Q2 did not significantly change from that of the free swimming cyprid at any settlement stage (figure 5.4c). This combined with the downregulation from the stage six nauplius to the cyprid strongly suggests Q2 is not a component of the temporary adhesive.

The SIPC was the only analysed transcript to exhibit significant upregulation from the free swimming cyprid to early juvenile stage (figure 4a). This again aligns with the qualitative Dreanno *et al.* (2006c) SDS-PAGE data for *B. amphitrite*, which indicated a slight increase in the SIPC protein from cyprid to juveniles and adults. *P. pollicipes* also exhibited an increase in SIPC expression following metamorphosis, measured by qPCR (Rocha, 2015), however Kotsiri *et al.* (2018) observed a gradual decrease in SIPC protein occurrence from cyprids to three-day old juveniles by SDS-PAGE. *Semibalanus balanoides* cyprids exhibit equal settlement responses to adult and cyprid extracts (Hills *et al.*, 1998). This, in addition to the low concentrations of SIPC required to induce permanent settlement, an EC_{50} of 100 ng per 0.8 cm^2 for *B. amphitrite* (Dreanno *et al.*, 2007), would suggest that an upregulation of cuticle bound SIPC is unnecessary to stimulate gregarious settlement post-metamorphosis. Instead, the increase in expression may be attributed to the growth of new cuticle in juveniles,

requiring new SIPC, against the non-growing cyprid, which would only require turnover for maintaining constant levels.

5.5.3. Whole mount in-situ hybridisation

By combining RNA-seq analysis with qPCR, a small number of primary candidates for the temporary adhesive protein(s) emerged. These candidates were assayed by ISH, in the expectation of localising expression of the temporary adhesive in the proximal first antennular segment (Raine *et al.*, 2020).

For the probes being tested, the existing WISH protocols published for cyprids proved ineffective, providing either poor signal, or excessive background (Gibert *et al.*, 2000; Rabet *et al.*, 2001; Dreanno *et al.*, 2006; Chen *et al.*, 2011). The following adjustments were made. To improve sensitivity, cyprids were incubated in 0.75% w/v SDS prior to initial dehydration (tables 4, 5). In the WISH of mollusc larvae, 0.5-1% SDS treatment between fixation and dehydration, depending on the probe target, increased sensitivity and permeability (Hohagen *et al.*, 2015). To further improve permeability, cyprids were incubated overnight in reducing solution (tables 4, 5). Treatment with a reducing solution containing DTT reportedly increases detection in impermeable regions, and improves sensitivity (Pearson *et al.*, 2009). The addition of an acetylation step pre-hybridization and RNase treatment post-hybridisation were included to reduce non-specific background staining (tables 4, 5). Acetylation with a triethanolamine and acetic anhydride solution is effective at reducing background staining, reducing the binding of charged probes to tissues (Jensen, 2014; Hohagen *et al.*, 2015). Other studies have reported that RNase treatments do not significantly reduce background, and can even reduce signal (Hohagen *et al.*, 2015), however this was not the case in cyprids. Finally, 10% dextran sulphate was included in the hybridisation buffer (tables 4, 5). Dextran sulphate acts as a volume exclusion agent, increasing the hybridisation speed without increasing background (Ostromohov, *et al.*, 2018). For future WISH studies on cyprids, a systematic review and optimisation of ISH conditions would be beneficial, as there is currently no consensus regarding optimal methodologies or best practice.

The expression pattern of the SIPC matched that identified by Dreanno *et al.* (2006c), occurring in the thoracic appendages, antennules and carapace (figure 5a-c). This served as a pseudo-positive control for the methodology, verifying its efficacy, and improving confidence of the candidate transcript assays.

The spatial expression pattern of candidate Q1 is patchy, distributed across the carapace (figure 6a-c). This expression pattern did not match the location of the temporary adhesive glands in the proximal first antennular segment (Raine *et al.*, 2020). This renders it highly unlikely that it plays a role in the temporary adhesive system. However, the uniformity between cyprids suggests that the expression is spatially fixed, and possibly associated with a specific structure. The pattern bears some resemblance to that displayed by mannose receptors associated with the lattice organs (Chen *et al.*, 2011; Rybakov *et al.*, 2003). However, the comparatively irregular distribution, more linear shape and larger size of the Q1 expression sites suggests it is unlikely Q1 is also associated with these structures.

As Q1 bears homology with a HA binding protein, an alternative hypothesis is that the protein encoded by Q1 acts to support cuticle and/or carapace formation and/or repair by HA matrix assembly. While there is no direct evidence for HA occurrence in cyprids, glucosamine, an important for component HA synthesis, can be extracted from chitin in crustacean exoskeletons (Jerosch, 2011). The formation of hyaline cartilage (Fukui *et* al., 2014) is related to HA presence in chelicerate arthropods (Bitsch and Bitsch 2002; Cole and Hall, 2004), and hyaline cells are present in Crustacea (Johansson *et al.*, 2000).

5.6. Conclusions

Identification of temporary adhesive protein(s) from the candidates identified in chapter 4 was attempted through determination of their spatial and ontogenetic expression patterns via a combination of qPCR, RNA-seq differential expression analysis and WISH. While several candidates displayed trends in expression matching those hypothesised for a temporary adhesive protein, none could be confirmed. The most promising candidate, Q1, instead appeared to be associated with cuticular or carapace-based structures. A role in synthesis and repair was

hypothesised for this candidate. Additionally, some broader expression patterns across the settlement process were highlighted, indicating that cyprids may not fully begin downregulation of cyprid-associated genes until post-metamorphosis, and that upregulation of juvenile-associated genes may begin prior to metamorphosis.

Chapter 6. Synthesis and future thoughts

6.1. Synthesis

At the outset, considerable gaps in knowledge surrounding the cyprid temporary adhesive protein(s) were identified, in particular regarding its characterisation and the anatomy relating to secretion.

This work provided new evidence that the temporary adhesive gland is located in the proximal first antennular segment in acorn barnacles (Raine *et al.*, 2020). This updated the original theory of unicellular glands located in the distal second antennular segment (Nott and Foster, 1969), and noted differences compared to the stalked barnacle *Octolasmis angulata*, in which the temporary adhesive gland is multicellular and located behind the eye (Yap *et al.*, 2017). Additionally, unlike the permanent cement secretory system and the temporary adhesive system in *Octolasmis angulata*, the temporary adhesive systems of *Balanus amphitrite* and *Megabalanus coccopoma* were non branching, with single cells feeding single ducts. The original 'glands' identified by Nott and Foster (1969) were putatively reclassified as collecting structures, allowing for on-demand secretion upon contact. The temporary adhesive was constitutively synthesised in the gland cells, packaged into homogenous vesicles and transported to the third antennular segment. The homogeneity of the vesicles indicated that the temporary adhesive is a single-phased release, unlike the permanent adhesive (Aldred *et al.*, 2013a; Gohad *et al.*, 2014). Identification of the temporary adhesive gland location facilitated the assaying of candidates by whole mount in-situ hybridisation (WISH).

The route to characterisation of the temporary adhesive protein(s) began with collection of the material. The low abundance of deposited material per footprint has been an historic barrier to characterisation, thus a novel method to collect working quantities of material was established. Comparisons of footprint deposit extracts from actively exploring cyprids and inactive cyprids highlighted a number of prominent differences in band pattern on SDS-PAGE. These bands were present when footprint extracts were assayed with antibodies raised against the C-terminus amino acid sequence of the settlement-inducing protein complex (SIPC). The bands were not concurrent with the typical 88 and 76 kDa subunits of the SIPC (Dreanno *et al.*, 2006c),

indicating that the component(s) of the footprint deposit is not the SIPC protein identified previously in larvae and adults, and may instead be a functional analogue. Further interrogation of the transcriptome for SIPC C- and N-terminal antibody peptide target coding sequences only revealed transcripts which also aligned with the SIPC mRNA sequence. As such, the difference between these materials may be greater than originally thought.

From the protein bands which cross reacted with the SIPC C-terminal antibody, candidates were selected by peptide mass fingerprinting combined with existing and generated transcriptome data. These candidates were put forward for expression analyses. Several candidates exhibited promising patterns of expression, increasing from nauplius to cyprid, and decreasing from cyprid to early juvenile. Only one was able to be successfully interrogated for spatial expression with WISH. This candidate occurred in consistent regions on the carapace, rendering it unlikely to be a component of the temporary adhesive. For this candidate, a putative role in the repair or synthesis of the carapace or cuticle was hypothesised, along with a potential role of hyaluronic acid, or an analogue. The SDS-PAGE band from which this candidate was identified did not contain mannose residues as detected by LCA. It seems likely that the adhesive, or at least the component that stimulates gregarious settlement, is present in the bands that reacted to both SIPC C- terminus antibody and LCA.

Aside from the temporary adhesive, some broad expression patterns in *B. improvisus* were observed. These patterns potentially indicate significant increases in variable expression once attachment and metamorphosis begin, over a highly consistent free-swimming and close searching expression pattern. Further investigation would be necessary to confirm these ontogenetic expression patterns. Additionally, some evidence of delayed downregulation of cyprid specific genes until post-metamorphosis, and early upregulation of juvenile genes pre-metamorphosis, was observed.

6.2. Directions for future work

The research presented here could be expanded in a number of directions. Firstly, while the location of the temporary adhesive gland is concurrent between two species

of acorn barnacle, the serial block face scanning electron microscopy method presented here could be expanded to other species, such as *Semibalanus balanoides*, the species on which the original identification of the 'glands' was made (Nott and Foster, 1969). Furthermore, the differences noted between the acorn barnacles and the stalked barnacle *Octolasmis angulata* (Yap *et al.*, 2017) would require further investigation, and determine if this is a widespread difference between the groups. Additionally, characterising the anatomy and ultrastructure of the temporary adhesion system in non-fouling acorn barnacle species such as *Balanus spongicola*, which settles epibiotically, could be used to determine differences by ecological niche, and whether this correlates with variations in antennular structure (Chan *et al.*, 2017). On a smaller scale, some evidence of some minor species-specific differences between *B. amphitrite* and *M. coccopoma* was observed, but more investigation would be required to determine if these are consistent amongst their respective species. The glands themselves, now located, could be imaged over the course of their development, and determine if formation begins in the stage six nauplius, or is limited to the cyprid stage. This information would assist in the assessment of candidate temporary adhesive proteins by expression patterns. Finally, an analysis of structural changes in the temporary adhesive system as cyprids age and become more 'desperate' to settle could contribute to further understanding of the settlement decision-making process (Pechenik *et al.*, 1993).

In regard to the characterisation of temporary adhesive protein(s), further optimisation of the process could be valuable. For protein collection, more potent solvents, such as hexafluoroisopropanol, which act against cured adult cement could be applied to footprint extraction process to improve yield and efficiency (So *et al.*, 2016). The SIPC antibodies, despite the potential difference in structure of the SIPC compared to the temporary adhesive protein(s), still exhibit reactivity, and would therefore allow immunoprecipitation for collection directly from whole cyprid extracts. Identification of locality of the temporary adhesive gland could be beneficial for targeted protein extraction, although the first antennular segment is hard to access cleanly in dissection, and the abundance of protein available at any individual moment is likely to be low, given its constitutive production and secretion. Instead, spatial RNA-seq methods to analyse differential expression between the antennule and cyprid body could assist in identifying or confirming candidate transcripts. To further this avenue,

single cell RNA-seq, could be applied to the antennule, and potentially localise expression of candidate transcripts to the temporary adhesive gland cells.

For broader scale expression studies on acorn barnacle larvae, while much work has been done between life stages, nauplii, cyprid and adult, further investigation into the expression patterns of acorn barnacles between settlement stages may be required. This would help to elucidate the apparent increase in variation in expression exhibited during attachment and early juvenile stages and determine if this was a sampling artefact. In addition, functional pathway analysis could identify which genes are being up and down-regulated at each settlement stage and determine whether the downregulation of cyprid-specific genes is delayed until post-metamorphosis, as the data presented here suggest, and vice versa for upregulation of juvenile genes pre-metamorphosis.

Further investigation of the putative involvement of the SIPC in the temporary adhesive is required, as the data presented here indicate that the SIPC is not involved, despite footprints of the temporary adhesive reacting with antibodies to the N- and C-termini of the SIPC. The footprint deposits also have a demonstrable ability to induce gregarious conspecific settlement, so SIPC or an analogue seems likely to be present (Clare et al., 1994; Head et al., 2003; 2004; Elbourne et al., 2008).

Finally, testing of the remaining candidates identified here by WISH remains to be concluded. Room also remains for in depth study into optimal in-situ techniques in barnacle larvae, both whole mount and slide based, in order to assay candidates more efficiently. Should the temporary adhesive protein(s) be successfully characterised it would provide a major benefit to the design of anti-fouling and fouling-release materials targeting larval settlement. Knowing the mode of action of the larval adhesive and designing surfaces to have a low affinity for that material would be considerably more efficient than attempting to counter the adhesives of already established adults. The role temporary adhesion strength plays in surface selectivity is still being investigated, but there is some evidence of a correlation (O'Connor & Richardson 1994; Dahlström *et al.*, 2004; Di Fino *et al.*, 2014: Gatley-Montross *et al.*, 2017: Abramova, 2019). Identifying variations in temporary adhesives between acorn barnacle species, particularly those with differing ecological niches, could additionally reveal the role adhesion strength plays in surface selection, as larvae would

presumably produce a temporary adhesive with a higher affinity for surfaces on which settlement is preferable.

In conclusion, the study of temporary adhesion in acorn barnacle cyprids is still in its infancy and will require a great deal of multi-disciplinary study to fully elucidate this complex process. The fruits of such effort would yield information vital to understanding the settlement ecology of these organisms, and in turn enhance the development of anti-fouling technologies.

7. References

Abramova, A., 2019. Molecular biology of barnacle *Balanus improvisus* settlement. (Doctoral dissertation, University of Gothenburg).

Abramova, A., Lind, U., Blomberg, A. and Rosenblad, M.A., 2019b. The complex barnacle perfume: identification of waterborne pheromone homologues in *Balanus improvisus* and their differential expression during settlement. Biofouling, 35(4), 416-428.

Abramova, A., Rosenblad, M.A., Blomberg, A. and Larsson, T.A., 2019a. Sensory receptor repertoire in cyprid antennules of the barnacle *Balanus improvisus*. PLoS ONE, 14(5), e0216294.

Ahmed, N., Murosaki, T., Kurokawa, T., Kakugo, A., Yashima, S., Nogata, Y. and Gong, J.P., 2014. Prolonged morphometric study of barnacles grown on soft substrata of hydrogels and elastomers. Biofouling, 30(3), 71-279.

Al-Aidaroos, A.M., Satheesh, S. and Devassy, R.P., 2016. Biochemical analysis of adhesives produced by the cypris larvae of barnacle *Amphibalanus amphitrite*. Thalassas: An International Journal of Marine Sciences, 32(1), 7-42.

Al-Aqeel, S., Ryu, T., Zhang, H., Chandramouli, K.H. and Ravasi, T., 2016. Transcriptome and proteome studies reveal candidate attachment genes during the development of the barnacle *Amphibalanus amphitrite*. Frontiers in Marine Science, 3, 171.

Albeiroti, S., Soroosh, A. and de la Motte, C.A., 2015. Hyaluronan's role in fibrosis: a pathogenic factor or a passive player?. BioMed Research International, 2015, e790203.

Aldred, N. and Clare, A.S., 2009. Mechanisms and principles underlying temporary adhesion, surface exploration and settlement site selection by barnacle cyprids: A short review. In Functional surfaces in biology, Gorb, S.N., Ed., Springer, Dordrecht, Netherlands, 43-65.

Aldred, N. and Nelson, A., 2019. Microbiome acquisition during larval settlement of the barnacle *Semibalanus balanoides*. Biology Letters, 15(6), 20180763.

Aldred, N., Alsaab, A. and Clare, A.S., 2018. Quantitative analysis of the complete larval settlement process confirms Crisp's model of surface selectivity by barnacles. Proceedings of the Royal Society B: Biological Sciences, 285(1872), 20171957.

Aldred, N., Gatley-Montross, C.M., Lang, M., Detty, M.R. and Clare, A.S., 2019. Correlative assays of barnacle cyprid behaviour for the laboratory evaluation of antifouling coatings: A study of surface energy components. Biofouling, 35(2),159-172.

Aldred, N., Gohad, N.V., Petrone, L., Orihuela, B., Liedberg, B., Ederth, T., Mount, A., Rittschof, D. and Clare, A.S., 2013a. Confocal microscopy-based goniometry of barnacle cyprid permanent adhesive. Journal of Experimental Biology, 216(11), 969-1972.

Aldred, N., Høeg, J.T., Maruzzo, D. and Clare, A.S., 2013b. Analysis of the behaviours mediating barnacle cyprid reversible adhesion. PLoS One, 8(7), e68085.

Aldred, N., Phang, I.Y., Conlan, S.L., Clare, A.S. and Vancso, G.J., 2008. The effects of a serine protease, Alcalase®, on the adhesives of barnacle cyprids (*Balanus amphitrite*). Biofouling, 24(2), 97-107.

Aldred, N., San Chan, V.B., Emami, K., Okano, K., Clare, A.S. and Mount, A.S., 2020. Chitin is a functional component of the larval adhesive of barnacles. Communications Biology, 3(1), 1-8.

Aldred, N., Scardino, A., Cavaco, A., de Nys, R. and Clare, A.S., 2010. Attachment strength is a key factor in the selection of surfaces by barnacle cyprids (*Balanus amphitrite*) during settlement. Biofouling, 26(3), 287-299.

Alsaab, A., Aldred, N. and Clare, A.S., 2017. Automated tracking and classification of the settlement behaviour of barnacle cyprids. Journal of The Royal Society Interface, 14(128), 20160957.

Altschul, S.F., Gish, W., Miller, W., Myers, E.W. and Lipman, D.J., 1990. Basic local alignment search tool. Journal of Molecular Biology, 215, 403-410.

Al-Yahya, H., Chen, H.N., Chan, B.K., Kado, R. and Høeg, J.T., 2016. Morphology of cyprid attachment organs compared across disparate barnacle taxa: Does it relate to habitat?. The Biological Bulletin, 231(2), 120-129.

Anderson, D.T., 1993. Barnacles: structure, function, development and evolution. Chapman and Hall, London

Anil, A.C., Desai, D. and Khandeparker, L., 2001. Larval development and metamorphosis in *Balanus amphitrite* Darwin (Cirripedia; Thoracica): Significance of food concentration, temperature and nucleic acids. Journal of Experimental Marine Biology and Ecology, 263(2), 125-141.

Aranda, P.S., LaJoie, D.M. and Jorcyk, C.L., 2012. Bleach gel: a simple agarose gel for analyzing RNA quality. Electrophoresis, 33(2), 366-369.

Baragi, L.V. and Anil, A.C., 2017. Influence of elevated temperature, pCO2, and nutrients on larva-biofilm interaction: Elucidation with acorn barnacle, *Balanus amphitrite* Darwin (Cirripedia: Thoracica). Estuarine, Coastal and Shelf Science, 185, 107-119.

Barlow, D.E., Dickinson, G.H., Orihuela, B., Kulp III, J.L., Rittschof, D. and Wahl, K.J., 2010. Characterization of the adhesive plaque of the barnacle *Balanus amphitrite*: Amyloid-like nanofibrils are a major component. Langmuir, 26(9), 6549-6556.

Belevich, I., Joensuu, M., Kumar, D., Vihinen, H. and Jokitalo, E., 2016. Microscopy image browser: A platform for segmentation and analysis of multidimensional datasets. PLoS Biology, 14, e1002340.

Berglin, M. and Gatenholm, P., 2003. The barnacle adhesive plaque: morphological and chemical differences as a response to substrate properties. Colloids and Surfaces B: Biointerfaces, 28(2-3), 107-117.

Berntsson, K.M., Jonsson, P.R., Larsson, A.I. and Holdt, S., 2004. Rejection of unsuitable substrata as a potential driver of aggregated settlement in the barnacle *Balanus improvisus*. Marine Ecology Progress Series, 275, 199-210.

Berntsson, K.M., Jonsson, P.R., Lejhall, M. and Gatenholm, P., 2000. Analysis of behavioural rejection of micro-textured surfaces and implications for recruitment by

the barnacle *Balanus improvisus*. Journal of Experimental Marine Biology and Ecology, 251(1), 59-83.

Bielecki, J., Chan, B.K., Hoeg, J.T. and Sari, A., 2009. Antennular sensory organs in cyprids of balanomorphan cirripedes: Standardizing terminology using *Megabalanus rosa*. Biofouling, 25(3), 203-214.

Bitsch, C. and Bitsch, J., 2002. The endoskeletal structures in arthropods: cytology, morphology and evolution. Arthropod Structure and Development, 30(3), 159-177.

Bouchet, P., 2006. The magnitude of marine biodiversity. In The exploration of marine biodiversity: scientific and technological challenges, Duarte, C., Ed., BBVA Foundation, Bilbao, Spain, 31-62

Bray, N.L., Pimentel, H., Melsted, P. and Pachter, L., 2016. Near-optimal probabilistic RNA-seq quantification. Nature Biotechnology, 34(5), 525-527.

Browne, K.A. and Zimmer, R.K., 2001. Controlled field release of a waterborne chemical signal stimulates planktonic larvae to settle. The Biological Bulletin, 200(1), 87-91.

Burden, D.K., Barlow, D.E., Spillmann, C.M., Orihuela, B., Rittschof, D., Everett, R.K. and Wahl, K.J., 2012. Barnacle *Balanus amphitrite* adheres by a stepwise cementing process. Langmuir, 28(37), 13364-13372.

Burden, D.K., Spillmann, C.M., Everett, R.K., Barlow, D.E., Orihuela, B., Deschamps, J.R., Fears, K.P., Rittschof, D. and Wahl, K.J., 2014. Growth and development of the barnacle *Amphibalanus amphitrite*: Time and spatially resolved structure and chemistry of the base plate. Biofouling, 30(7), 799-812.

Cano-Gomez, A., Goulden, E.F., Owens, L. and Høj, L., 2010. *Vibrio owensii* sp. nov., isolated from cultured crustaceans in Australia. FEMS microbiology letters, 302(2), 175-181.

Cassidy, A. and Jones, J., 2014. Developments in in situ hybridisation. Methods, 70(1), 39-45.

Chan, B.K.K., Corbari, L., Rodriguez Moreno, P.A. and Tsang, L.M., 2017. Molecular phylogeny of the lower acorn barnacle families (Bathylasmatidae, Chionelasmatidae, Pachylasmatidae and Waikalasmatidae)(Cirripedia: Balanomorpha) with evidence for

revisions in family classification. Zoological Journal of the Linnean Society, 180(3), 542-555.

Chaw, K.C., Dickinson, G.H., Ang, K.Y., Deng, J. and Birch, W.R., 2011. Surface exploration of *Amphibalanus amphitrite* cyprids on microtextured surfaces. Biofouling, 27(4), 413-422.

Chen, Z.F., Matsumura, K., Wang, H., Arellano, S.M., Yan, X., Alam, I., Archer, J.A., Bajic, V.B. and Qian, P.Y., 2011. Toward an understanding of the molecular mechanisms of barnacle larval settlement: A comparative transcriptomic approach. PLoS ONE, 6(7), e22913.

Chen, Z.F., Wang, H., Matsumura, K. and Qian, P.Y., 2012. Expression of calmodulin and myosin light chain kinase during larval settlement of the barnacle *Balanus amphitrite*. PLoS ONE, 7(2), e31337.

Chen, Z.F., Zhang, H., Wang, H., Matsumura, K., Wong, Y.H., Ravasi, T. and Qian, P.Y., 2014. Quantitative proteomics study of larval settlement in the barnacle *Balanus amphitrite*. PLoS ONE, 9(2), e88744.

Clare, A.S., 1996. Signal transduction in barnacle settlement: calcium re-visited. Biofouling, 10(1-3), 141-159.

Clare, A.S. and Matsumura, K., 2000. Nature and perception of barnacle settlement pheromones. Biofouling, 15(1-3), 57-71.

Clare, A.S. and Nott, J.A., 1994. Scanning electron microscopy of the fourth antennular segment of *Balanus amphitrite amphitrite*. Journal of the Marine Biological Association of the United Kingdom, 74(4), 967-970.

Clare, A.S. and Yamazaki, M., 2000. Inactivity of glycyl-glycyl-arginine and two putative (QSAR) peptide analogues of barnacle waterborne settlement pheromone. Journal of the Marine Biological Association of the United Kingdom, 80(5), 945-946.

Clare, A., Freet, R. and McClary, M., 1994. On the antennular secretion of the cyprid of *Balanus amphitrite amphitrite*, and its role as a settlement pheromone. Journal of the Marine Biological Association of the United Kingdom, 74(1), 243-250.

Clare, A.S., Rittschof, D. and Costlow Jr, J.D., 1992. Effects of the nonsteroidal ecdysone mimic RH 5849 on larval crustaceans. Journal of Experimental Zoology, 262(4), 436-440.

Cole, A.G. and Hall, B.K., 2004. The nature and significance of invertebrate cartilages revisited: Distribution and histology of cartilage and cartilage-like tissues within the Metazoa. Zoology, 107(4), 261-273.

Crickenberger, S. and Moran, A., 2013. Rapid range shift in an introduced tropical marine invertebrate. PloS ONE, 8(10), e78008.

Crisp, D.J. and Bourget, E., 1985. Growth in barnacles. In Advances in marine biology, Blaxter, J.H.S., Russell, F.S. and Yonge, M. Ed., Academic Press, Cambridge, USA, 22, 199-244.

Crisp, D.J. and Spencer, C.P., 1958. The control of the hatching process in barnacles. Proceedings of the Royal Society B: Biological Sciences, 149(935), 278-299.

Crisp, D.J., 1976. Settlement responses in marine organisms. In Adaptations to Environment: Essays on the Physiology of Marine Animals, Newell, R.C., Ed. Butterworths, London, UK, 83-124.

Crisp, D.T., 1961. Territorial behaviour in barnacle settlement. Journal of Experimental Biology, 38(2), 429-446.

Dahlström, M., Jonsson, H., Jonsson, P.R. and Elwing, H., 2004. Surface wettability as a determinant in the settlement of the barnacle *Balanus improvisus* (Darwin). Journal of Experimental Marine Biology and Ecology, 305(2), 223-232.

Darwin, C.R., 1853. Living Cirripedia, a monograph on the sub-class Cirripedia, with figures of all the species. The Lepadidæ; or, pedunculated cirripedes. Annals and Magazine of Natural History, 12(72), 444-448.

Darwin, C.R., 1854. A Monograph on the Sub-class Cirripedia: The Balanidae (or sessile cirrepedes), the Verrucidae. The Ray society, London, 2.

Davenport, J. and Irwin, S., 2003. Hypoxic life of intertidal acorn barnacles. Marine Biology, 143(3), 555-563.

De Gregorio, B.T., Stroud, R.M., Burden, D.K., Fears, K.P., Everett, R.K. and Wahl, K.J., 2015. Shell structure and growth in the base plate of the barnacle *Amphibalanus amphitrite*. ACS Biomaterials Science & Engineering, 1(11), 1085-1095.

De Gregoris, T., Borra, M., Biffali, E., Bekel, T., Burgess, J.G., Kirby, R.R. and Clare, A.S., 2009. Construction of an adult barnacle (*Balanus amphitrite*) cDNA library and selection of reference genes for quantitative RT-PCR studies. BMC molecular biology, 10(1), 1-12.

De Gregoris, T.B., Khandeparker, L., Anil, A.C., Mesbahi, E., Burgess, J.G. and Clare, A.S., 2012. Characterisation of the bacteria associated with barnacle, *Balanus amphitrite*, shell and their role in gregarious settlement of cypris larvae. Journal of Experimental Marine Biology and Ecology, 413, 7-12.

De Gregoris, T.B., Rupp, O., Klages, S., Knaust, F., Bekel, T., Kube, M., Burgess, J.G., Arnone, M.I., Goesmann, A., Reinhardt, R. and Clare, A.S., 2011. Deep sequencing of naupliar-, cyprid-and adult-specific normalised Expressed Sequence Tag (EST) libraries of the acorn barnacle *Balanus amphitrite*. Biofouling, 27(4), 367-374.

Deerinck, T.J., Bushong, E.A., Lev-Ram, V., Shu, X., Tsien, R.Y. and Ellisman, M.H., 2010. Enhancing serial block-face scanning electron microscopy to enable high resolution 3-D nanohistology of cells and tissues. Microscopy and Microanalysis, 16, 1138-1139.

Di Fino, A., 2015. Comparative approach to barnacle adhesive-surface interactions (Doctoral dissertation, Newcastle University).

Di Fino, A., Petrone, L., Aldred, N., Ederth, T., Liedberg, B. and Clare, A.S., 2014. Correlation between surface chemistry and settlement behaviour in barnacle cyprids (*Balanus improvisus*). Biofouling, 30(2), 143-152.

Dreanno, C., Kirby, R.R. and Clare, A.S., 2006a. Smelly feet are not always a bad thing: The relationship between cyprid footprint protein and the barnacle settlement pheromone. Biology letters, 2(3), 423-425.

Dreanno, C., Kirby, R.R. and Clare, A.S., 2006b. Locating the barnacle settlement pheromone: Spatial and ontogenetic expression of the settlement-inducing protein

complex of *Balanus amphitrite*. Proceedings of the Royal Society B: Biological Sciences, 273(1602), 2721-2728.

Dreanno, C., Kirby, R.R. and Clare, A.S., 2007. Involvement of the barnacle settlement-inducing protein complex (SIPC) in species recognition at settlement. Journal of Experimental Marine Biology and Ecology, 351(1-2), 276-282.

Dreanno, C., Matsumura, K., Dohmae, N., Takio, K., Hirota, H., Kirby, R.R. and Clare, A.S., 2006c. An α2-macroglobulin-like protein is the cue to gregarious settlement of the barnacle *Balanus amphitrite*. Proceedings of the National Academy of Sciences, 103(39), 14396-14401.

Eckman, J.E., 1990. A model of passive settlement by planktonic larvae onto bottoms of differing roughness. Limnology and Oceanography, 35(4), 887-901.

Eckman, J.E., Savidge, W.B. and Gross, T.F., 1990. Relationship between duration of cyprid attachment and drag forces associated with detachment of *Balanus amphitrite* cyprids. Marine Biology, 107(1), 111-118.

Elbourne, P.D. and Clare, A.S., 2010. Ecological relevance of a conspecific, waterborne settlement cue in *Balanus amphitrite* (Cirripedia). Journal of Experimental Marine Biology and Ecology, 392(1-2), 99-106.

Elbourne, P.D., 2008. Ecological role of an adult-derived, waterborne cue in cyprid settlement in the barnacle *Balanus amphitrite* Darwin (Doctoral dissertation, University of Newcastle Upon Tyne).

Elbourne, P.D., Veater, R.A. and Clare, A.S., 2008. Interaction of conspecific cues in *Balanus amphitrite* Darwin (Cirripedia) settlement assays: Continued argument for the single-larva assay. Biofouling, 24(2), 87-96.

Endo, N., Nogata, Y., Yoshimura, E. and Matsumura, K., 2009. Purification and partial amino acid sequence analysis of the larval settlement-inducing pheromone from adult extracts of the barnacle, *Balanus amphitrite* (= *Amphibalanus amphitrite*). Biofouling, 25(5), 429-434.

Endo, N., Sato, K., Matsumura, K., Yoshimura, E., Odaka, Y. and Nogata, Y., 2010. Species-specific detection and quantification of common barnacle larvae from the Japanese coast using quantitative real-time PCR. Biofouling, 26(8), 901-911.

Essock-Burns, T., Gohad, N.V., Orihuela, B., Mount, A.S., Spillmann, C.M., Wahl, K.J. and Rittschof, D., 2017. Barnacle biology before, during and after settlement and metamorphosis: A study of the interface. Journal of Experimental Biology, 220(2), 194-207.

Ewers-Saucedo, C., Owen, C.L., Pérez-Losada, M., Høeg, J.T., Glenner, H., Chan, B. and Crandall, K.A., 2019. Towards a barnacle tree of life: Integrating diverse phylogenetic efforts into a comprehensive hypothesis of thecostracan evolution. PeerJ, 7, e7387.

Fears, K.P., Orihuela, B., Rittschof, D. and Wahl, K.J., 2018. Acorn barnacles secrete phase-separating fluid to clear surfaces ahead of cement deposition. Advanced Science, 5(6), 1700762.

Ferrier, G.A., Kim, S.J., Kaddis, C.S., Loo, J.A., Ann Zimmer, C. and Zimmer, R.K., 2016. MULTIFUNCin: A multifunctional protein cue induces habitat selection by, and predation on, barnacles. Integrative and Comparative Biology, 56(5), 901-913.

Finlay, J.A., Bennett, S.M., Brewer, L.H., Sokolova, A., Clay, G., Gunari, N., Meyer, A.E., Walker, G.C., Wendt, D.E., Callow, M.E. and Callow, J.A., 2010. Barnacle settlement and the adhesion of protein and diatom microfouling to xerogel films with varying surface energy and water wettability. Biofouling, 26(6), 657-666.

Franco, S.C., Aldred, N., Cruz, T. and Clare, A.S., 2016. Modulation of gregarious settlement of the stalked barnacle, *Pollicipes pollicipes*: A laboratory study. Scientia Marina, 80(2), 217-228.

Freeman, J.A. and Costlow, J.D., 1983. The cyprid molt cycle and its hormonal control in the barnacle *Balanus amphitrite*. Journal of Crustacean Biology, 3(2), 173-182.

Freeman, S.C., Malik, A. and Basit, H., 2020. Physiology, Exocrine Gland. StatPearls Publishing, Treasure Island, USA, (Internet), Updated 24 August 2020. Available online: https://www.ncbi.nlm.nih.gov/books/NBK542322/ (accessed on 25 November 2020).

Fukui, T., Kitamura, N., Kurokawa, T., Yokota, M., Kondo, E., Gong, J.P. and Yasuda, K., 2014. Intra-articular administration of hyaluronic acid increases the volume of the hyaline cartilage regenerated in a large osteochondral defect by implantation of a

double-network gel. Journal of Materials Science: Materials in Medicine, 25(4), 1173-1182.

Fyhn, U.E. and Costlow, J.D., 1976. A histochemical study of cement secretion during the intermolt cycle in barnacles. The Biological Bulletin, 150(1), 47-56.

Gaonkar, C.C., Khandeparker, L., Desai, D.V., and Anil, A.C., 2015. Identification of *Balanus amphitrite* larvae from field zooplankton using species-specific primers. Journal of the Marine Biological Association of the United Kingdom, 95(3), 497-502.

Gasteiger, E., Gattiker, A., Hoogland, C., Ivanyi, I., Appel, R.D. and Bairoch, A., 2003. ExPASy: The proteomics server for in-depth protein knowledge and analysis. Nucleic Acids Research, 31(13), 3784-3788.

Gatley-Montross, C.M., Finlay, J.A., Aldred, N., Cassady, H., Destino, J.F., Orihuela, B., Hickner, M.A., Clare, A.S., Rittschof, D., Holm, E.R. and Detty, M.R., 2017. Multivariate analysis of attachment of biofouling organisms in response to material surface characteristics. Biointerphases, 12(5), 051003.

Gibert, J.M., Mouchel-Vielh, E., Quéinnec, E. and Deutsch, J.S., 2000. Barnacle duplicate engrailed genes: Divergent expression patterns and evidence for a vestigial abdomen. Evolution and Development, 2(4), 194-202.

Gohad, N.V., Aldred, N., Hartshorn, C.M., Lee, Y.J., Cicerone, M.T., Orihuela, B., Clare, A.S., Rittschof, D. and Mount, A.S., 2014. Synergistic roles for lipids and proteins in the permanent adhesive of barnacle larvae. Nature communications, 5(1), 1-9.

Gohad, N.V., Aldred, N., Orihuela, B., Clare, A.S., Rittschof, D. and Mount, A.S., 2012. Observations on the settlement and cementation of barnacle (*Balanus amphitrite*) cyprid larvae after artificial exposure to noradrenaline and the locations of adrenergic-like receptors. Journal of Experimental Marine Biology and Ecology, 416, 153-161.

Golden, J.P., Burden, D.K., Fears, K.P., Barlow, D.E., So, C.R., Burns, J., Miltenberg, B., Orihuela, B., Rittshof, D., Spillmann, C.M. and Wahl, K.J., 2016. Imaging active surface processes in barnacle adhesive interfaces. Langmuir, 32(2), 541-550.

Grabherr, M.G., Haas, B.J., Yassour, M., Levin, J.Z., Thompson, D.A., Amit, I., Adiconis, X., Fan, L., Raychowdhury, R., Zeng, Q. and Chen, Z., 2011. Full-length

transcriptome assembly from RNA-Seq data without a reference genome. Nature Biotechnology, 29(7), 644-652.

Guerette, P.A., Hoon, S., Ding, D., Amini, S., Masic, A., Ravi, V., Venkatesh, B., Weaver, J.C. and Miserez, A., 2014. Nanoconfined β-sheets mechanically reinforce the supra-biomolecular network of robust squid sucker ring teeth. ACS Nano, 8(7), 7170-7179.

Guerette, P.A., Hoon, S., Seow, Y., Raida, M., Masic, A., Wong, F.T., Ho, V.H., Kong, K.W., Demirel, M.C., Pena-Francesch, A. and Amini, S., 2013. Accelerating the design of biomimetic materials by integrating RNA-seq with proteomics and materials science. Nature Biotechnology, 31(10), 908-915.

Guo, S., Puniredd, S.R., Jańczewski, D., Lee, S.S.C., Teo, S.L.M., He, T., Zhu, X. and Vancso, G.J., 2014. Barnacle larvae exploring surfaces with variable hydrophilicity: Influence of morphology and adhesion of “footprint” proteins by AFM. ACS Applied Materials and Interfaces, 6(16), 13667-13676.

He, L.S., Zhang, G. and Qian, P.Y., 2013. Characterization of two 20kDa-cement protein (cp20k) homologues in *Amphibalanus amphitrite*. PLoS ONE, 8(5), e64130.

He, L.S., Zhang, G., Wang, Y., Yan, G.Y. and Qian, P.Y., 2018. Toward understanding barnacle cementing by characterization of one cement protein-100kDa in *Amphibalanus amphitrite*. Biochemical and Biophysical Research Communications, 495(1), 969-975.

Head, R., Overbeke, K., Klijnstra, J., Biersteker, R. and Thomason, J., 2003. The effect of gregariousness in cyprid settlement assays. Biofouling, 19(4), 269-278.

Head, R.M., Berntsson, K.M., Dahlström, M., Overbeke, K. and Thomason, J.C., 2004. Gregarious settlement in cypris larvae: The effects of cyprid age and assay duration. Biofouling, 20(2), 123-128.

Herbert, B., 1999. Advances in protein solubilisation for two-dimensional electrophoresis. ELECTROPHORESIS: An International Journal, 20(4-5), 660-663.

Higgins, M.J., Crawford, S.A., Mulvaney, P. and Wetherbee, R., 2002. Characterization of the adhesive mucilages secreted by live diatom cells using atomic force microscopy. Protist, 153(1), 25-38.

Higuchi, R., Fockler, C., Dollinger, G. and Watson, R., 1993. Kinetic PCR analysis: real-time monitoring of DNA amplification reactions. Bio/technology, 11(9), 1026-1030.

Hills, J.M., Thomason, J.C., Davis, H., Köhler, J. and Millett, E., 2000. Exploratory behaviour of barnacle larvae in field conditions. Biofouling, 16(2-4), 171-179.

Hills, J.M., Thomason, J.C., Milligan, J.L. and Richardson, M., 1998. Do barnacle larvae respond to multiple settlement cues over a range of spatial scales?. In Recruitment, colonization and physical-chemical forcing in marine biological systems, Baden, S., Pihl, L., Rosenberg, R., Strömberg, J. O., Svane, I. and Tiselius, P. Ed., Springer, Dordrecht, Netherlands, 101-111.

Hoch, J.M., Schneck, D.T. and Neufeld, C.J., 2016. Ecology and evolution of phenotypic plasticity in the penis and cirri of barnacles. Integrative and Comparative Bbiology, 56(4), 728-740.

Høeg, J.T., 1987. Male cypris metamorphosis and a new male larval form, the trichogon, in the parasitic barnacle *Sacculina carcini* (Crustacea: Cirripedia: Rhizocephala). Philosophical Transactions of the Royal Society B, Biological Sciences, 317(1183), 47-63.

Høeg, J.T. and Møller, O.S., 2006. When similar beginnings lead to different ends: Constraints and diversity in cirripede larval development. Invertebrate Reproduction and Development, 49(3), 125-142.

Hohagen, J., Herlitze, I. and Jackson, D.J., 2015. An optimised whole mount in situ hybridisation protocol for the mollusc *Lymnaea stagnalis*. BMC Developmental Biology, 15(1), 1-13.

Holm, E.R., McClary Jr, M. and Rittschof, D., 2000. Variation in attachment of the barnacle *Balanus amphitrite*: Sensation or something else?. Marine Ecology Progress Series, 202, 153-162.

Horton, T., Kroh, A., Ahyong, S., Bailly, N., Boyko, C.B., Brandão, S.N., Gofas, S., Hooper, J.N.A., Hernandez, F., Holovachov, O., *et al.,* 2020. World Register of Marine Species. Available from https://www.marinespecies.org at VLIZ. Accessed 18th May 2020.

Jalili, V., Afgan, E., Gu, Q., Clements, D., Blankenberg, D., Goecks, J., Taylor, J. and Nekrutenko, A., 2020. The Galaxy platform for accessible, reproducible and collaborative biomedical analyses: 2020 update. Nucleic Acids Research, 48(1), 395-402.

Jensen, E., 2014. Technical review: in situ hybridization. The Anatomical Record, 297(8), 1349-1353.

Jerosch, J., 2011. Effects of glucosamine and chondroitin sulfate on cartilage metabolism in OA: Outlook on other nutrient partners especially omega-3 fatty acids. International journal of rheumatology, 2011, e969012.

Johansson, M.W., Keyser, P., Sritunyalucksana, K. and Söderhäll, K., 2000. Crustacean haemocytes and haematopoiesis. Aquaculture, 191(1-3), 45-52.

Jonker, J.L., Abram, F., Pires, E., Coelho, A.V., Grunwald, I. and Power, A.M., 2014. Adhesive proteins of stalked and acorn barnacles display homology with low sequence similarities. Plos ONE, 9(10).

Kamino, K., 2013. Mini-review: Barnacle adhesives and adhesion. Biofouling, 29(6), 735-749.

Kamino K., 2016 Barnacle underwater attachment. In Biological adhesives, Smith M.A. and Callow., J.A., Ed., Springer-Verlag, Berlin, Germany, 153-176.

Kamino, K. and Shizuri, Y., 1998. Structure and function of barnacle cement proteins. In New developments in marine biotechnology, Le Gal, Y. and Halvorson, H.O., Ed., Springer, Boston, USA, 77-80

Kamino, K., Inoue, K., Maruyama, T., Takamatsu, N., Harayama, S. and Shizuri, Y., 2000. Barnacle cement proteins importance of disulfide bonds in their insolubility. Journal of Biological Chemistry, 275(35), 27360-27365.

Kamino, K., Nakano, M. and Kanai, S., 2012. Significance of the conformation of building blocks in curing of barnacle underwater adhesive. The FEBS Journal, 279(10), 1750-1760.

Kamino, K., Odo, S. and Maruyama, T., 1996. Cement proteins of the acorn-barnacle, *Megabalanus rosa*. The Biological Bulletin, 190(3), 403-409.

Kamperman, M., Kroner, E., del Campo, A., McMeeking, R.M. and Arzt, E., 2010. Functional adhesive surfaces with “gecko” effect: The concept of contact splitting. Advanced Engineering Materials, 12(5), 335-348.

Kato-Yoshinaga, Y., Nagano, M., Mori, S., Clare, A.S., Fusetani, N. and Matsumura, K., 2000. Species specificity of barnacle settlement-inducing proteins. Comparative Biochemistry and Physiology Part A: Molecular and Integrative Physiology, 125(4), 511-516.

Kavanagh, C. J., Quinn, R. D. and Swain, G. W., 2005. Observations of barnacle detachment from silicones using high-speed video. The Journal of Adhesion, 81(7-8), 843-868.

Khandeparker, L., Anil, A.C. and Raghukumar, S., 2002. Exploration and metamorphosis in *Balanus amphitrite* Darwin (Cirripedia; Thoracica) cyprids: significance of sugars and adult extract. Journal of Experimental Marine Biology and Ecology, 281(1-2), 77-88.

Kim, J.H., Kim, H., Kim, H., Chan, B.K., Kang, S. and Kim, W., 2019. Draft genome assembly of a fouling barnacle, *Amphibalanus amphitrite* (Darwin, 1854): The first reference genome for Thecostraca. Frontiers in Ecology and Evolution, 7, 465.

Klieber, M.A., Underhill, C., Hammond, G.L. and Muller, Y.A., 2007. Corticosteroid-binding globulin, a structural basis for steroid transport and proteinase-triggered release. Journal of Biological Chemistry, 282(40), 29594-29603.

Knight-Jones, E.W. and Crisp, D.J., 1953. Gregariousness in barnacles in relation to the fouling of ships and to anti-fouling research. Nature, 171(4364), 1109-1110.

Knight-Jones, E.W., 1955. The gregarious setting reaction of barnacles as a measure of systematic affinity. Nature, 175(4449), 266-266.

Knudson, C.B. and Knudson, W., 1993. Hyaluronan-binding proteins in development, tissue homeostasis, and disease. The Journal of the Federation of American Societies for Experimental Biology, 7(13), 1233-1241.

Koivusalo, L., Kauppila, M., Samanta, S., Parihar, V.S., Ilmarinen, T., Miettinen, S., Oommen, O.P. and Skottman, H., 2019. Tissue adhesive hyaluronic acid hydrogels

for sutureless stem cell delivery and regeneration of corneal epithelium and stroma. Biomaterials, 225, e119516.

Koressaar, T. and Remm, M., 2007. Enhancements and modifications of primer design program Primer3. Bioinformatics, 23(10), 1289-91.

Koressaar, T., Lepamets, M., Kaplinski, L., Raime, K., Andreson, R. and Remm, M., 2018. Primer3_masker: integrating masking of template sequence with primer design software. Bioinformatics, 34(11), 1937-1938.

Kotsiri, M., Protopapa, M., Mouratidis, S., Zachariadis, M., Vassilakos, D., Kleidas, I., Samiotaki, M. and Dedos, S.G., 2018. Should I stay or should I go? The settlement-inducing protein complex guides barnacle settlement decisions. Journal of Experimental Biology, 221(22), 185348.

Lagersson, N. and Høeg, J., 2002. Settlement behavior and antennulary biomechanics in cypris larvae of *Balanus amphitrite* (Crustacea: Thecostraca: Cirripedia). Marine Biology, 141(3), 513-526.

Larsson, A.I., Granhag, L.M. and Jonsson, P.R., 2016. Instantaneous flow structures and opportunities for larval settlement: barnacle larvae swim to settle. PloS ONE, 11(7).

Law, R.H., Zhang, Q., McGowan, S., Buckle, A.M., Silverman, G.A., Wong, W., Rosado, C.J., Langendorf, C.G., Pike, R.N., Bird, P.I. and Whisstock, J.C., 2006. An overview of the serpin superfamily. Genome biology, 7(5), 1-11.

Lee, H., Scherer, N.F. and Messersmith, P.B., 2006. Single-molecule mechanics of mussel adhesion. Proceedings of the National Academy of Sciences, 103(35), 12999-13003.

Lennon, F.E. and Singleton, P.A., 2011. Role of hyaluronan and hyaluronan-binding proteins in lung pathobiology. American Journal of Physiology-Lung Cellular and Molecular Physiology, 301(2), 137-147.

Liang, C., Strickland, J., Ye, Z., Wu, W., Hu, B. and Rittschof, D., 2019. Biochemistry of barnacle adhesion: An updated review. Frontiers in Marine Science, 6, 565.

Liang, C., Ye, Z., Xue, B., Zeng, L., Wu, W., Zhong, C., Cao, Y., Hu, B. and Messersmith, P.B., 2018. Self-assembled nanofibers for strong underwater adhesion: The trick of barnacles. ACS Applied Materials and Interfaces, 10(30), 25017-25025.

Lin, H.C., Wong, Y.H., Tsang, L.M., Chu, K.H., Qian, P.Y. and Chan, B.K., 2014. First study on gene expression of cement proteins and potential adhesion-related genes of a membranous-based barnacle as revealed from Next-Generation Sequencing technology. Biofouling, 30(2), 169-181.

Lind, U., Järvå, M., Alm Rosenblad, M., Pingitore, P., Karlsson, E., Wrange, A.L., Kamdal, E., Sundell, K., André, C., Jonsson, P.R. and Havenhand, J., 2017. Analysis of aquaporins from the euryhaline barnacle *Balanus improvisus* reveals differential expression in response to changes in salinity. PLoS ONE, 12(7), e0181192.

Lind, U., Rosenblad, M.A., Wrange, A.L., Sundell, K.S., Jonsson, P. R., André, C., Havenhand, J. and Blomberg, A., 2013. Molecular characterization of the α-subunit of Na+/K+ ATPase from the euryhaline barnacle *Balanus improvisus* reveals multiple genes and differential expression of alternative splice variants. PLoS ONE, 8(10), e77069.

Liu, X., Liang, C., Zhang, X., Li, J., Huang, J., Zeng, L., Ye, Z., Hu, B. and Wu, W., 2017. Amyloid fibril aggregation: An insight into the underwater adhesion of barnacle cement. Biochemical and Biophysical Research Communications, 493(1), 654-659.

Livak, K.J. and Schmittgen, T.D., 2001. Analysis of relative gene expression data using real-time quantitative PCR and the 2− ΔΔCT method. Methods, 25(4), 402-408.

Lorenz, M.W., Kellner, R. and Hoffmann, K.H., 1995. Identification of two allatostatins from the cricket, *Gryllus bimaculatus* de Geer (Ensifera, Gryllidae): Additional members of a family of neuropeptides inhibiting juvenile hormone biosynthesis. Regulatory Peptides, 57(3), 227-236.

Lucas, M.I., Walker, G., Holland, D.L. and Crisp, D.J., 1979. An energy budget for the free-swimming and metamorphosing larvae of *Balanus balanoides* (Crustacea: Cirripedia). Marine Biology, 55(3), 221-229.

Maki, J.S., Rittschof, D., Costlow, J.D. and Mitchell, R., 1988. Inhibition of attachment of larval barnacles, *Balanus amphitrite*, by bacterial surface films. Marine Biology, 97(2), 199-206.

Maki, J.S., Yule, A.B., Rittschof, D. and Mitchell, R., 1994. The effect of bacterial films on the temporary adhesion and permanent fixation of cypris larvae, *Balanus amphitrite* Darwin. Biofouling, 8(2), 121-131.

Mala, J.G.S. and Rose, C., 2010. Interactions of heat shock protein 47 with collagen and the stress response: an unconventional chaperone model?. Life sciences, 87(19-22), 579-586.

Maleschlijski, S., Bauer, S., Aldred, N., Clare, A.S. and Rosenhahn, A., 2015. Classification of the pre-settlement behaviour of barnacle cyprids. Journal of The Royal Society Interface, 12(102), 20141104.

Maréchal, J.P., Matsumura, K., Conlan, S. and Hellio, C., 2012. Competence and discrimination during cyprid settlement in *Amphibalanus amphitrite*. International Biodeterioration and Biodegradation, 72, 59-66.

Maruzzo, D., Conlan, S., Aldred, N., Clare, A.S. and Høeg, J.T., 2011. Video observation of surface exploration in cyprids of *Balanus amphitrite*: The movements of antennular sensory setae. Biofouling, 27(2), 225-239.

Matsumura, K. and Qian, P.Y., 2014. Larval vision contributes to gregarious settlement in barnacles: Adult red fluorescence as a possible visual signal. Journal of Experimental Biology, 217(5), 743-750.

Matsumura, K., Nagano, M. and Fusetani, N., 1998. Purification of a larval settlement-inducing protein complex (SIPC) of the barnacle, *Balanus amphitrite*. Journal of Experimental Zoology, 281(1), 12-20.

Miron, G., Walters, L.J., Tremblay, R. and Bourget, E., 2000. Physiological condition and barnacle larval behavior: A preliminary look at the relationship between TAG/DNA ratio and larval substratum exploration in *Balanus amphitrite*. Marine Ecology Progress Series, 198, 303-310.

Mishra, J.K. and Kitamura, H., 2000. The effect of mono-amino acids on larval settlement of the barnacle, *Balanus amphitrite* Darwin. Biofouling, 14(4), 299-203.

Mori, Y., Urushida, Y., Nakano, M., Uchiyama, S. and Kamino, K., 2007. Calcite-specific coupling protein in barnacle underwater cement. The FEBS Journal, 274(24), 6436-6446.

Mullineaux, L.S. and Butman, C.A., 1991. Initial contact, exploration and attachment of barnacle (*Balanus amphitrite*) cyprids settling in flow. Marine Biology, 110(1), 93-103.

Noirot, C. and Quennedey, A., 1974. Fine structure of insect epidermal glands. Annual Review of Entomology, 19, 61-80.

Nott, J.A. and Foster, B., 1969. On the structure of the antennular attachment organ of the cypris larva of *Balanus balanoides* (L.). Philosophical Transactions of the Royal Society B, Biological Sciences, 256(803), 115-134.

Nott, J.A., 1969. Settlement of barnacle larvae: Surface structure of the antennular attachment disc by scanning electron microscopy. Marine Biology, 2(3), 248-251.

O'Connor, N.J. and Richardson, D.L., 1994. Comparative attachment of barnacle cyprids (*Balanus amphitrite* Darwin, 1854; *B. improvisus* Darwin, 1854; & *B. ebumeus* Gould, 1841) to polystyrene and glass substrata. Journal of Experimental Marine Biology and Ecology, 183(2), 213-225.

Ödling, K., Albertsson, C., Russell, J.T. and Mårtensson, L.G., 2006. An in vivo study of exocytosis of cement proteins from barnacle *Balanus improvisus* (D.) cyprid larva. Journal of Experimental Biology, 209(5), 956-964.

Okano, K., Shimizu, K., Satuito, C. and Fusetani, N. 1996. Visualization of cement exocytosis in the cypris cement gland of the barnacle *Megabalanus rosa*. Journal of Experimental Biology, 199(10), 2131-2137.

Olivier, F., Tremblay, R., Bourget, E. and Rittschof, D., 2000. Barnacle settlement: Field experiments on the influence of larval supply, tidal level, biofilm quality and age on *Balanus amphitrite* cyprids. Marine Ecology Progress Series, 199, 185-204.

Ostromohov, N., Huber, D., Bercovici, M. and Kaigala, G.V., 2018. Real-time monitoring of fluorescence in situ hybridization kinetics. Analytical chemistry, 90(19), 11470-11477.

Pagett, H.E., Abrahams, J.L., Bones, J., O'Donoghue, N., Marles-Wright, J., Lewis, R.J., Harris, J.R., Caldwell, G.S., Rudd, P.M. and Clare, A.S., 2012. Structural characterisation of the N-glycan moiety of the barnacle settlement-inducing protein complex (SIPC). Journal of Experimental Biology, 215(7), 1192-1198.

Patil, J.S. and Anil, A.C., 2005. Influence of diatom exopolymers and biofilms on metamorphosis in the barnacle *Balanus amphitrite*. Marine Ecology Progress Series, 301, 231-245.

Pearson, B.J., Eisenhoffer, G.T., Gurley, K.A., Rink, J.C., Miller, D.E. and Sánchez Alvarado, A., 2009. Formaldehyde-based whole-mount in situ hybridization method for planarians. Developmental dynamics, 238(2), 443-450.

Pechenik, J.A., 1999. On the advantages and disadvantages of larval stages in benthic marine invertebrate life cycles. Marine Ecology Progress Series, 177, 269-297.

Pechenik, J.A., Rittschof, D. and Schmidt, A.R., 1993. Influence of delayed metamorphosis on survival and growth of juvenile barnacles *Balanus amphitrite*. Marine Biology, 115(2), 287-294.

Pérez-Losada, M., Harp, M., Høeg, J.T., Achituv, Y., Jones, D., Watanabe, H. and Crandall, K.A., 2008. The tempo and mode of barnacle evolution. Molecular Phylogenetics and Evolution, 46(1), 328-346.

Pérez-Losada, M., Høeg, J.T. and Crandall, K.A., 2004. Unravelling the evolutionary radiation of the thoracican barnacles using molecular and morphological evidence: A comparison of several divergence time estimation approaches. Systematic Biology, 53, 278-298.

Petrone, L., Aldred, N., Emami, K., Enander, K., Ederth, T. and Clare, A.S., 2015. Chemistry-specific surface adsorption of the barnacle settlement-inducing protein complex. Interface Focus, 5(1), 20140047.

Petrone, L., Di Fino, A., Aldred, N., Sukkaew, P., Ederth, T., Clare, A.S. and Liedberg, B., 2011. Effects of surface charge and Gibbs surface energy on the settlement behaviour of barnacle cyprids (*Balanus amphitrite*). Biofouling, 27(9), 1043-1055.

Pfeiffer, F., Gröber, C., Blank, M., Händler, K., Beyer, M., Schultze, J. L. and Mayer, G., 2018. Systematic evaluation of error rates and causes in short samples in next-generation sequencing. Scientific Reports, 8(1), 1-14.

Phang, I.Y., Aldred, N., Clare, A.S. and Vancso, G.J., 2008. Towards a nanomechanical basis for temporary adhesion in barnacle cyprids (*Semibalanus balanoides*). Journal of the Royal Society Interface, 5(21), 397-402.

Phang, I.Y., Aldred, N., Clare, A.S., Callow, J.A. and Vancso, G.J., 2006. An in situ study of the nanomechanical properties of barnacle (*Balanus amphitrite*) cyprid cement using atomic force microscopy (AFM). Biofouling, 22(4), 245-250.

Phang, I.Y., Aldred, N., Ling, X.Y., Huskens, J., Clare, A.S. and Vancso, G.J., 2010. Atomic force microscopy of the morphology and mechanical behaviour of barnacle cyprid footprint proteins at the nanoscale. Journal of the Royal Society Interface, 7(43), 285-296.

Phang, I.Y., Aldred, N., Ling, X.Y., Tomczak, N., Huskens, J., Clare, A.S. and Vancso, G.J., 2009. Chemistry-specific interfacial forces between barnacle (*Semibalanus balanoides*) cyprid footprint proteins and chemically functionalised AFM tips. The Journal of Adhesion, 85(9), 616-630.

Pimentel, H., Bray, N.L., Puente, S., Melsted, P. and Pachter, L., 2017. Differential analysis of RNA-seq incorporating quantification uncertainty. Nature Methods, 14(7), 687-690.

Prendergast, G.S., Zurn, C.M., Bers, A.V., Head, R.M., Hansson, L.J. and Thomason, J.C., 2008. Field-based video observations of wild barnacle cyprid behaviour in response to textural and chemical settlement cues. Biofouling, 24(6), 449-459.

Qian, P.Y., Thiyagarajan, V., Lau, S.C.K. and Cheung, S.C.K., 2003. Relationship between bacterial community profile in biofilm and attachment of the acorn barnacle *Balanus amphitrite*. Aquatic Microbial Ecology, 33(3), 225-237.

Quennedey, A., 1998. Insect epidermal gland cells: Ultrastructure and morphogenesis. In Microscopic anatomy of invertebrates, Harrison, F. and Locke, M., Ed., Wiley-Liss, Hoboken, USA, 177-207.

Rabet, N., Gibert, J.M., Quéinnec, É., Deutsch, J.S. and Mouchel-Vielh, E., 2001. The caudal gene of the barnacle *Sacculina carcini* is not expressed in its vestigial abdomen. Development Genes and Evolution, 211(4), 172-178.

Raine, J.J., Aldred, N. and Clare, A.S., 2020. Anatomy and Ultrastructure of the Cyprid Temporary Adhesive System in Two Species of Acorn Barnacle. Journal of Marine Science and Engineering, 8(12), 968.

Raman, S., Karunamoorthy, L., Doble, M., Kumar, R. and Venkatesan, R., 2013. Barnacle adhesion on natural and synthetic substrates: Adhesive structure and composition. International Journal of Adhesion and Adhesives, 41, 140-143.

Rappsilber, J., Mann, M. and Ishihama, Y., 2007. Protocol for micro-purification, enrichment, pre-fractionation and storage of peptides for proteomics using StageTips. Nature Protocols, 2(8), 1896-906.

Rittschof, D., 1985. Oyster drills and the frontiers of chemical ecology: Unsettling ideas. Bulletin of the American Maritime Union, 1, 111-116.

Rittschof, D., 1993. Body odors and neutral-basic peptide mimics: A review of responses by marine organisms. American Zoologist, 33(6), 487-493.

Rittschof, D., Branscomb, E.S. and Costlow, J.D., 1984. Settlement and behaviour in relation to flow and surface in larval barnacles, *Balanus amphitrite* Darwin. Journal of Experimental Marine Biology and Ecology, 82(2-3), 131-146.

Rittschof, D., Maki, J., Mitchell, R. and Costlow, J.D., 1986. Ion and neuropharmacological studies of barnacle settlement. Netherlands Journal of Sea Research, 20(2-3), 269-275.

Robson, M.A., Williams, D., Wolff, K. and Thomason, J.C., 2009. The effect of surface colour on the adhesion strength of *Elminius modestus* Darwin on a commercial non-biocidal antifouling coating at two locations in the UK. Biofouling, 25(3), 215-227.

Rocha, M.S., 2015. Molecular targets involved in the goose barnacle *Pollicipes pollicipes* (Cirripedia) larvae metamorphosis and settlement. (Doctoral dissertation, University of Porto.

Ruppert, E.E. and Barnes, R.D., 1994. Invertebrate Zoology,. Saunders College Publishing, Florida, USA, 6th edition.

Rybakov, A.V., Høeg, J.T., Jensen, P.G. and Kolbasov, G.A., 2003. The chemoreceptive lattice organs in cypris larvae develop from naupliar setae (Thecostraca: Cirripedia, Ascothoracida and Facetotecta). Zoologischer Anzeiger-A Journal of Comparative Zoology, 242(1), 1-20.

Satuito, C.G., Shimizu, K., Natoyama, K., Yamazaki, M. and Fusetani, N., 1996. Age-related settlement success by cyprids of the barnacle *Balanus amphitrite*, with special reference to consumption of cyprid storage protein. Marine Biology, 127(1), 125-130.

Schmidt, M., Cavaco, A., Gierlinger, N., Aldred, N., Fratzl, P., Grunze, M. and Clare, A.S., 2009. In situ imaging of barnacle (*Balanus amphitrite*) cyprid cement using confocal Raman microscopy. The Journal of Adhesion, 85(2-3), 139-151.

Schultzhaus, J.N., Dean, S.N., Leary, D.H., Hervey, W.J., Fears, K.P., Wahl, K.J. and Spillmann, C.M., 2019. Pressure cycling technology for challenging proteomic sample processing: Application to barnacle adhesive. Integrative Biology, 11(5), 235-247.

Senkbeil, T., Mohamed, T., Simon, R., Batchelor, D., Di Fino, A., Aldred, N., Clare, A.S. and Rosenhahn, A., 2016. In vivo and in situ synchrotron radiation-based μ-XRF reveals elemental distributions during the early attachment phase of barnacle larvae and juvenile barnacles. Analytical and Bioanalytical Chemistry, 408(5), 1487-1496.

Shimizu, H., Shimoda, M., Mochizuki, S., Miyamae, Y., Abe, H., Chijiiwa, M., Yoshida, H., Shiozawa, J., Ishijima, M., Kaneko, K. and Kanaji, A., 2018. Hyaluronan-binding protein involved in hyaluronan depolymerization is up-regulated and involved in hyaluronan degradation in human osteoarthritic cartilage. The American Journal of Pathology, 188(9), 2109-2119.

Shimizu, K., Satuito, C.G., Saikawa, W. and Fusetani, N., 1996. Larval storage protein of the barnacle, *Balanus amphitrite*: Biochemical and immunological similarities to vitellin. Journal of Experimental Zoology, 276(2), 87-94.

Shimoda, M., Yoshida, H., Mizuno, S., Hirozane, T., Horiuchi, K., Yoshino, Y., Hara, H., Kanai, Y., Inoue, S., Ishijima, M. and Okada, Y., 2017. Hyaluronan-binding protein involved in hyaluronan depolymerization controls endochondral ossification through hyaluronan metabolism. The American Journal of Pathology, 187(5), 1162-1176.

Shiomoto, S., Yamaguchi, Y., Yamaguchi, K., Nogata, Y. and Kobayashi, M., 2019. Adhesion force measurement of live cypris tentacles by scanning probe microscopy in seawater. Polymer Journal, 51(1), 51-59.

Smith, P.A., Clare, A.S., Rees, H.H., Prescott, M.C., Wainwright, G. and Thorndyke, M.C., 2000. Identification of methyl farnesoate in the cypris larva of the barnacle, *Balanus amphitrite*, and its role as a juvenile hormone. Insect Biochemistry and Molecular Biology, 30(8-9), 885-890.

So, C.R., Fears, K.P., Leary, D.H., Scancella, J.M., Wang, Z., Liu, J.L., Orihuela, B., Rittschof, D., Spillmann, C.M. and Wahl, K.J., 2016. Sequence basis of barnacle cement nanostructure is defined by proteins with silk homology. Scientific Reports, 6(1), 1-14.

So, C.R., Scancella, J.M., Fears, K.P., Essock-Burns, T., Haynes, S.E., Leary, D.H., Diana, Z., Wang, C., North, S., Oh, C.S. and Wang, Z., 2017. Oxidase activity of the barnacle adhesive interface involves peroxide-dependent catechol oxidase and lysyl oxidase enzymes. ACS Applied Materials and Interfaces, 9(13), 11493-11505.

So, C.R., Yates, E.A., Estrella, L.A., Fears, K.P., Schenck, A.M., Yip, C.M. and Wahl, K.J., 2019. Molecular recognition of structures is key in the polymerization of patterned barnacle adhesive sequences. ACS Nano, 13(5), 5172-5183.

Stark, R., Grzelak, M. and Hadfield, J., 2019. RNA sequencing: the teenage years. Nature Reviews Genetics, 20(11), 631-656.

Sullan, R.M.A., Gunari, N., Tanur, A.E., Chan, Y., Dickinson, G.H., Orihuela, B., Rittschof, D. and Walker, G.C., 2009. Nanoscale structures and mechanics of barnacle cement. Biofouling, 25(3), 263-275.

Talbot, P. and Demers, D., 1993. Tegumental glands of Crustacea. In Crustacean integument: Morphology and biochemistry, Horst, M.N. and Freeman, J.A., Ed., CRC Press, Boca Raton, USA, 151-191.

Tegtmeyer, K. and Rittschof, D., 1989. Synthetic peptide analogs to barnacle settlement pheromone. Peptides, 9(6), 1403-1406.

Thiyagarajan, V. and Qian, P.Y., 2008. Proteomic analysis of larvae during development, attachment, and metamorphosis in the fouling barnacle, *Balanus amphitrite*. Proteomics, 8(15), 3164-3172.

Thiyagarajan, V., Harder, T., Qiu, J.W. and Qian, P.Y., 2003. Energy content at metamorphosis and growth rate of the early juvenile barnacle *Balanus amphitrite*. Marine Biology, 143(3), 543-554.

Tilbury, M.A., McCarthy, S., Domagalska, M., Ederth, T., Power, A.M. and Wall, J.G., 2019. The expression and characterization of recombinant cp19k barnacle cement protein from *Pollicipes pollicipes*. Philosophical Transactions of the Royal Society B, 374(1784), 20190205.

Turley, E.A., Austen, L., Vandeligt, K. and Clary, C., 1991. Hyaluronan and a cell-associated hyaluronan binding protein regulate the locomotion of ras-transformed cells. The Journal of Cell Biology, 112(5), 1041-1047.

Untergasser, A., Cutcutache, I., Koressaar, T., Ye, J., Faircloth, B.C., Remm, M. and Rozen, S.G., 2012. Primer3--new capabilities and interfaces. Nucleic Acids Research, 40(15), e115.

Urushida, Y., Nakano, M., Matsuda, S., Inoue, N., Kanai, S., Kitamura, N., Nishino, T. and Kamino, K., 2007. Identification and functional characterization of a novel barnacle cement protein. The FEBS Journal, 274(16), 4336-4346.

Visscher, J.P., 1928. Reactions of the cyprid larvae of barnacles at the time of attachment. The Biological Bulletin, 54(4), 327-335.

Walker, G. A., 1971. Study of the cement apparatus of the cypris larva of the barnacle *Balanus balanoides*. Marine Biology, 9, 205-212.

Walker, G. and Yule, A.B., 1984. Temporary adhesion of the barnacle cyprid: The existence of an antennular adhesive secretion. Journal of the Marine Biological Association of the United Kingdom, 64(3), 679-686.

Walker, G., 1970. The histology, histochemistry and ultrastructure of the cement apparatus of three adult sessile barnacles, *Elminius modestus*, *Balanus balanoides* and *Balanus hameri*. Marine Biology, 7(3), 239-248.

Walker, G., 1972. The biochemical composition of the cement of two barnacle species, *Balanus hameri* and *Balanus crenatus*. Journal of the Marine Biological Association of the United Kingdom, 52(2), 429-435.

Walker, G., 1977. Observations by scanning electron microscope (SEM) on the oviducal gland sacs of *Balanus balanoides* at egg-laying. Journal of the Marine Biological Association of the United Kingdom, 57(4), 969-972.

Wang, X., Wang, C., Xu, B., Wei, J., Xiao, Y. and Huang, F., 2018. Adsorption of intrinsically disordered barnacle adhesive proteins on silica surface. Applied Surface Science, 427, 942-949.

Wang, Z., Leary, D.H., Liu, J., Settlage, R.E., Fears, K.P., North, S.H., Mostaghim, A., Essock-Burns, T., Haynes, S.E., Wahl, K.J. and Spillmann, C.M., 2015. Molt-dependent transcriptomic analysis of cement proteins in the barnacle *Amphibalanus amphitrite*. BMC Genomics, 16(1), 859.

Wiegemann, M. and Watermann, B., 2003. Peculiarities of barnacle adhesive cured on non-stick surfaces. Journal of Adhesion Science and Technology, 17(14), 1957-1977.

Yamamoto, H., Kawaii, S., Yoshimura, E., Tachibana, A. and Fusetani, N., 1997b. 20-hydroxyecdysone regulates larval metamorphosis of the barnacle, *Balanus amphitrite*. Zoological Science, 14(6), 887-892.

Yamamoto, H., Okino, T., Yoshimura, E., Tachibana, A., Shimizu, K. and Fusetani, N., 1997a. Methyl farnesoate induces larval metamorphosis of the barnacle, *Balanus amphitrite* via protein kinase C activation. Journal of Experimental Zoology, 278(6), 349-355.

Yamamoto, H., Shimizu, K., Tachibana, A. and Fusetani, N., 1999. Roles of dopamine and serotonin in larval attachment of the barnacle, *Balanus amphitrite*. Journal of Experimental Zoology, 284(7), 746-758.

Yamamoto, H., Tachibana, A., Kawaii, S., Matsumura, K. and Fusetani, N., 1996. Serotonin involvement in larval settlement of the barnacle, *Balanus amphitrite*. Journal of Experimental Zoology, 275(5), 339-345.

Yan, G., Sun, J., Wang, Z., Qian, P.Y. and He, L., 2020. Insights into the synthesis, secretion and curing of barnacle cyprid adhesive via transcriptomic and proteomic analyses of the cement gland. Marine Drugs, 18(4), 186.gibert

Yan, G., Zhang, G., Huang, J., Lan, Y., Sun, J., Zeng, C., Wang, Y., Qian, P.Y. and He, L., 2017. Comparative transcriptomic analysis reveals candidate genes and pathways involved in larval settlement of the barnacle *Megabalanus volcano*. International Journal of Molecular Sciences, 18(11), 2253.

Yan, X.C., Chen, Z.F., Sun, J., Matsumura, K., Wu, R.S. and Qian, P.Y., 2012. Transcriptomic analysis of neuropeptides and peptide hormones in the barnacle *Balanus amphitrite*: Evidence of roles in larval settlement. PLoS ONE, 7(10), e46513.

Yap, F.C., Wong, W.L., Maule, A.G., Brennan, G.P., Chong, V.C. and Lim, L.H.S., 2017. First evidence for temporary and permanent adhesive systems in the stalked barnacle cyprid, *Octolasmis angulata*. Scientific Reports, 7, 44980.

Yates, E.A., Estrella, L.A., Ryou, H., Wahl, K.J. and So, C.R., 2020. Measuring the physical properties of synthetic cement derived barnacle adhesive nanomaterials from the barnacle *Amphibalanus amphitrite*. Biophysical Journal, 118(3), 163a.

Yorisue, T., Matsumura, K., Hirota, H., Dohmae, N. and Kojima, S., 2012. Possible molecular mechanisms of species recognition by barnacle larvae inferred from multi-specific sequencing analysis of proteinaceous settlement-inducing pheromone. Biofouling, 28(6), 605-611.

Yu, W., Wanka, R., Finlay, J.A., Clarke, J.L., Clare, A.S. and Rosenhahn, A., 2020. Degradable hyaluronic acid/chitosan polyelectrolyte multilayers with marine fouling-release properties. Biofouling, 36(9), 1049-1064.

Yule, A.B. and Crisp, D.J., 1983. Adhesion of cypris larvae of the barnacle, *Balanus balanoides*, to clean and arthropodin treated surfaces. Journal of the Marine Biological Association of the United Kingdom, 63(2), 261-271.

Yule, A.B. and Walker, G., 1984. The temporary adhesion of barnacle cyprids: Effects of some differing surface characteristics. Journal of the Marine Biological Association of the United Kingdom, 64(2), 429-439.

Yule, A.B. and Walker, G., 1987. Adhesion in barnacles. In Barnacle biology, Southward, A.J., Ed., Balkema, Rotterdam, Netherlands, 389-402.

Zhang, G., Yang, X.X., Leung, P.M., He, L.S., Chan, T.Y., Yan, G.Y., Zhang, Y., Sun, J., Xu, Y. and Qian, P.Y., 2016. Secretory locations of SIPC in *Amphibalanus amphitrite* cyprids and a novel function of SIPC in biomineralization. Scientific Reports, 6(1), 1-11.

Zhang, Y., He, L.S., Zhang, G., Xu, Y., Lee, O.O., Matsumura, K. and Qian, P.Y., 2012. The regulatory role of the NO/cGMP signal transduction cascade during larval attachment and metamorphosis of the barnacle *Balanus* (= *Amphibalanus*) *amphitrite*. Journal of Experimental Biology, 215(21), 3813-3822.

Zimmer, R.K., Ferrier, G.A., Kim, S.J., Kaddis, C.S., Zimmer, C.A. and Loo, J.A., 2016. A multifunctional chemical cue drives opposing demographic processes and structures ecological communities. Ecology, 97(9), 2232-2239.

8. Appendix A

Table A1. Generic homology search. Top BLASTn sequence alignments with the NCBI nucleotide database. Entries shaded red have over 70% cover and identity in both transcripts to an existing database entry and have been rejected as candidates. 'Gel band' indicates which SDS PAGE gel band the transcript is associated with from those considered for peptide mass fingerprinting.

Sequence Identifier	Best alignment	Cover	Identity	E value	Total score	Accession	Gel band (kDa)
k75_2466758/ NODE_29304	PREDICTED: *Pollicipes policipes* rab proteins geranylgeranyltransferase component A 2-like (LOC119092279), mRNA	58%/ 74%	81.07/ 78.46%	4e-178/ 0.0	638/ 774	XM_037215250.1	30-35
k55_4809949/ NODE_26814	PREDICTED: Pollicipes pollicipes leishmanolysin-like peptidase (LOC119103683), mRNA	100%/ 92%	81.27%/ 81.91%	7e-178/ 0.0	636/ 1316	XM_037227299.1	30-35
k45_6229312/ NODE_11739	PREDICTED: *Pollicipes policipes* glycine receptor subunit alpha-2-like (LOC119103720), mRNA	50%/ 16%	83.95%/ 83.44%	5e-84/ 8e-88	324/ 339	XM_037227351.1	30-32.5
k55_4766728/ NODE_15688	PREDICTED: *Pollicipes policipes* copper-transporting ATPase 2-like (LOC119092178), mRNA	100%/ 93%	71.78%/ 76.17%	3e-127/ 0.0	533/ 1251	XM_037215155.1	35
k45_6236322/ NODE_1719	PREDICTED: *Pollicipes policipes* tuberin-like (LOC119098352), mRNA	85%/ 29%	80.00%/ 84.46%	0.0/ 0.0	1119/ 1110	XM_037221273.1	35
k65_3283434/ NODE_42329	None/ PREDICTED: *Pollicipes policipes* serpin B4-like (LOC119109435), mRNA	-/ 52%	-/ 66.86%	-/ 9e-27	-/ 135	- / XM_037233051.1	35

k65_3660540/ NODE_2621	PREDICTED: *Rhipicephalus sanguineus* uncharacterized protein K02A2.6-like (LOC119388994), mRNA brown dog tick	20%/ 17%	64.18%/ 64.00%	1e-10/ 2e-09	83.3/ 78.8	XM_03765630 2.1	30
k65_364217/ NODE_1889	PREDICTED: *Pollicipes pollicipes* collagen alpha-3(IX) chain-like (LOC119105727), mRNA	99%/ 86%	79.68%/ 77.36%	2e-119/ 0.0	442/ 2260	XM_03722921 2.1	30
k75_2505784/ NODE_3504	PREDICTED: *Pollicipes pollicipes* nicotinate phosphoribosyltrans ferase-like (LOC119102206), transcript variant X2, mRNA	100%/ 54%	82.89%/ 83.75%	0.0/ 0.0	689/ 1702	XM_03722556 5.1	35
k85_1882426/ NODE_33480	PREDICTED: *Pollicipes pollicipes* choline-phosphate cytidylyltransferase A-like (LOC119110432), transcript variant X3, mRNA	99%/ 65%	88.43%/ 87.05%	4e-127/ 0.0	466/ 914	XM_03723426 4.1	35
k65_2820919/ NODE_67014	PREDICTED: *Pollicipes pollicipes* fat-like cadherin-related tumor suppressor homolog (LOC119090030), partial mRNA	99%/ 99%	80.92%/ 80.90%	2e-99/ 4e-162	375/ 584	XM_03721282 6.1	32.5
k75_645919/ NODE_13780	PREDICTED: *Onthophagus taurus* neurotrimin-like (LOC111429336), transcript variant X2, mRNA/ PREDICTED: *Pollicipes pollicipes* lachesin-like (LOC119099779), mRNA	17%/ 44%	85.48%/ 75.64%	3e-07/ 4e-155	68.9/ 562	XM_02306521 7.1/ XM_03722285 1.1	32.5

k75_2476289/ NODE_5283	PREDICTED: *Pollicipes policipes* uncharacterized aarF domain-containing protein kinase 5-like (LOC119108991), transcript variant X1, mRNA	97%/ 56%	78.01%/ 83.16%	5e-68/ 0.0	270/ 1526	XM_03723253 6.1	30
k85_1827598/ NODE_11929 0	*Coregonus* sp. 'balchen' genome assembly, chromosome: 4/ -	1%/ -	88.64%/ -	0.005/ -	58.1/ -	LR778256.1/ -	30
k85_1877424/ NODE_7520	PREDICTED: *Pollicipes policipes* serine protease inhibitor A3N-like (LOC119106317), mRNA	34%/ 10%	69.11%/ 67.32%	0.028/ 4e-10	51.8/ 81.5	XM_03722993 1.1	35
k75_2496648/ NODE_5654	PREDICTED: *Pollicipes policipes* papilin-like (LOC119093526), mRNA	26%/ 32%	77.06%/ 74.01%	1e-09/ 1e-92	196/ 721	XM_03721648 5.1	35
k65_3659377/ NODE_4268	PREDICTED: *Pollicipes policipes* poly [ADP-ribose] polymerase 2-like (LOC119105858), mRNA	87%/ 77%	77.36%/ 70.73%	9e-80/ 0.0	309/ 1003	XM_03722941 4.1	35
k85_1893376/ NODE_6717	PREDICTED: *Pollicipes policipes* talin-2-like (LOC119098416), mRNA	100%/ 84%	88.39%/ 87.64%	8e-123/ 0.0	453 /2522	XM_03722133 2.1	35
k55_4432846/ NODE_26764	PREDICTED: *Pollicipes policipes* chitinase-3-like protein 1 (LOC119108611), mRNA	100%/ 86%	66.76%/ 70.23%	1e-13/ 2e-132	90.6/ 487	XM_03723221 2.1	35
k85_1857937/ NODE_8120	PREDICTED: *Pollicipes policipes* putative RNA-binding protein Luc7-like 2 (LOC119103302), mRNA	100%/ 45%	86.77%/ 79.77%	3e-168/ 0.0	603/ 945	XM_03722677 4.1	35

k45_6245999/ NODE_5445	PREDICTED: *Pollicipes policipes* cAMP-dependent protein kinase catalytic subunit 3-like (LOC119109653), mRNA	85%/ 40%	85.12%/ 85.12%	0.0/ 0.0	1177/ 1177	XM_03723337 1.1	32.5
k45_1194892/ NODE_16940	PREDICTED: *Pollicipes policipes* mitotic spindle assembly checkpoint protein MAD2B-like (LOC119111867), mRNA	86%/ 34%	70.97%/ 68.75%	2e-28/ 5e-52	139/ 220	XM_03723570 5.1	32.5
k85_1841077/ NODE_21781	PREDICTED: *Pollicipes policipes* dipeptidyl peptidase 9-like (LOC119090647), mRNA	97%/ 76%	84.53%/ 82.33%	1e-167/ 0.0	601/ 1134	XM_03721349 3.1	30
k85_1859180/ NODE_897	PREDICTED: *Pollicipes policipes* fasciclin-1-like (LOC119098674), transcript variant X2, mRNA	87%/ 37%	66.78%/ 65.97%	4e-29/ 1e-70	142/ 377	XM_03722165 9.1	30
k85_1865598/ NODE_6813	PREDICTED: *Pollicipes policipes* cell migration-inducing and hyaluronan-binding protein-like (LOC119092219), mRNA	68%/ 69%	76.11%/ 72.21%	2e-82/ 1e-106	319/ 768	XM_03721519 4.1	125
k45_6243571/ NODE_12522	PREDICTED: *Stomoxys calcitrans* actin-5C (LOC106087830), mRNA/ Sepia officinalis mRNA for actin I (gene ACTI)	93%/ 99%	84.17%/ 91.46%	0.0/ 0.0	1233/ 2699	XM_01325300 5.1/ HE687188.1	125
k85_1830366/ NODE_21933	PREDICTED: *Pollicipes policipes* uncharacterized LOC119109749	26%/ 5%	71.79%/ 79.49%	3e-27/ 0.003	136/ 57.2	XM_03723350 1.1/ GU722576.1	30

(LOC119109749), mRNA/ *Locusta migratoria* clone LmigCSP1 hypothetical protein mRNA, complete cds

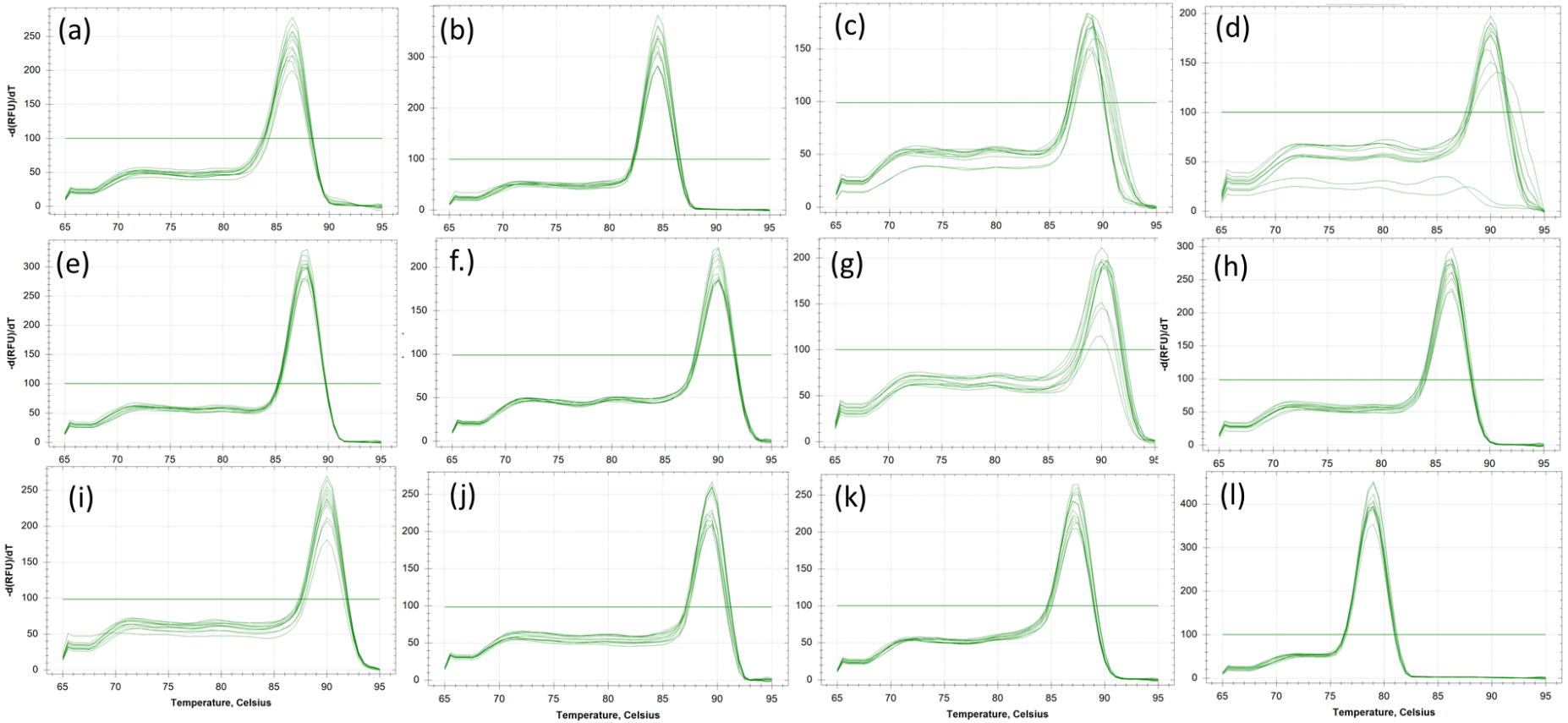

Figure A1. Melt curve analysis for the primer pairs designed for candidate transcripts and reference genes. **(a)** = SIPC, **(b-e) =** Q1-4**, (f-g)** = B1-2, **(h-j)** = H1-3, **(k)** = *ef1a*, **(l) =** *mt-cyb*.

Table A2. Summary table of figure X.X and statistical analyses. Each candidate was subjected to a two sample T test (Minitab 18). Green = significant difference ($p < 0.07$) in log_2 mean fold expression between stage 6 nauplii and cyprids. All statistical analyses were performed on log_2 fold expression values. NMFE = normalised mean fold expression; S6N = stage six nauplii; CYP = cyprids; CI = confidence interval; SD = standard deviation; SEM = standard error of the mean; DF = degrees of freedom.

Candidate tag	S6N NMFE	CYP NMFE	95% CI +	95% CI -	P value	Log_2 S6N mean	Log_2 NPL SD	Log_2 NPL SEM	Log_2 CYP mean	Log_2 CYP SD	Log_2 CYP SEM	T value	DF
SIPC	1	5.23	16.00	1.71	0.02	0.00	0.62	0.36	2.39	0.62	0.36	-4.71	2.00
Q4	1	2.53	3.13	2.04	0.00	0.00	0.12	0.07	1.34	0.12	0.07	-13.74	2.00
Q1	1	1.83	3.18	1.05	0.04	0.00	0.07	0.04	0.87	0.31	0.18	-4.70	2.00
H2	1	1.35	2.77	0.65	0.22	0.00	0.42	0.24	0.43	0.02	0.01	-1.77	2.00
H3	1	1.10	1.37	0.88	0.28	0.00	0.13	0.08	0.13	0.12	0.07	-1.30	2.00
B1	1	1.00	2.73	0.37	0.99	0.00	0.54	0.31	0.00	0.23	0.13	-0.01	2.00
H1	1	0.92	1.42	0.60	0.59	0.00	0.23	0.13	-0.12	0.25	0.14	0.60	2.00
B2	1	0.79	1.66	0.38	0.31	0.00	0.43	0.03	-0.34	0.06	0.03	1.37	2.00
Q3	1	0.69	2.66	0.18	0.36	0.00	0.76	0.44	-0.53	0.18	0.11	1.18	2.00
Q2	1	0.50	1.15	0.22	0.07	0.00	0.14	0.08	-1.00	0.46	0.27	3.57	2.00